Supporting Information

# 1.   Synthesis of *N*-aryl-1,2,3,4-tetrahydroisoquinolines (1a-f)

General procedure. The two-neck flask equipped with a reflux condenser and a stir bar was charged with palladium(II) acetate (3 mol%), *rac*-BINAP (5 mol%) and sodium *tert*–butylate (2 equiv.) and then the vessel was purged with dry argon. Dry toluene (1.6 mL) was added under an argon stream, and the mixture was stirred for *ca.* 5 min. Afterward, aryl bromide (1 mmol) and 1,2,3,4-tetrahydroisoquinoline (NH-THIQ, 2 equiv.) were added, and argon was bubbled through the solution *via* a needle for 10 min. Then, the flask was sealed with a septum, and the reaction mixture was stirred at 110 ºC for 20–24 h under an argon atmosphere. After cooling to room temperature, the reaction mixture was rotary evaporated. The product was isolated by column chromatography on silica gel using ethyl acetate/hexanes mixture as an eluent. The products are colorless to slightly yellowish oils that quickly form white solids and are best stored in a fridge. The product yields can probably be increased using classical ratio of Pd(OAc)$_2$: *rac*-BINAP (1:2) in the synthesis.
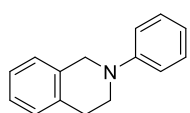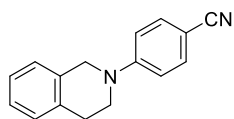
2-Phenyl-1,2,3,4-tetrahydroisoquinoline (**1a**)[1] was obtained from bromobenzene (2.355 g, 1.575 mL, 15 mmol) and NH-THIQ (3.99 g, 30 mmol). Eluent: ethyl acetate/hexanes 1:20 v/v. Yield: 2.910 g (93%), white solid. ^{1}H NMR (CDCl$_3$, 400 MHz): δ 7.32 (dd, 2H, *J* = 8.6 Hz, *J* = 7.3 Hz, Ar), 7.23–7.17 (m, 4H, Ar), 7.03 (d, 2H, *J* = 8.1 Hz, Ar), 6.87 (t, 1H, *J* = 7.3 Hz, Ar), 4.45 (s, 2H, NCH$_2$Ar), 3.60 (t, 2H, *J* = 5.9 Hz, NCH$_2$CH$_2$), 3.02 (t, 2H, *J* = 5.9 Hz, NCH$_2$CH$_2$).
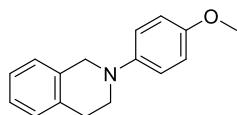
2-(4-Methoxyphenyl)-1,2,3,4-tetrahydroisoquinoline (**1b**)[1] was obtained from 4-bromoanizole (1.870 g, 1.25 mL, 10 mmol) and NH-THIQ (2.66 g, 20 mmol). Eluent: ethyl acetate/hexanes 1:5 v/v. Yield: 0.887 g (37%), white solid. ^{1}H NMR (CDCl$_3$, 400 MHz): δ 7.20–7.14 (m, 4H, Ar), 7.01 (d, 2H, *J* = 9.1 Hz, Ar), 6.89 (d, 2H, *J* = 9.1 Hz, Ar), 4.32 (s, 2H, NCH$_2$Ar), 3.79 (s, 3H, OCH$_3$), 3.46 (t, 2H, *J* = 5.9 Hz, NCH$_2$CH$_2$), 3.01 (t, 2H, *J* = 5.9 Hz, NCH$_2$CH$_2$).
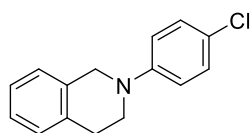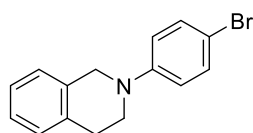
2-(4-Chlorophenyl)-1,2,3,4-tetrahydroisoquinoline (**1c**)[1] was obtained from 1-bromo-4-chlorobenzene (0.995 g, 5 mmol) and NH-THIQ (1.33 g, 10 mmol). Eluent: ethyl acetate/hexanes 1:10 v/v. Yield: 0.585 g (47%), white solid. ^{1}H NMR (CDCl$_3$, 400 MHz): δ 7.25 (d, 2H, *J* = 8.9 Hz, Ar), 7.24–7.17 (m, 4H, Ar), 6.91 (d, 2H, *J* = 8.9 Hz, Ar), 4.40 (s, 2H, NCH$_2$Ar), 3.55 (t, 2H, *J* = 5.8 Hz, NCH$_2$CH$_2$), 3.00 (t, 2H, *J* = 5.8 Hz, NCH$_2$CH$_2$).

2-(4-Cyanophenyl)-1,2,3,4-tetrahydroisoquinoline (**1d**)[1] was obtained from 4-bromobenzonitrile (1.820 g, 10 mmol) and NH-THIQ (2.66 g, 20 mmol). Eluent: ethyl acetate/hexanes 1:3 v/v. Yield: 1.661 g (71%), white solid. ^{1}H NMR (CDCl$_3$, 400 MHz): δ 7.52 (d, 2H, J = 8.9 Hz, Ar), 7.26–7.18 (m, 4H, Ar), 6.88 (d, 2H, J = 8.9 Hz, Ar), 4.50 (s, 2H, NCH$_2$Ar), 3.63 (t, 2H, J = 5.9 Hz, NCH$_2$CH$_2$), 3.00 (t, 2H, J = 5.9 Hz, NCH$_2$CH$_2$).

2-(4-Bromophenyl)-1,2,3,4-tetrahydroisoquinoline (**1e**)[1] was obtained from 1,4-dibromobenzene (590 mg, 2.5 mmol) and NH-THIQ (333 mg, 0.25 mL). Eluent: ethyl acetate/hexanes 1:20 v/v. Yield: 0.365 g (50%), white solid. ^{1}H NMR (CDCl$_3$, 400 MHz): δ 7.37 (d, 2H, J = 8.4 Hz, Ar), 7.22–7.18 (m, 4H, Ar), 6.85 (d, 2H, J = 8.4 Hz, Ar), 6.89 (d, 2H, J = 9.1 Hz, Ar), 4.39 (s, 2H, NCH$_2$Ar), 3.54 (t, 2H, J = 5.8 Hz, NCH$_2$CH$_2$), 2.99 (t, 2H, J = 5.8 Hz, NCH$_2$CH$_2$).
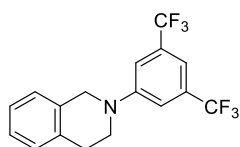
2-(3,5-Bis(trifluoromethyl)phenyl)-1,2,3,4-tetrahydroisoquinoline (**1f**)[2] was obtained from 1-bromo-3,5-bis(trifluoromethyl)benzene (4.395 g, 2.586 mL, 15 mmol) and NH-THIQ (3.99 g, 30 mmol). Eluent: ethyl acetate/hexanes 1:10 v/v. Yield 5.000 g (96%), white solid. ^{1}H NMR (CDCl$_3$, 400 MHz): δ 7.30–7.24 (m, 7H, Ar and Ar$_F$), 4.52 (s, 2H, NCH$_2$), 3.87 (t, 2H, J = 5.9 Hz, NCH$_2$CH$_2$), 3.07 (t, 2H, J = 5.9 Hz, NCH$_2$CH$_2$). ^{13}C{^{1}H} NMR (CDCl$_3$, 125 MHz): δ 150.0 (s, 1C, NC(Ar$_F$)), 134.3 (s, 1C, C1 (Ph)), 132.8 (s, 1C, C2 (Ph)), 132.0 (q, 2C, $J_{C,F}$ = 32.1 Hz, C3 and C5 (Ar$_F$)), 127.9 (s, 1C, C6 (Ph)), 126.5 (s, 1C, C2 (Ph)), 126.1 (s, 2C, C5 and C3 (Ph)), 124.1 (q, 2C, $J_{C,F}$ = 272.8 Hz, CF$_3$), 112.4 (s, 2C, C2 and C6 (Ar$_F$), 110.0 (s, 1C, C4, (Ar$_F$), 49.0 (s, 1C, NCH$_2$Ar), 44.9 (s, 1C, NCH$_2$CH$_2$Ph), 28.6 (s, 1C, NCH$_2$CH$_2$Ph).

2. Optimization of hydrolysis of complex Ru-4,7PEt and phosphonate-substituted phenanthroline ligand 4,7PEt.

Table S1. Optimization of hydrolysis of complex **Ru-4,7PEt**.[1]

Ru-4,7PH$_1$Et$_3$: n = 1, m = 0
Ru-4,7PHEt : n = m = 1
Ru-4,7PH$_3$Et$_1$: n = 2, m = 1
Ru-4,7PH : n = m = 2

Ent-ry	Solvent (mL)	Reagent	T[2] (°C)	Time (h)	Conversion[3] (%)	Yield[3] (%)			
						Ru-PH$_1$Et$_3$	Ru-4,7PHEt	Ru-PH$_3$Et$_1$	Ru-4,7PH
1	EtOH	H$_2$O	100	2	86	30	56	0	0
2	EtOH (2)	NaOH	100	2	100	0	99 [4]	0	0
3	EtOH (2)	HCl (1 M)	100	2	89	36	53	0	0
4	H$_2$O (4)	-	100	2	100	30	70	0	0
				16	100	10	90	0	0
				30	100	6	94	0	0
5	H$_2$O (4)	-	130	4	100	0	99 [5]	0	0
6	H$_2$O (4)	-	150	6	100	0	0	65	35
				20	100	0	0	13	87
				48	100	0	0	0	99 (94 [5])

[1] Reaction conditions: Ru(II) complex (0.1 mmol), reagent (*ca.* 2 equiv.) and solvent were refluxed in a glass pressure resistant tube with a screw cap. A crude sample of **Ru-4,7PEt** was used in all experiments (a mixture of **Ru-4,7PEt** and **Ru-PH$_1$Et$_3$**, *ca.* 1:1) and complex loading was calculated based on this composition of starting material. [2] The temperature of the oil bath is given. [3] Conversion and yields were determined by ^{31}P and ^{1}H NMR spectroscopies. [4] Attempts to isolate the pure product by precipitation from acidic aqueous solutions failed due to the high solubility of the complex. [5] Isolated yield.

Table S2. Optimization of hydrolysis of phenanthroline **4,7PEt**.[1]

Ru-4,7PEt → Reagent, EtOH, 100 °C → Ru-4,7PH₁Et₃ : n = 1, m = 0; Ru-4,7PHEt : n= m = 1
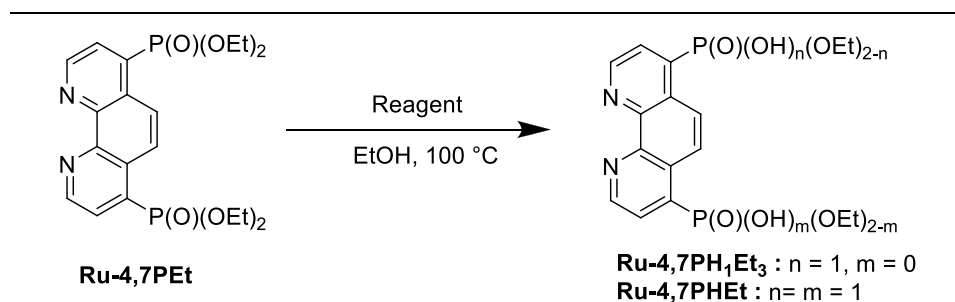
Entry	Reagent	Time (h)	Conversion [2] (%)	Yield [2] (%)	
				PH₁Et₃	4,7PHEt
1	H_2O	2	0	0	0
2	NaOH	2	94	59	35
3	HCl (1 M)	2	50	50	0

[1] Reaction conditions: **4,7PEt** (0.1 mmol), reagent (*ca.* 2 equiv.), and EtOH (2 mL) were refluxed in a glass pressure resistant tube with a screw cap.
[2] Conversion and yields were determined by ^{31}P and ^{1}H NMR spectroscopies.

3. Synthesis of Ru(II) complexes for NMR studies
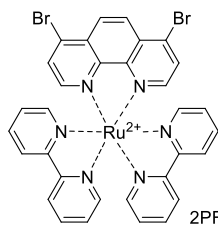
[Ru(4,7-Br-Phen)(bpy)₂](PF₆)₂ (Ru-4,7Br₂). 4,7-Dibromo-1,10-phenanthroline (260 mg, 0.77 mmol) and *cis*-Ru(bpy)₂Cl₂ (339 mg, 0.7 mmol) were refluxed in MeOH (23 mL) for 30 h. The hot solution was filtered, and the filtrate was allowed to cool to room temperature. Then, a saturated aqueous solution of NH₄PF₆ (3 mL) and water (30 mL) were added to this solution. The precipitate formed was collected, washed with water (3 × 10 mL) and dried under reduced pressure. Yield 676 mg (93%), orange powder. ^{1}H NMR (CD₃CN, 400 MHz): δ 7.24 (ddd, ^{3}J = 7.6 Hz, ^{3}J = 5.3 Hz, ^{4}J = 1.3 Hz, 2H, H5 (bpy)), 7.45 (ddd, ^{3}J = 7.7 Hz, ^{3}J = 5.6 Hz, ^{4}J = 1.3 Hz, 2H, H5' (bpy)), 7.58 (ddd, ^{3}J = 5.6 Hz, ^{4}J = 1.3 Hz, ^{5}J = 0.7 Hz, 2H, H6 (bpy)), 7.80 (ddd, ^{3}J = 5.6 Hz, ^{4}J = 1.3 Hz, ^{5}J = 0.7 Hz, 2H, H6' (bpy)), 7.94 (d, ^{3}J = 5.6 Hz, 2H, H3 and H8 (Phen)), 7.99–8.03 m (2H, H4 (bpy)), 8.04 д (2H, ^{3}J = 5.6, H2 and H9 (Phen)), 8.08–8.12 (m, H4' (bpy)), 8.49 (d, ^{3}J = 8.2 Hz, H5' (bpy)), 8.52 (d, ^{3}J = 8.2, 2H, H5 (bpy)), 8.53 (s, 2H, H5 and H6 (Phen)). Anal. Calcd. for C₃₂H₂₂Br₂F₁₂N₆P₂Ru: C, 36.91; H, 2.13; N, 8.07. Found: C, 37.11; H, 2.43; N, 7.83. HRMS (MALDI TOF) *m/z*: [M–2PF₆]⁺ Calcd. for C₃₂H₂₂Br₂N₆Ru 749.9316; Found 749.9360.

Analytically pure samples of **Ru-4,7PH₁Et₃** and **Ru-3,8PH₁Et₃** (Table S1) were prepared according the following general procedure:

A crude sample of **Ru-3,8PEt** or **Ru-4,7PEt** obtained as described in the Experimental part was dissolved in MeOH/water mixture (*ca*. 6 mL, 1:1 v/v) and a saturated aqueous solution of NH_4PF_6 (0.5 mL) was added to this solution. This aqueous phase was extracted with CH_2Cl_2 (1 × 5 mL) and the organic phase was dried over 3Å molecular sieves, evaporated to dryness under reduced pressure and redissolved in CH_2Cl_2 (*ca*. 5 mL). The Ru(II) complex was extracted with water (1 × 5 mL), and aqueous phase was evaporated under reduced pressure (2 Torr) at 55 °C to give an analytically pure sample of the target product as red glassy solids.
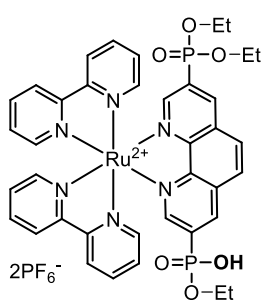
Ru-3,8PH₁Et₃ was obtained from **3,8PEt** (100 mg, 0.22 mmol) and *cis*-[Ru(bpy)₂Cl₂] (100 mg, 0.2 mmol). Yield 46 mg (20%), deep red glassy solid. ¹H NMR (CD₃CN, 400 MHz): δ 8.94 (dd, 1H, $^3J_{H,P}$ = 13.8 Hz, $^4J_{H,H}$ = 1.1 Hz, H7 (Phen)), 8.92 (d, 1H, $^3J_{H,P\ obs.}$ = 10.9 Hz, H4 (Phen)), 8.64–8.51 (m, 4H, (bpy)), 8.37 (d, 1H, $^3J_{H,H}$ = 8.9 Hz, 6H (Phen)), 8.29 (d, 1H, $^3J_{H,H}$ = 8.9 Hz, 5H (Phen)), 8.28 (7.94–7.90 (m, 2H, (bpy)), 8.16–8.12 (m, 2H), 8.08 (dd, 1H, $^3J_{H,P}$ = 6.8 Hz, $^4J_{H,H}$ = 1.1 Hz, H9 (Phen)), 8.01–7.96 (m, 2H, (bpy)), 7.94–7.89 (m, 2H, (bpy)), 7.62–7.58 (m, 2H, (bpy)), 7.51–7.49 (m, 2H, (bpy)), 7.26–7.21 (m, 2H, (bpy)), 4.11–3.98 (m, 4H, OCH₂ P(O)(OEt)₂), 3.56–3.49 (m, 2H, OCH₂ P(O)(OH)(OEt)), 1.18 (t, 6H, $^3J_{H,H}$ = 7.0 Hz, CH₃ P(O)(OEt)₂), 0.88 (t, 3H, $^3J_{H,H}$ = 7.0 Hz, CH₃ P(O)(OH)(OEt)). ³¹P{¹H} NMR (D₂O, 162.5 MHz): δ 11.02 (s, 1P, P(O)(OEt)₂), 1.35 (br. s., 1P, P(O)(OH)(OEt)), 144.51 (m, 1P, $J_{F,P}$ = 706.7 Hz, PF₆). MS MALDI TOF: [M–2PF₆–H]⁺ Calcd. for $C_{38}H_{37}N_6O_6P_2Ru^+$ 837.13; Found 837.15.
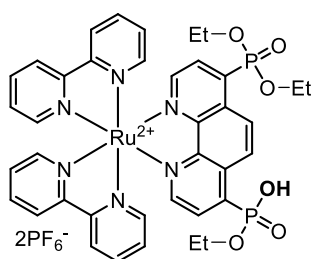
Ru-4,7PH₁Et₃ was obtained from **4,7PEt** (60 mg, 0.131 mmol).) and *cis*-[Ru(bpy)₂Cl₂] (60 mg, 0.12 mmol). Yield: 21 mg (16%), deep red glassy solid. ¹H NMR (CD₃CN, 400 MHz): δ 8.72 (d, 1H, $^3J_{H,H}$ = 9.5 Hz, H5 or H6 (Phen)), 8.92 (d, 1H, $^3J_{H,P\ obs.}$ = 10.9 Hz, H4 (Phen)), 8.60–8.51 (m, 4H,), 8.21 (dd, 1H, $^4J_{H,P}$ = 3.4 Hz, $^3J_{H,H}$ = 5.3 Hz, H9 or H2 (Phen)), 8.13–8.09 (m, 4H), 8.03 (dd, 1H, $^3J_{H,P}$ = 14.7 Hz, $^3J_{H,H}$ = 5.4 Hz, H3 or H8 (Phen)), 8.00–7.98 (m, 2H (bpy)), 7.84–7.81 (m, 2H, (bpy)),7.57–7.53 (m, 2H, (bpy)), 7.48–7.44 (m, 2H, (bpy)), 7.26–7.21 (m, 2H, (bpy)), 4.30–4.14 (m, 4H, OCH₂ P(O)(OEt)₂), 3.8–3.70 (m, 2H, OCH₂ P(O)(OH)(OEt)), 1.32 (td, 6H, $^3J_{H,H}$ = 7.0 Hz, $^4J_{H,P}$ = 3.7 Hz, CH₃ P(O)(OEt)₂), 1.06 (t, 3H, $^3J_{H,H}$ = 6.9 Hz, CH₃ P(O)(OH)(OEt)). ³¹P{¹H} NMR (D₂O, 162.5 MHz): δ 12.06 (s, 1P, P(O)(OEt)₂), 1.50 (s, 1P, P(O)(OH)(OEt)), 144.51 (m, 1P, $J_{F,P}$ = 706.7 Hz, PF₆). MS MALDI-TOF: [M–2PF₆–H]⁺ Calcd. for $C_{38}H_{37}N_6O_6P_2Ru^+$ 837.13; Found 837.16.

4. Photostability studies

A stirred 0.01 mM solutions of the ruthenium complex in various solvents was irradiated by a blue LED (12 W) at room temperature in a glass vial under air. The aliquots were periodically taken off and analyzed by UV–vis spectroscopy. The results are depicted in Figure S1.
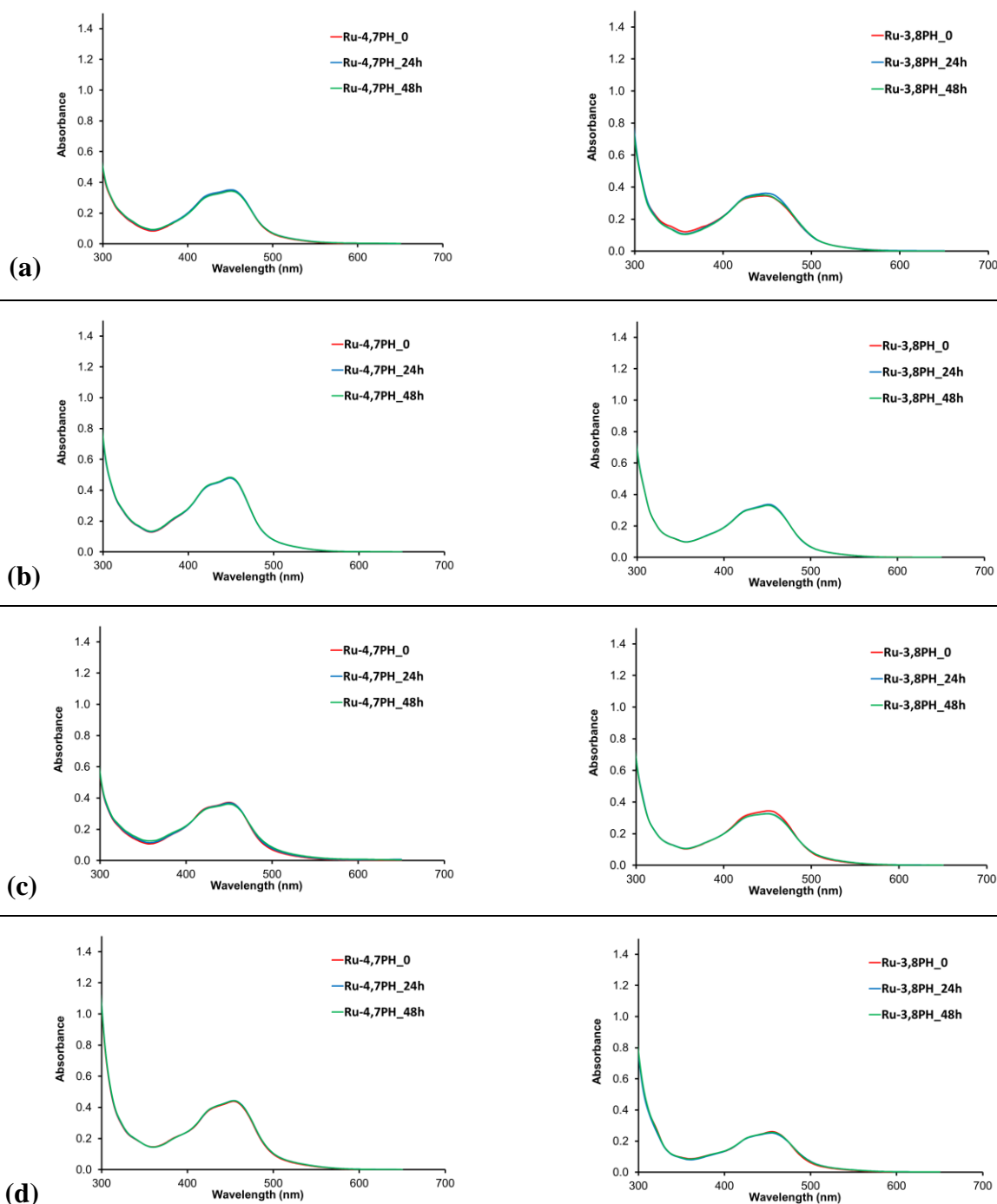
Figure S1. UV–vis spectra of the **Ru-4,7PH** (left) and **Ru-3,8PH** (right) solutions in water **(a)**, MeOH **(b)**, MeCN:H_2O (3:1) **(c)**, DMSO (4 vol% H_2O) **(d)**, before (red line) and after irradiation (blue LED, 12 W) for 24 h (blue line) and 48 h (green line).

5.   Single crystal analysis of Ru-4,7PH

The main problem we encountered within the search for all counterion is was the analysis of the Fourier density synthesis and atomic displacement parameters in order to "catch" the oxonium cation. The main difficulty is due to at least two different disorders that influence the occupancies of water molecules and/or oxonium cations. The disorder of PO_3 group led to decrease of O(6w) occupancy down to 0.5. Furthermore, the chloride anion is also disordered with two positions characterized by the occupancies 0.885(3) and 0.115(3). This disorder causes the decrease of O(5w) oxygen occupancy down to 0.885(3) while O(5w') occupancy is only 0.115(3). Clearly for correct description of such disordered supramolecular assembly (water, chloride anion, oxonium) one need to use the number of restraints: the same free variable for the same "part" of the disordered supramolecular moiety, as well as EADP in order to decrease the correlations. It should be mentioned that usage of all such constraints cause some increase in discrepancy factors and as one of the referee pointed out the "the refining all the entities in the solvent sphere with free occupancies will lead to a significant lowering of R1 to 5.65%" but unfortunately the matched model often degrades the residual electron density and discrepancy factors (see Figure S2b).
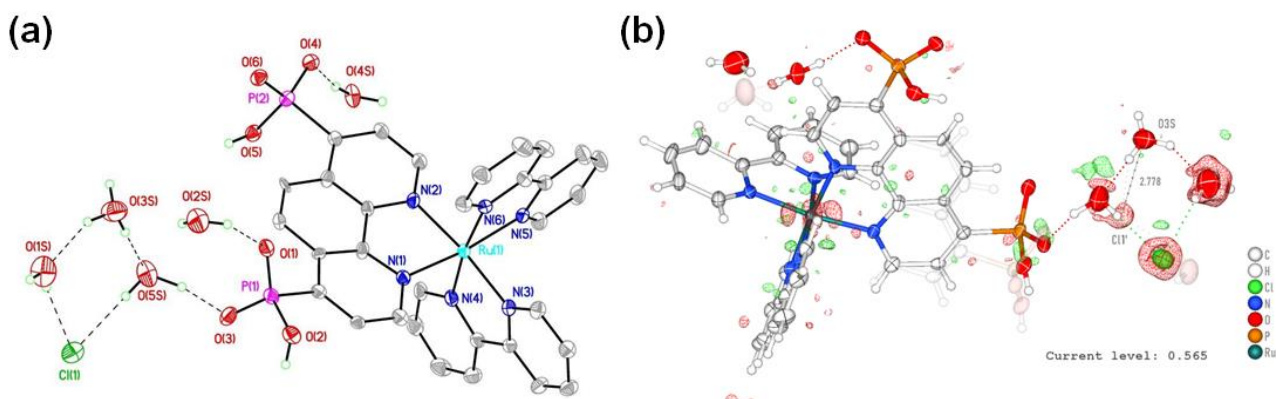
Figure S2. (a) Fragment of the crystalline structure of **Ru-4,7PH** showing the environment of the chloride and oxonium ions in the crystal. Minor disordered parts observed in the single crystal X-ray structure were omitted for clarity. **(b)** Residual density in the area of solvents and anions the crystalline structure of **Ru-4,7PH**.

Assuming the presence of partial disorder of chlorine anion and water molecules the exact position of oxonium cation is controversial. The choice of proposed position was based on the presence of shortened O····O separation that is commonly the characteristic of oxonium which form stronger H-bonds than water do (for e.g. see [3-5]). Assuming that the proposed position of oxonium is characterized by unrealistic O····Cl separation we can't exclude that some other position of oxonium can be observed or disorder is more complicated. But basing on the H-bonding pattern it

seems that such a position is one of the most probable and doubtful Cl····O distance can be the consequence of disorder influence.

6. Detailed NMR analysis of Ru(II) complexes.

Comparative analysis of spectral data for Ru(II) complexes containing asymmetric phen ligands.

As discussed in the article, a comparative analysis of the proton signals of two bpy (2,2'-bipyridine) ligands in $[Ru(bpy)_2(phen)]^{2+}$ complexes with D_3 symmetry (Figure S3) allows for easy assignment of all proton signals based on the data 1D and 2D ^1H NMR spectroscopy (Tables S3 and S4). However, when dealing with complexes containing asymmetric phen ligands, the two bpy ligands become non-equivalent, and the position of each ligand relative to the substituent on the phen ligand has to be determined.
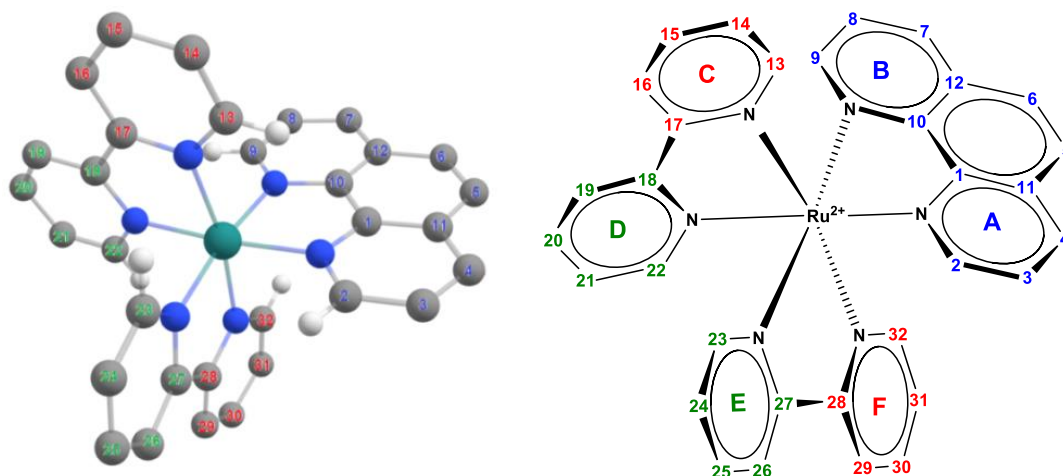
Figure S3. 3D schematic representation of the Ru(II) complexes showing atom labeling.

Table S5 summarized ^1H NMR spectral data for a series of asymmetric $[Ru(bpy)_2(phen)]^{2+}$ complexes that were reported previously by us and others and obtained in this work. Analyzing these data, one can conclude that α-H (H2, H9) of the phen ligands can be unambiguous assigned only for the compounds containing strong electron-donating or electron-withdrawing groups at positions 3 or 4 of the heterocycle. For these complexes, the α-H proton of the substituted py ring are upshifted or down-shifted, respectively, as generally observed in all aromatic organic compounds.

Table S3. Characteristic proton signals in ^{1}H NMR spectra of $[Ru(bpy)_2(phen)]^{2+}$ complexes.[1]

Ru-bpy

Ru-phen R = H
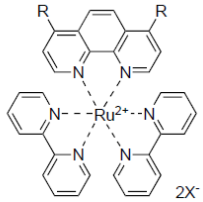Ru-4,7PEt R = P(O)(OEt)$_2$
Ru-4,7PH R = P(O)(OH)$_2$
X = Cl$^-$ or PF$_6^-$

Ru-4PEt

Complex	Solvent	H2	H9	H22	H23	H13	H32
Ru-bpy	CD$_3$CN	7.73	7.73	7.73	7.73	7.73	7.73
Ru-phen	CD$_3$CN	8.09	8.09	7.85	7.85	7.53	7.53
Ru-4,7PEt	CD$_3$CN	8.29	8.29	7.80	7.80	7.52	7.52
Ru-4PEt [2]	CD$_3$CN	8.24	8.14	7.82	7.84	7.48	7.57
Ru-4,7PH	D$_2$O	8.24	8.24	7.86	7.86	7.51	7.51

[1] Signals were assigned using detailed NMR investigations (the spectra are given in Figures S4–S30 at the end of this section). [2] Ref. [6]
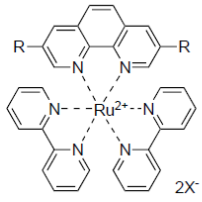
The α-H of the bpy ligands directed towards the phen ligand (H13 and H32) appear close to δ_H 7.53 ppm, i.e. the chemical shift of α-H in the parent (non-substituted) $[Ru(bpy)_2(phen)]^{2+}$ complex. However, in most cases, their position with respect to the substituent on the phen ligand cannot be defined due to the similarity of their chemical shifts. Proton directed towards the py ring with an electron-withdrawing substituent on the phen ligand (H32) experience a downshift compared to their analogs in the second bpy ligand (H13), but this downshift is clearly observed only for derivatives with strong electron-withdrawing groups. Additionally, the remaining two α-H protons of the bpy ligands (H22 and H23), directed towards the adjacent bpy ligand, exhibit very similar chemical shifts and appear close to δ_H 7.82 ppm. Consequently, when comparing the chemical shifts of the unknown complex with those of the parent $[Ru(bpy)_2(phen)]^{2+}$ complex and reported complexes of this series, six signals of α-H can be separated into three characteristic groups and unambiguously attributed to bpy or phen ligands. However, their relative positions in the coordination sphere of the metal ion can rarely be determined without additional structural analyses; in particular using two dimentional heteronuclear NMR techniques. Such 2D NMR analysis can be quite challenging due to the close similarity of chemical shifts for numerous protons and carbons, as well as the structural specificity of these compounds. For example, in **Ru-4PEt**, two α-H protons of the bpy ligands (H13 and H32) directed towards the phen ligand cannot be assigned based solely on quantitative NOESY experiments, as their cross-peak integrals are very similar. Proton assignment in this compound can only be accomplished by comparing the proton chemical
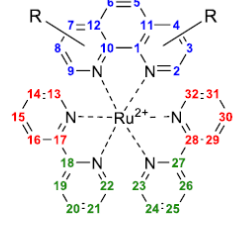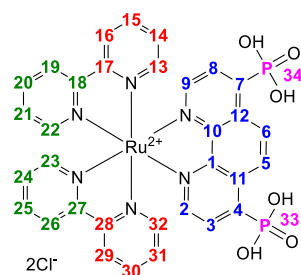
shifts observed in this compound with those **of Ru-4,7PEt**, and **Ru-phen** (Table S3). For complexes in which the difference in chemical shifts of H2 and H9 is less pronounced, complete attribution of signals in proton spectra can be very difficult or even impossible.

Table S4. Assignment of characteristic proton signals in ^{1}H NMR spectra of [Ru(bpy)$_2$(phen)]$^{2+}$ complexes with disubstituted phen ligands.

Complex	Solvent	H2(H9)	H22 (H23)	H13(H32)	Ref.
Ru-phen [1]	CD$_3$CN	8.09	7.85	7.53	this work
Ru-4,7PHEt	D$_2$O	8.24	7.85	7.48	this work
Ru-3,8PEt	CD$_3$CN	8.15	7.90	7.58	6
Ru-3,8PHEt	D$_2$O	8.18	7.91	7.57	this work
Ru-3,8PH	D$_2$O	8.26	7.85	7.53	this work
Ru-4,7PPh	CD$_3$CN	8.57	7.89	7.71	6
Ru-3,8COOH	CD$_3$OD	8.53	7.95	7.68	7
Ru-4,7Br$_2$	CD$_3$CN	8.04	7.80	7.58	this work

[1] Signals were assigned using detailed NMR investigations (the spectra are given in Figures S4–S30 at the end of this section).

Table S5. Assignment of α–H proton signals in ^{1}H NMR spectra of $[Ru(bpy)_2(phen)]^{2+}$ complexes with asymmetrical phen ligands.

Ru-3PPh	R = C$_6$H$_4$P(O)(OEt)$_2$ R$_1$ = H
Ru-3Br	R = Br R$_1$ = H
Ru-3NHEt	R = NH(CH$_2$)$_2$OAd R$_1$ = H
Ru-3,8PHEt$_3$	R = P(O)(OEt)$_2$ R$_1$ = P(O)(OH)(OEt)

| Ru-4PPh | R = C$_6$H$_4$P(O)(OEt)$_2$ R$_1$ = H |
| Ru-4,7PHEt$_3$ | R = P(O)(OEt)$_2$ R$_1$ = P(O)(OH)(OEt) |

Ru-5PEt	R = P(O)(OEt)$_2$
Ru-5PPh	R = C$_6$H$_4$P(O)(OEt)$_2$
Ru-5Me	R = Me
Ru-5NO$_2$	R = NO$_2$
Ru-5NHEt	R = NH(CH$_2$)$_2$OAd

Complex	Solvent	H2 or H9		H22 or H23		H13 or H32		Ref.
Ru-phen [1]	MeCN	8.09	8.09	7.85	7.85	7.53	7.53	this work
Ru-3PPh	MeCN	8.19	8.12	7.93	7.84	7.70	7.58	[6]
Ru-3Br	MeCN	8.10	8.08	7.84	7.78	7.62	7.48	[8]
Ru-3NHEt	MeCN	7.50	7.85	7.84	7.82	7.66	7.55	[9]
Ru-4PPh	MeCN	8.14	8.13	7.87	7.87	7.63	7.58	[6]
Ru-5PEt	MeCN	8.18	8.14	7.83	7.82	7.57	7.52	[6]
Ru-5PPh	MeCN	8.14	8.13	7.88	7.88	7.61	7.59	[6]
Ru-5Me	MeCN	8.05	8.02	7.85	7.85	7.53	7.53	[10]
Ru-5NO$_2$	MeCN	8.22	8.27	7.82	7.82	7.55	7.55	[10]
Ru-5NHEt	MeCN	7.65	8.04	7.84	7.82	7.59	7.54	[9]
Ru-3,8PH$_1$Et$_3$	MeCN	8.28	8.07	7.93	7.89	7.61	7.59	this work
Ru-4,7PH$_1$Et$_3$	MeCN	8.19	7.99	7.82	7.81	7.55	7.53	this work

[1] Signals were assigned using ^{1}H–^{13}C HMBC experiments.

*Assignment of signals for complexes **Ru-4,7PH, RU-4PEt** and **Ru-phen***.
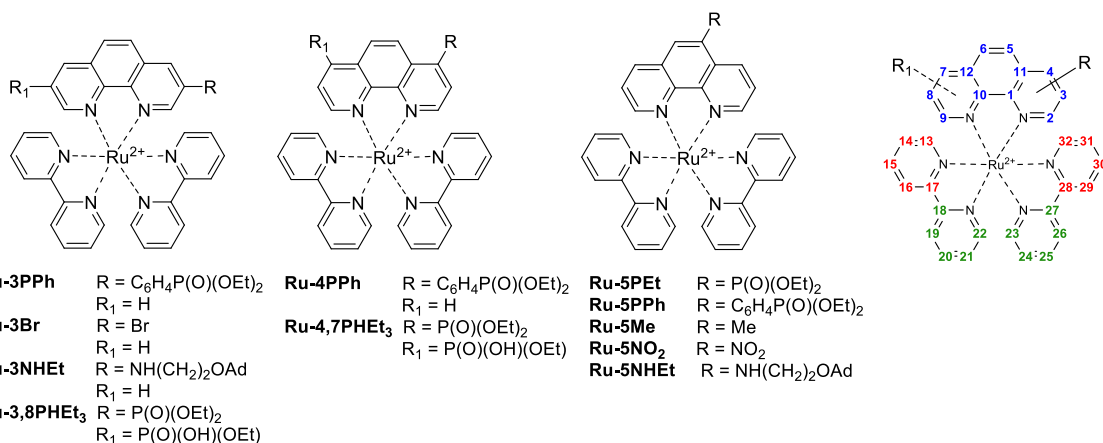
Table S6. Signal assignment in NMR spectra of **Ru-4,7PH**.

Ru-4,7PH

Assignment	Chemical shift (ppm)			J (Hz)			
	^{31}P	^{1}H	^{13}C	H–H	H–P	C–P	
1			148.0			10.5 (33) 2.3 (34)	
2		8.24	152.0	5.3	2.8	12.8	
3		7.96	127.8	5.3	13.5	7.9	
4			142.3			168.8	
5		8.84	127.6			4.5	
6		8.84	127.6			4.5	
7			142.3			168.8	
8		7.96	127.8	5.3	13.5	7.9	
9		8.24	152.0	5.3	2.8	12.8	
10			148.0			10.5 (34) 2.3 (33)	
11			130.1			9.4	
12			130.1			9.4	
13		7.86	151.5	5.7 (14) 1.5 (15)			
14		7.38	127.2	7.2 5.7 (13) 1.2			
15		8.04	137.8	7.9 7.9 1.5 (13)			
16		8.52	124.0	8.2			
17			157.0				
18			156.9				
19		8.47	124.0	8.2			
20		7.92	137.7	7.9 7.9 1.4 (22)			
21		7.13	127.0	7.3 5.7 (21) 1.2			
22		7.51	151.3	5.7 (21) 1.4 (20)			
23		7.51	151.3	5.7 (24) 1.4 (25)			
24		7.13	127.0	7.3 5.7 (23) 1.2			
25		7.92	137.7	7.9 7.9 1.4 (25)			
26		8.47	124.0	8.2			
27			156.9				
28			157.0				
29		8.52	124.0	8.2			
30		8.04	137.8	7.9 7.9 1.5 (32)			
31		7.38	127.2	7.2 5.7 (32) 1.2			
32		7.86	151.5	5.7 (31) 1.5 (32)			
33	5.4						
34	5.4						
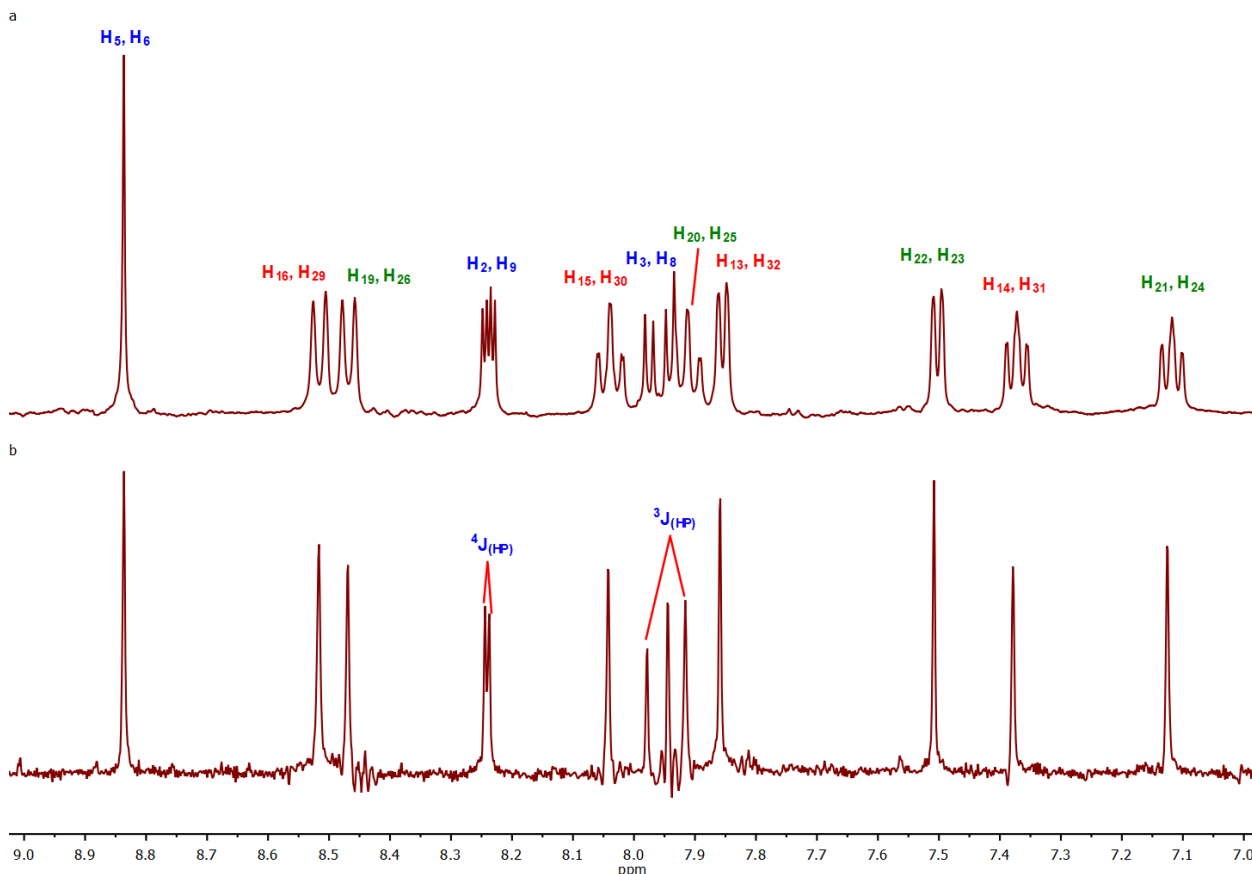
Figure S4. (a) ^{1}H NMR spectrum of **Ru-4,7PH** (400 MHz, D$_2$O, 298 K); (b) PSYCHE ^{1}H NMR spectrum of **Ru-4,7PH** (400 MHz, D$_2$O, 298 K) in the aromatic region.
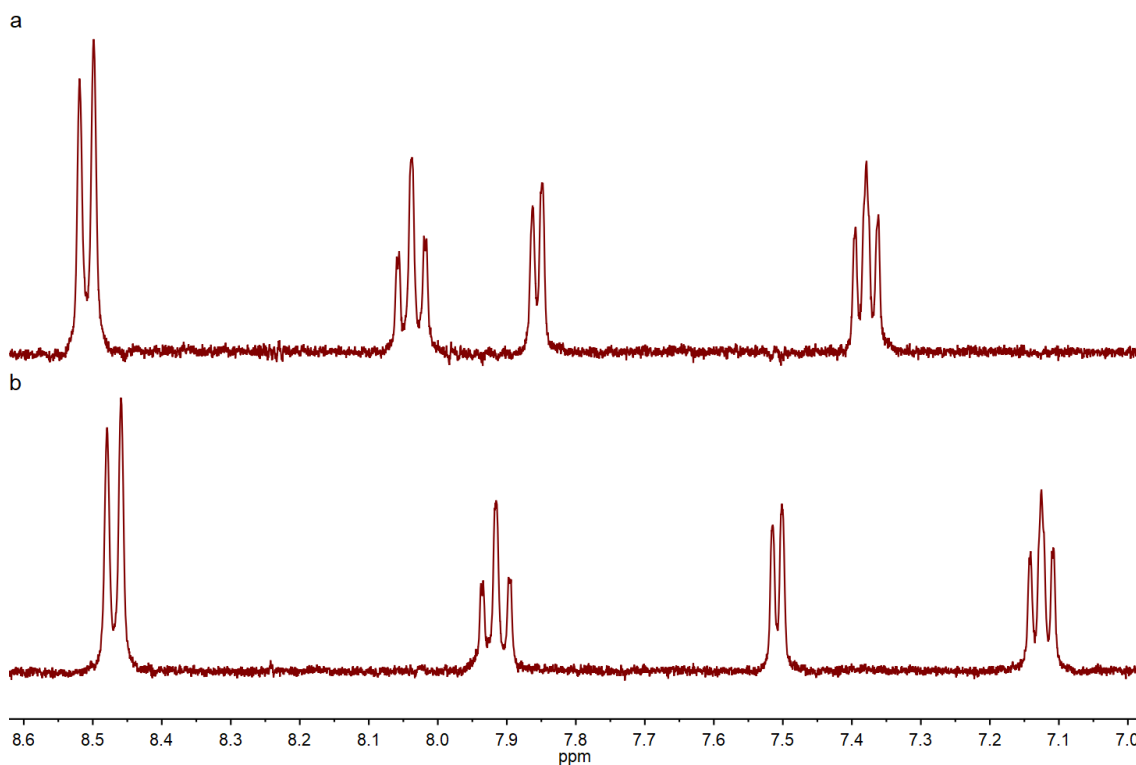
Figure S5. Partial view of selective TOCSY NMR spectra of **Ru-4,7PH** with excitation at (a) δ_H 7.38 ppm, (b) δ_H 7.13 ppm (400 MHz, D$_2$O, 298 K).
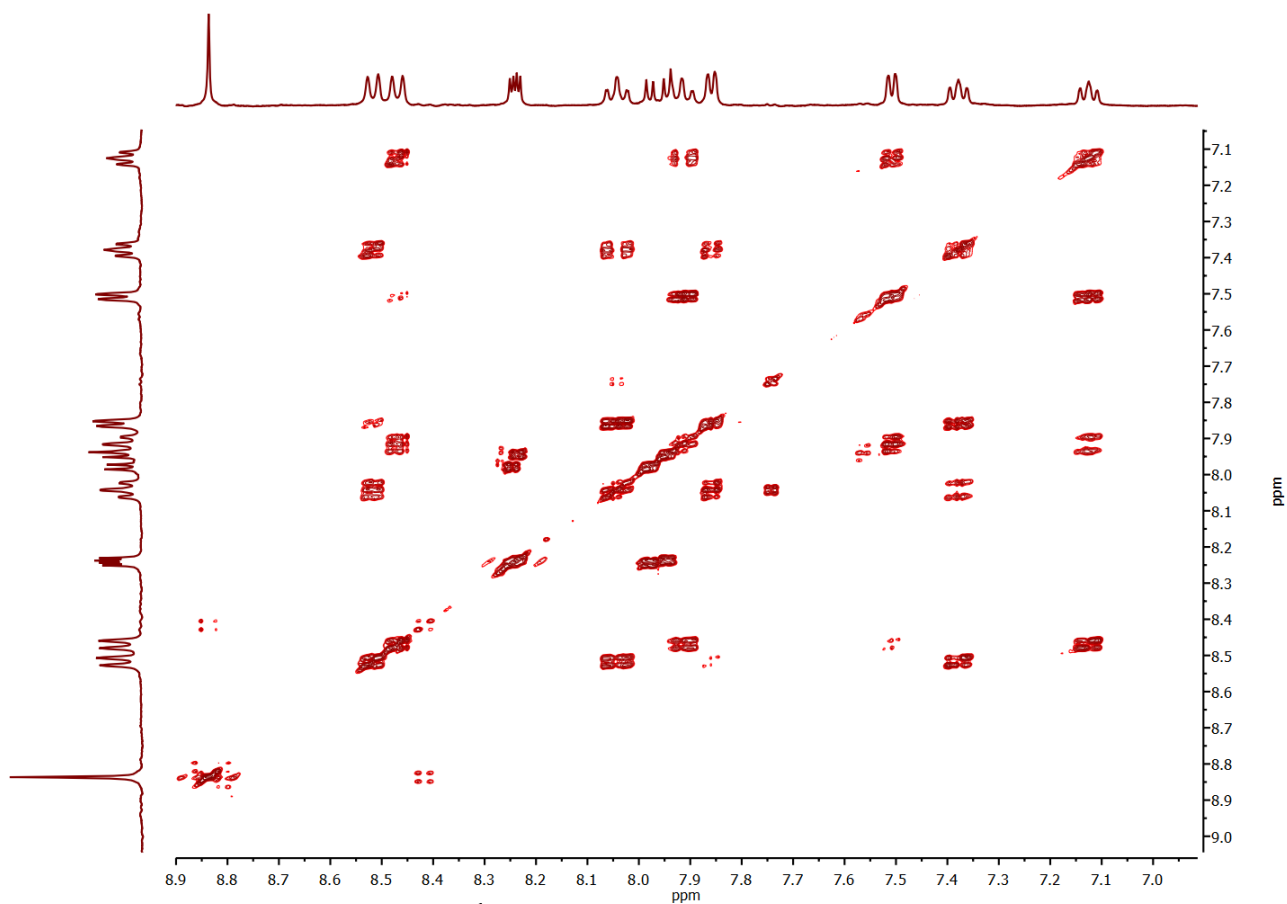
Figure S6. Aromatic region of COSY ^{1}H spectrum of **Ru-4,7PH** (400 MHz, D$_2$O, 298 K).
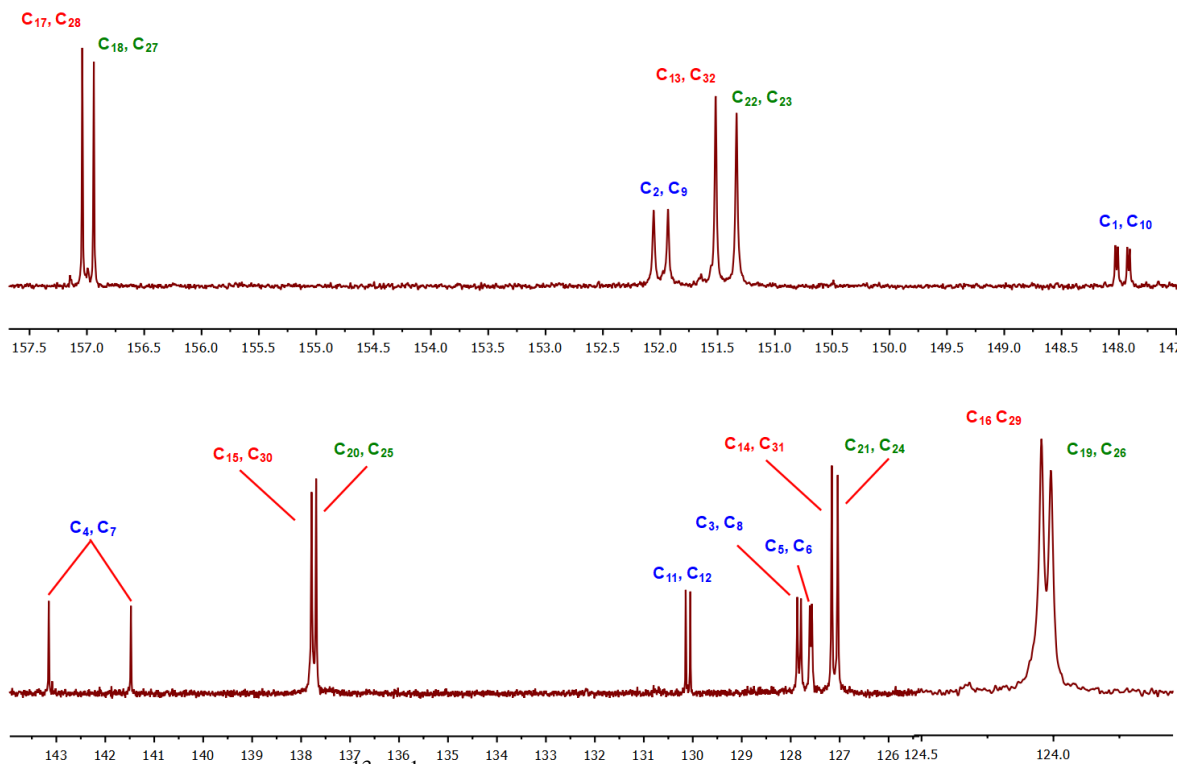
Figure S7. Aromatic region of ^{13}C{^{1}H} NMR spectrum of **Ru-4,7PH** (100 MHz, D$_2$O, 298 K).
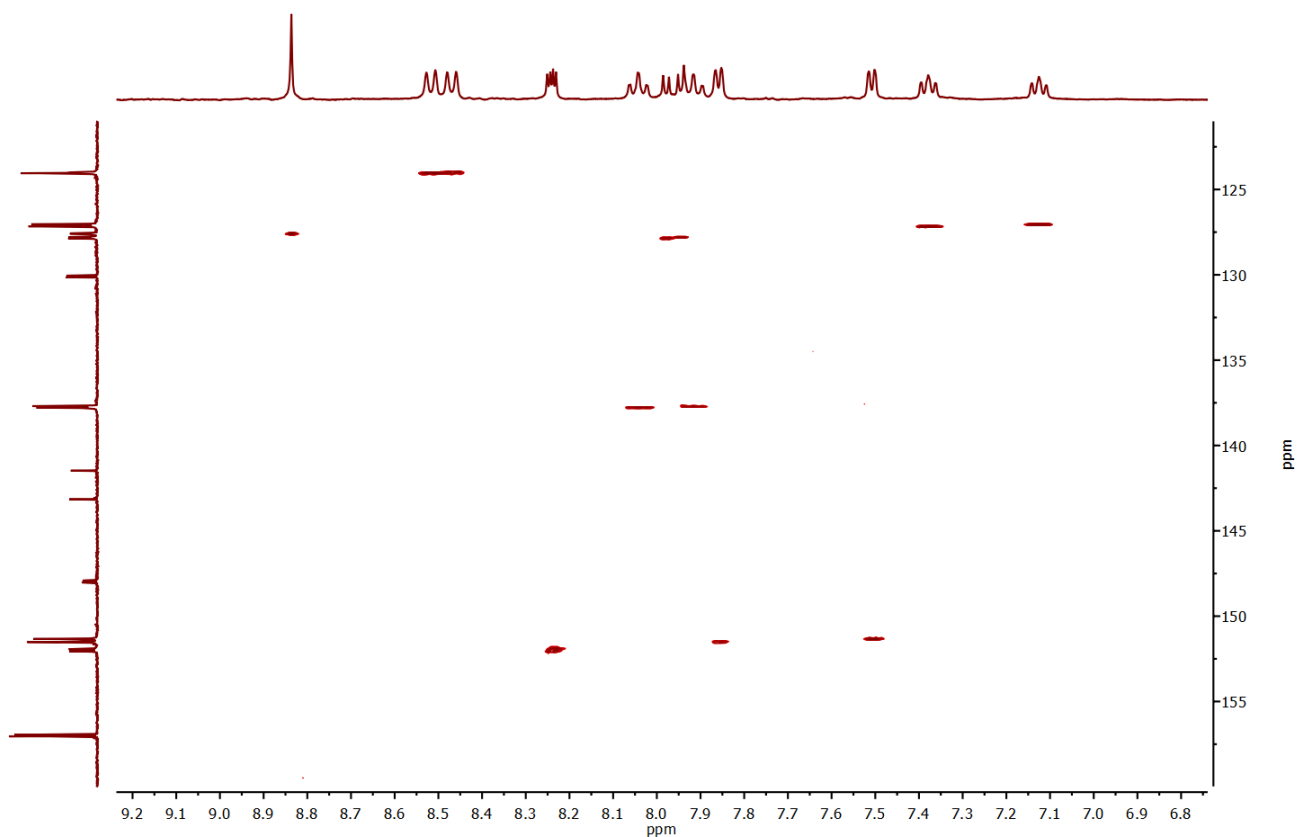
Figure S8. Aromatic region of gHSQCAD spectrum of **Ru-4,7PH** (400 MHz, D$_2$O, 298 K).
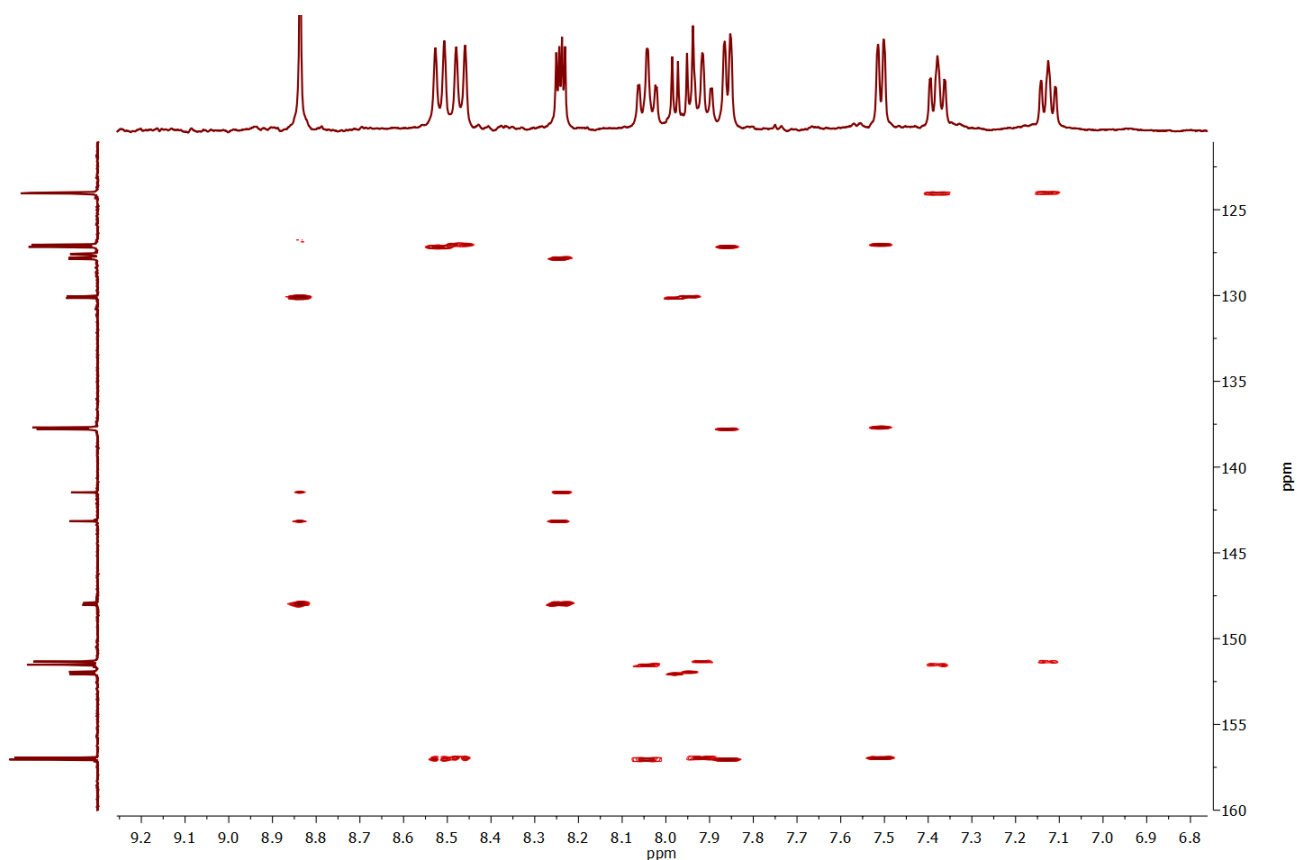
Figure S9. Aromatic region of gHMBCAD spectrum of **Ru-4,7PH** (400 MHz, D$_2$O, 298 K, $J = 8$ Hz).
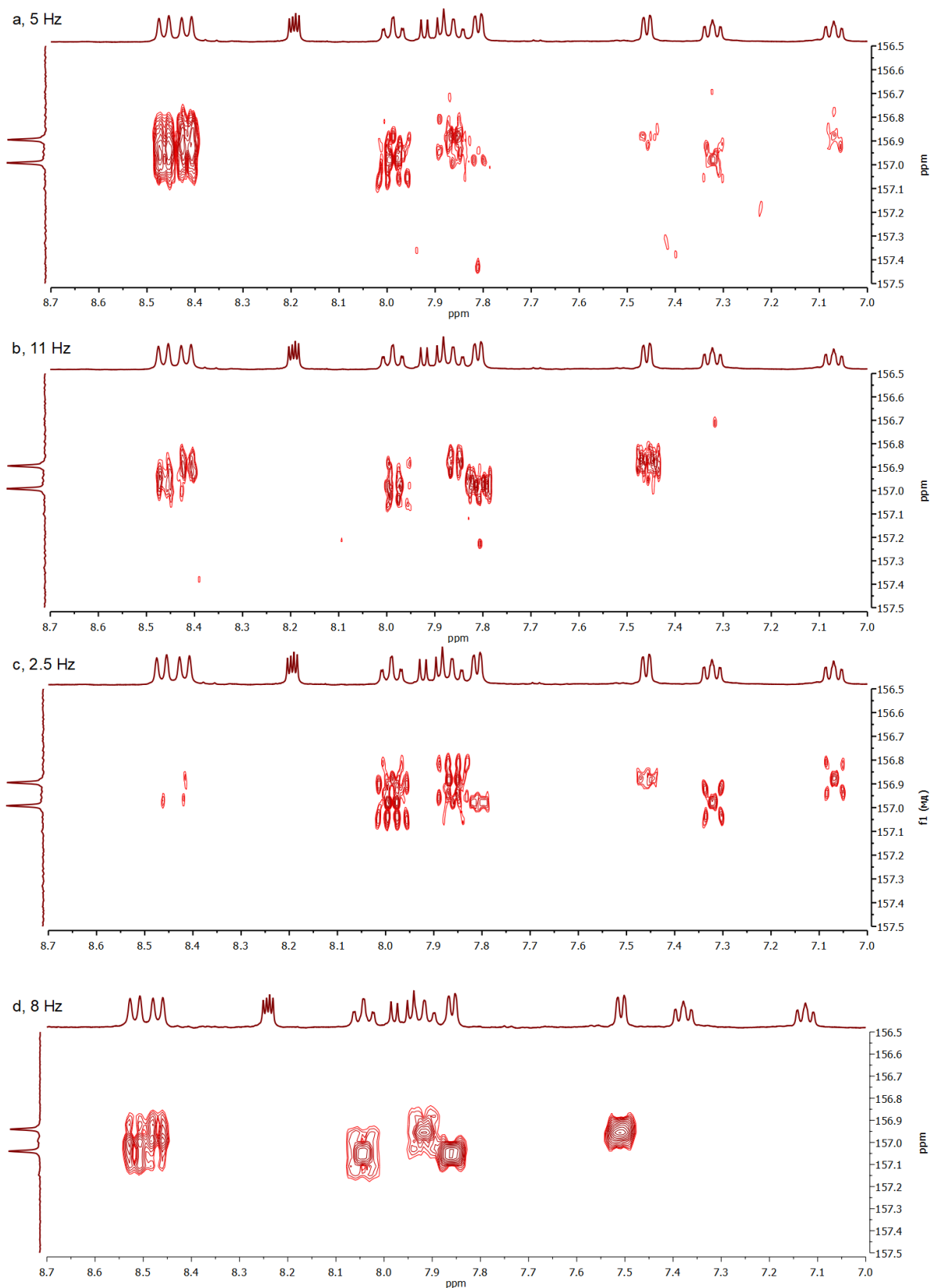
Figure S10. Partial view of gHMBCAD spectrum of **Ru-4,7PH** recorded with different values of J (a) $J = 5$ Hz, (b) $J = 11$ Hz, (c) $J = 2.5$ Hz, (d) $J = 8$ Hz (400 MHz, D$_2$O, 298 K).
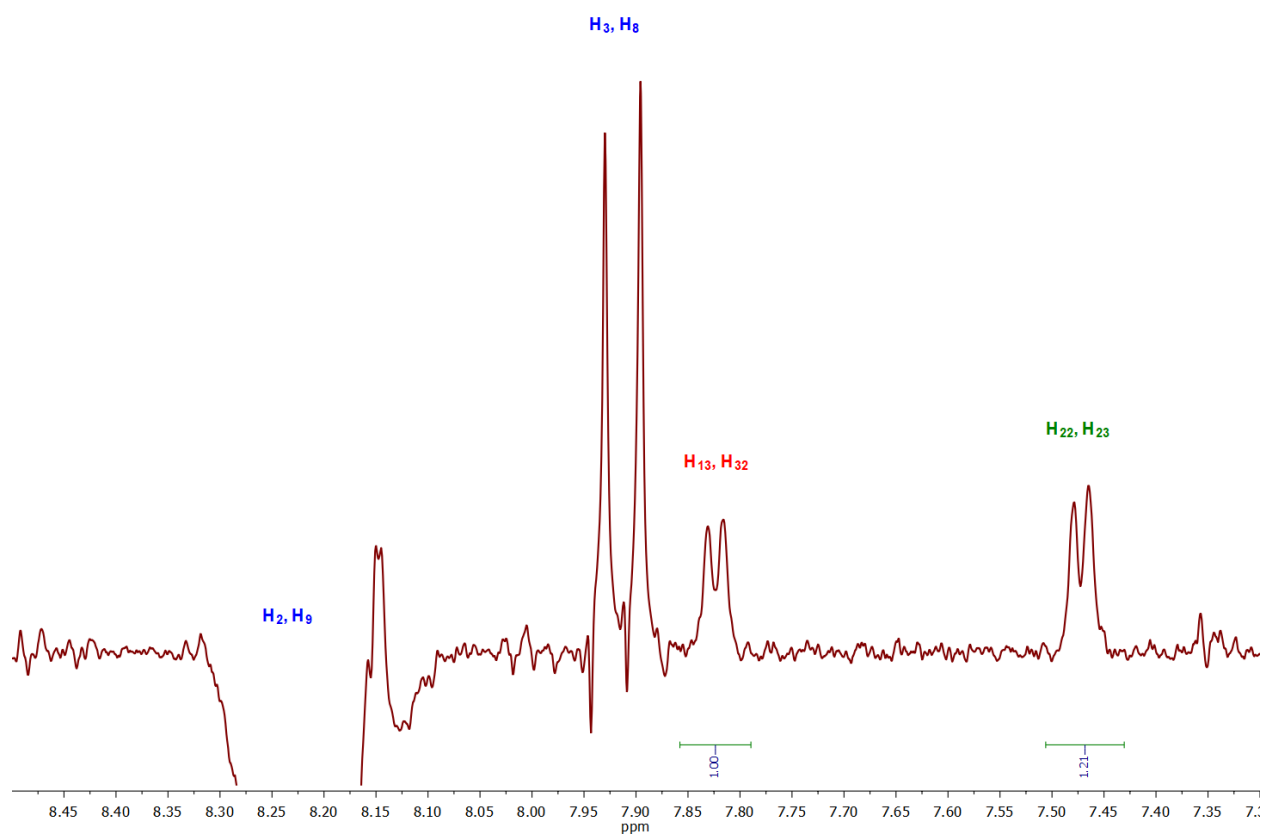
Figure S11. GEMSTONE NOESY spectrum of **Ru-4,7PH** recorded with excitation at δ_H 8.20 ppm (400 MHz, D_2O, 298 K).

Table S7. Signal assignment in NMR spectra of **Ru-4,7PEt**.
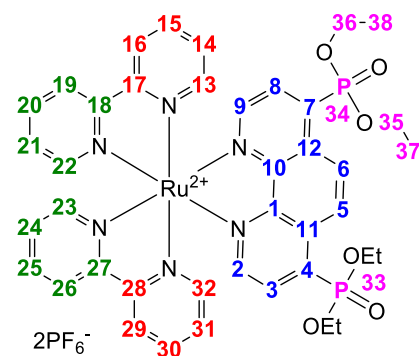
Assignment	Chemical shift (ppm)			J (Hz)				
	³¹P	¹H	¹³C	H–H			H–P	C–P
1			149.1					11.8 (33) 2.6 (34)
2		8.29	153.8	5.3			2.8	13.8
3		8.07	131.0	5.3			14.7	7.9
4			136.2					183.2
5		8.88	128.6					4.0 (33) 1.0 (34)
6		8.88	128.6					4.0 (34) 1.0 (33)
7			136.2					183.2
8		8.07	131.0	5.3			14.7	7.9
9		8.29	153.8	5.3			2.8	13.8
10			149.1					11.8 (34) 2.6 (33)
11			131.1					10.2
12			131.1					10.2
13		7.52	152.6	5.6 (14)	1.5 (15)	0.7 (16)		
14		7.24	128.5	7.7 (15)	5.6 (13)	1.3 (16)		
15		8.02	139.1	8.3 (16)	7.7 (14)	1.5 (13)		
16		8.51	125.3	8.3 (15)	1.3 (14)	0.7 (13)		
17			157.6					
18			157.8					
19		8.56	125.3	8.3 (20)	1.3 (21)	0.7 (22)		
20		8.13	139.2	8.3 (19)	7.7 (21)	1.5 (22)		
21		7.48	128.6	7.7 (20)	5.6 (22)	1.3 (29)		
22		7.80	153.1	5.6 (21)	1.5 (20)	0.7 (19)		
23		7.80	153.1	5.6 (24)	1.5 (25)	0.7 (26)		
24		7.48	128.6	7.7 (25)	5.6 (23)	1.3 (26)		
25		8.13	139.2	8.3 (26)	7.7 (24)	1.5 (23)		
26		8.56	125.3	8.3 (25)	1.3 (24)	0.7 (23)		
27			157.8					
28			157.6					
29		8.51	125.3	8.3 (30)	1.3 (31)	0.7 (32)		
30		8.02	139.1	8.3 (29)	7.7 (31)	1.5 (32)		
31		7.24	128.5	7.7 (30)	5.6 (32)	1.3 (29)		
32		7.52	152.6	5.6 (31)	1.5 (30)	0.7 (29)		
33	11.4							
34	11.4							
35		1.331	16.5	7.1 (37)			8.7	6.2
36		1.326	16.5	7.1 (38)			8.7	6.2
37		4.23(2)	64.6	7.1 (35)			0.6	5.9
38		4.23(2)	64.5	7.1 (36)			0.6	5.9
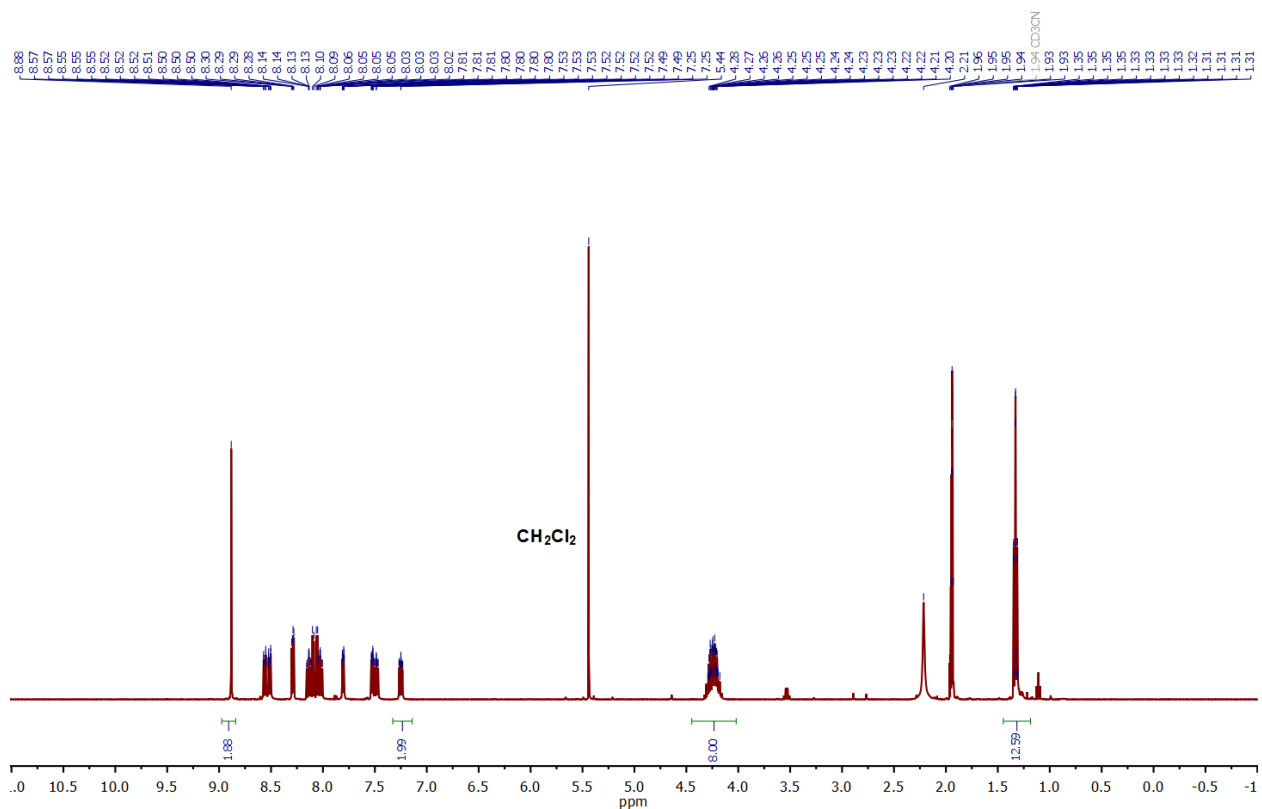
Figure S12. ^{1}H NMR spectrum of **Ru-4,7PEt** (400 MHz, CD$_3$CN, 300K).
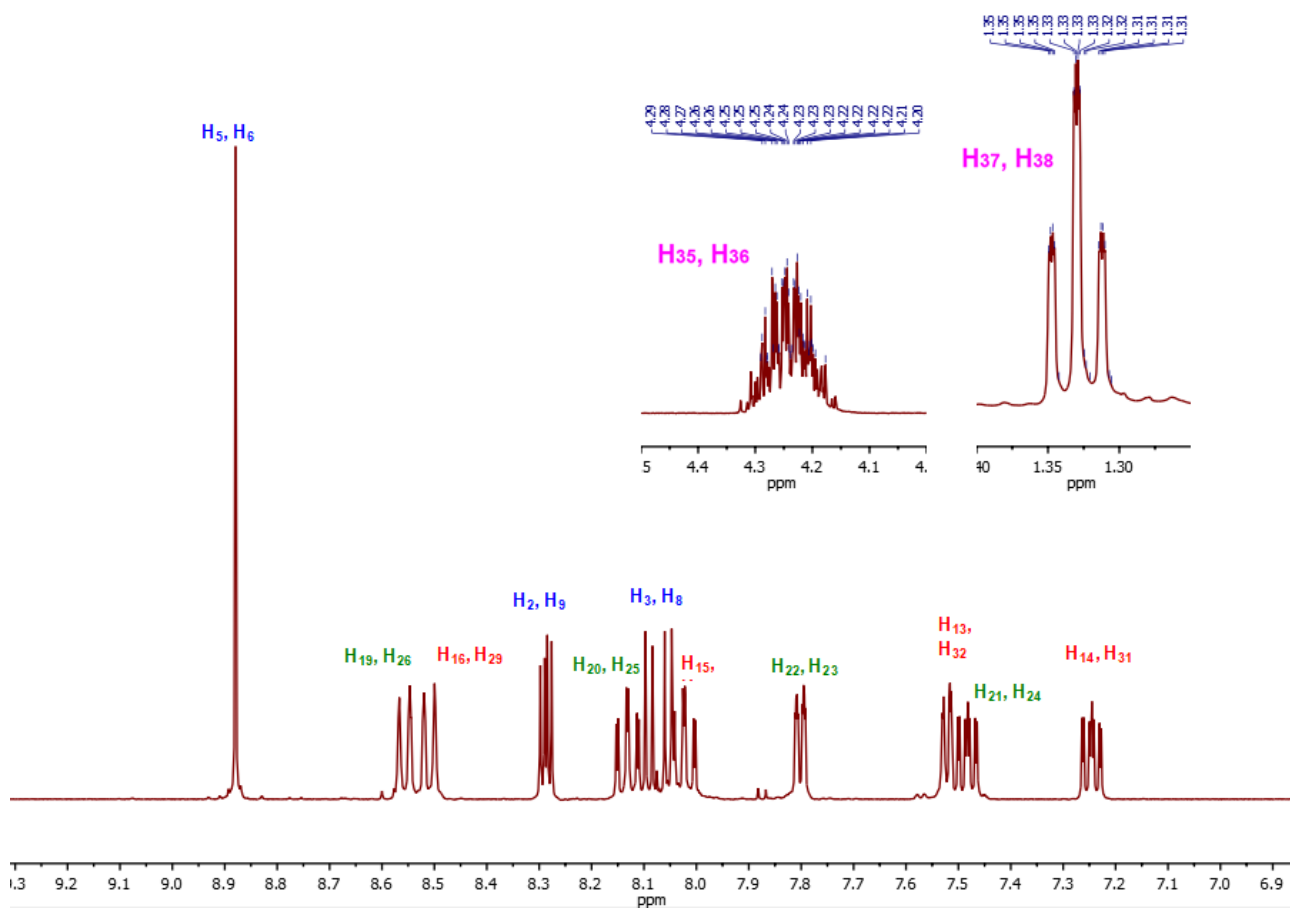
Figure S13. Aromatic region of ^{1}H NMR spectrum of **Ru-4,7PEt** (400 MHz, CD$_3$CN, 300K).
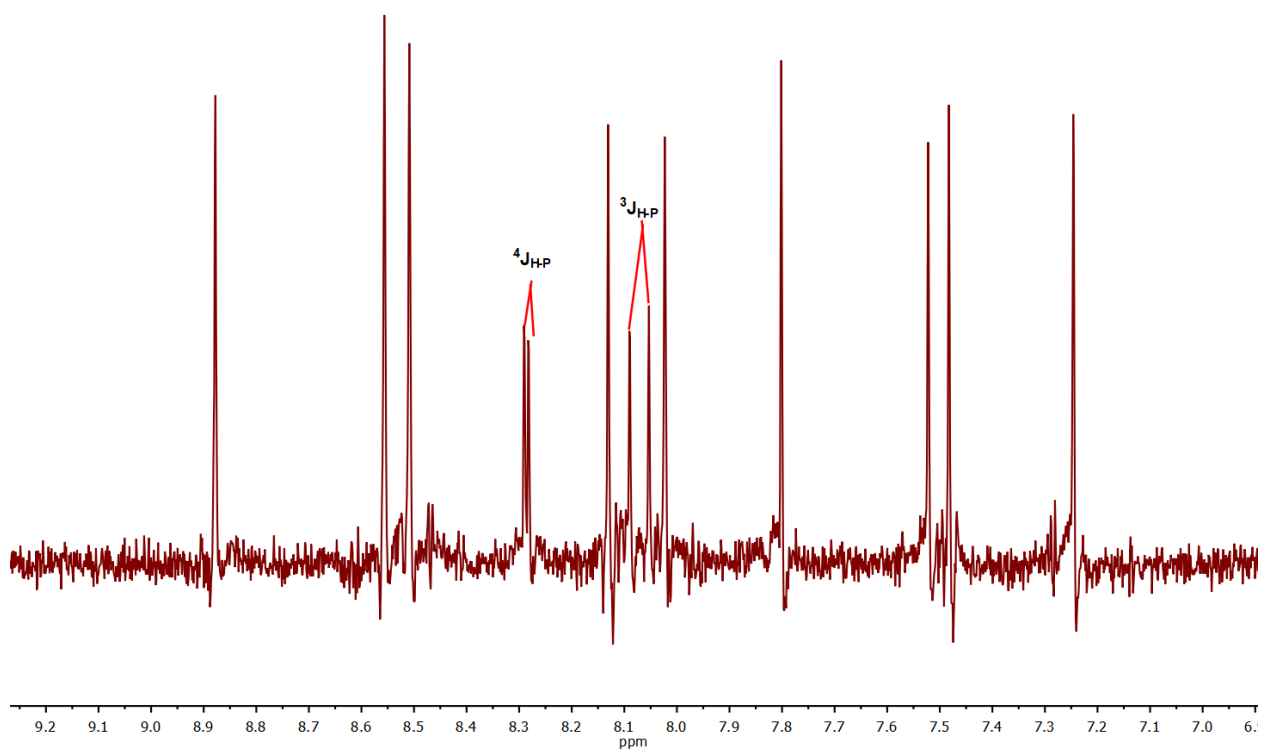
Figure S14. Aromatic region of PSYCHE ^{1}H NMR spectrum of **Ru-4,7PEt** (400 MHz, CD$_3$CN, 300K).
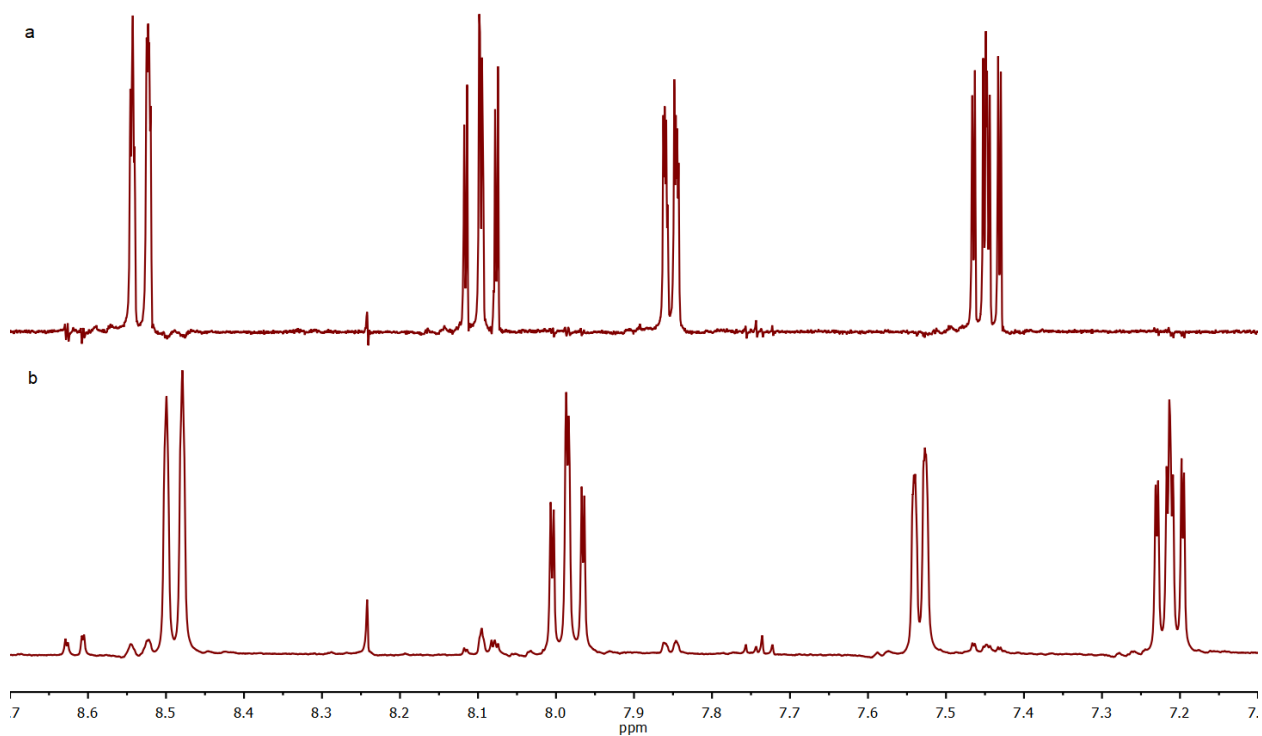
Figure S15. Selective ^{1}H TOCSY spectra of **Ru-4,7PEt** recorded with excitation at δ_H 7.21 ppm (a), 7.44 ppm (b) (400 MHz, CD$_3$CN, 300K).
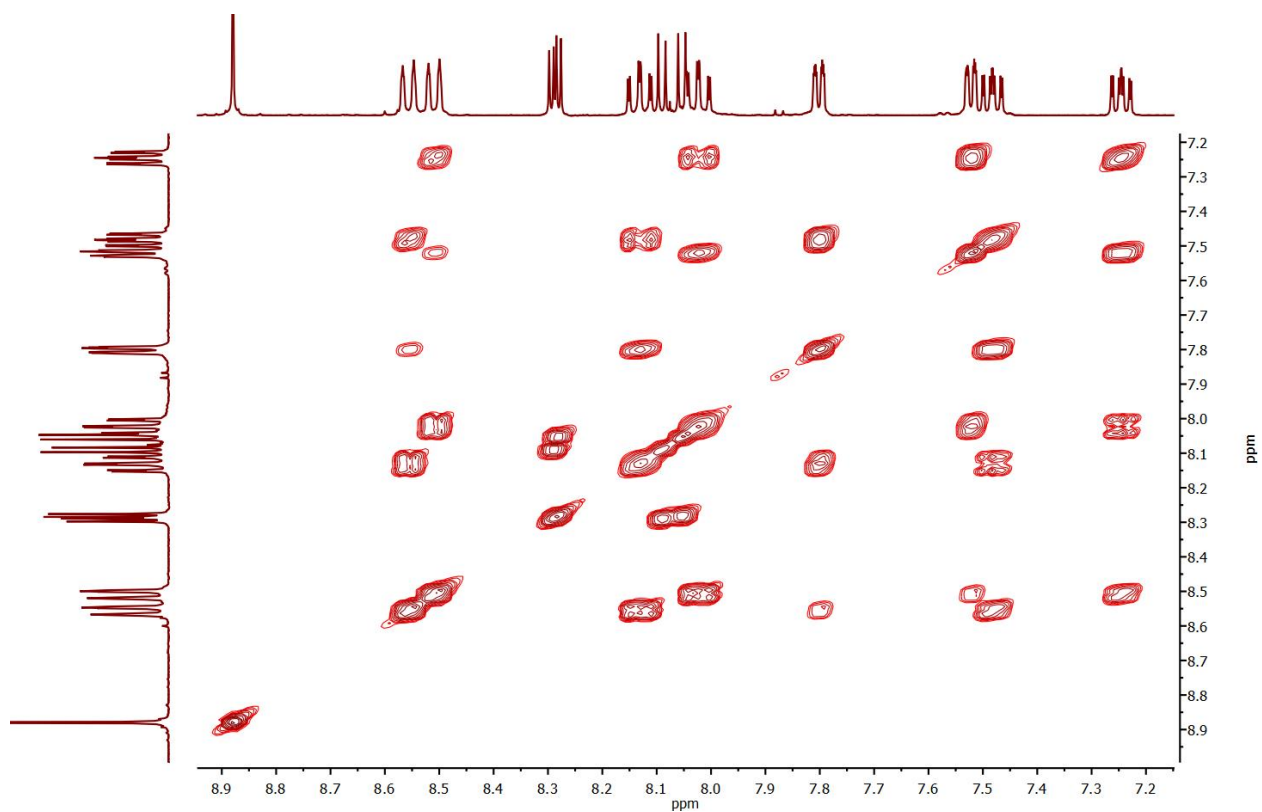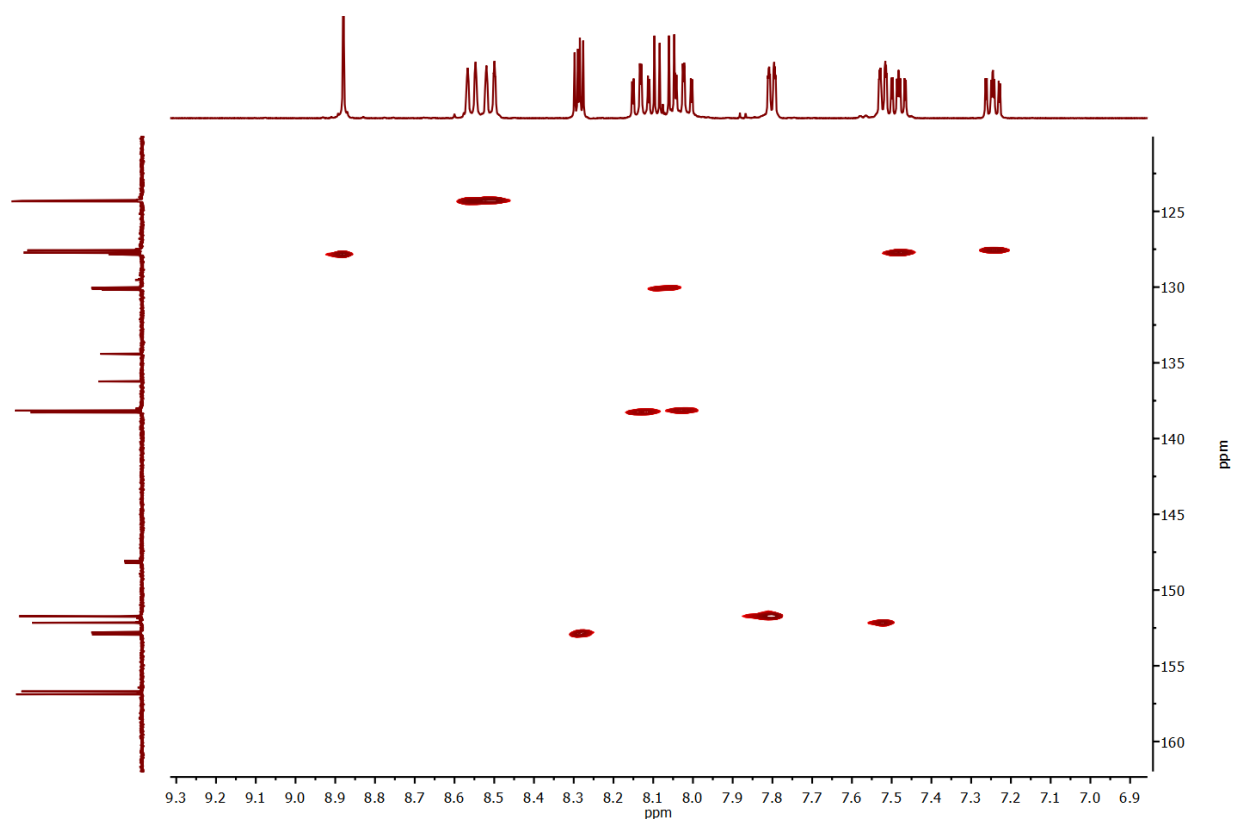
S21

Figure S16. $^{13}C\{^1H\}$ NMR spectrum of **Ru-4,7PEt** (100 MHz, CD$_3$CN, 300K).

Figure S17. Aromatic region of $^{13}C\{^1H\}$ NMR spectrum of **Ru-4,7PEt** (100 MHz, CD$_3$CN, 300K).
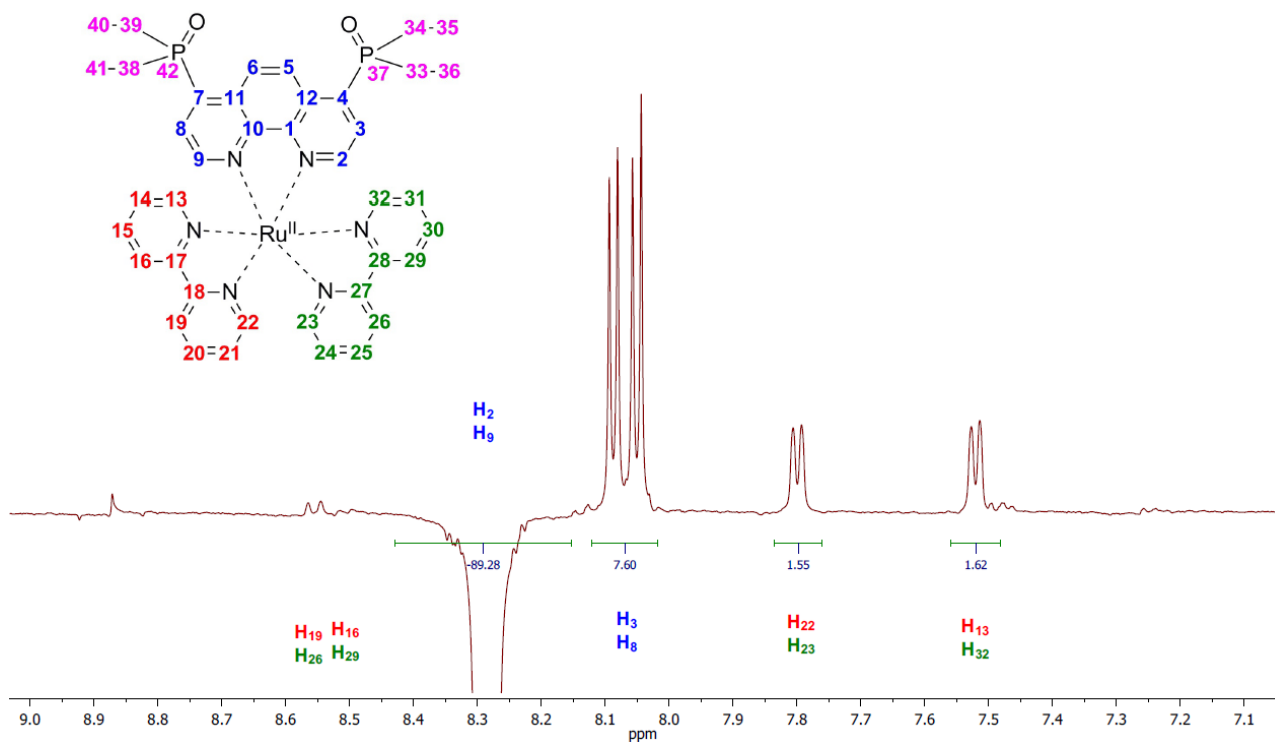
Figure S18. Partial view of GEMSTONE NOESY spectrum of **Ru-4,7PEt** recorded with the excitation at δ_H 8.29 ppm (400 MHz, D$_2$O, 298 K).
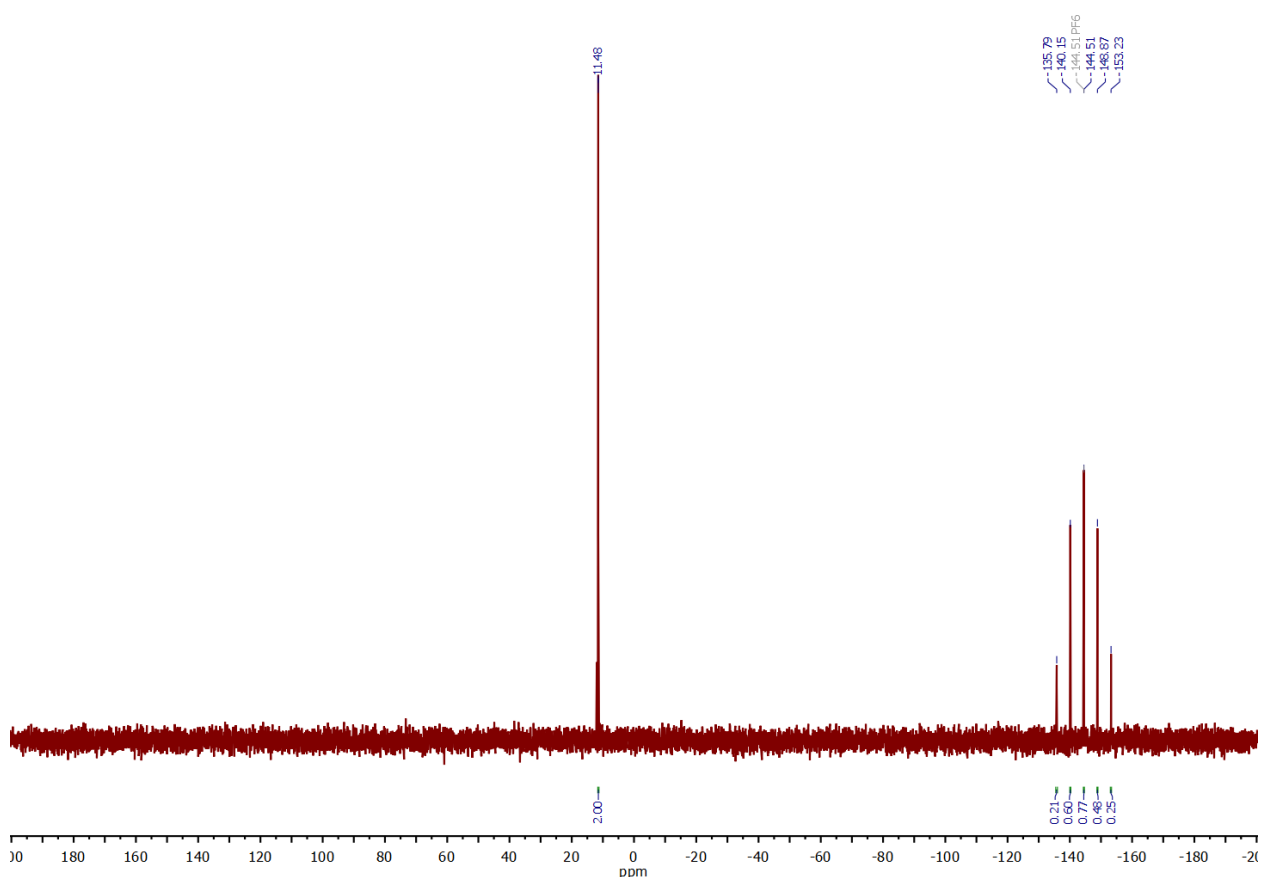
Figure S19. ^{31}P{^{1}H} NMR spectrum of **Ru-4,7PEt**. (161.9 MHz, CD$_3$CN, 300K).

Figure S20. Aromatic region of gCOSY ^{1}H NMR spectrum of **Ru-4,7PEt** (CD$_3$CN, 300K).

Figure S21. Aromatic region of gHSQCAD NMR spectrum of **Ru-4,7PEt** (400 MHz, CD$_3$CN, 300K).
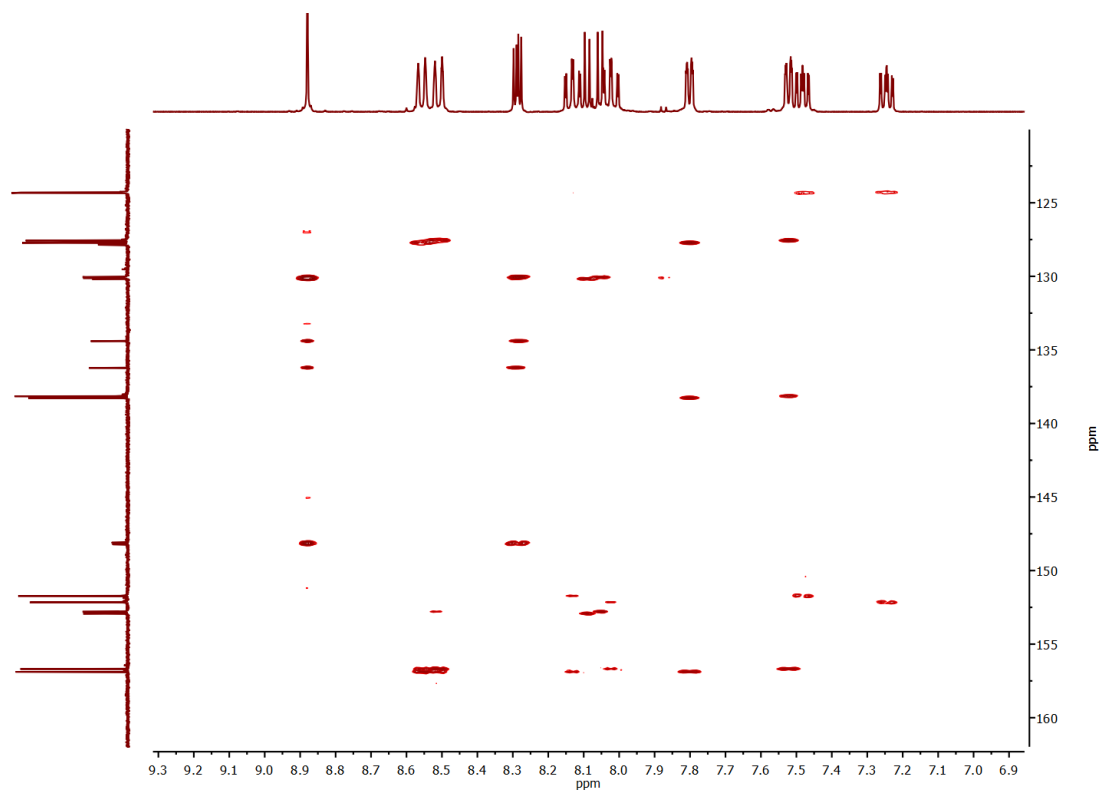
Figure S22. Aromatic region of gHMBCAD NMR spectrum of **Ru-4,7PEt**, recorded for $J = 8$ Hz. (400 MHz, CD$_3$CN, 300K).
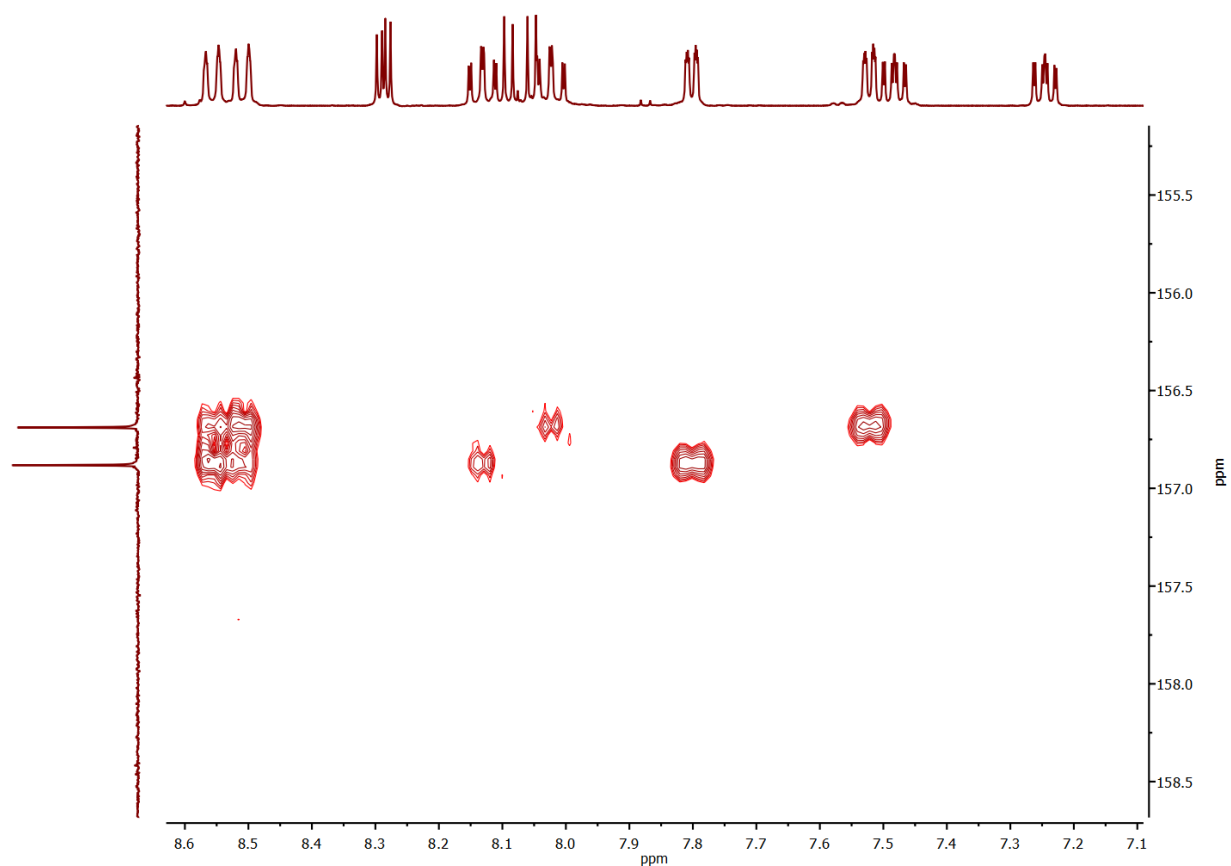
Figure S23. Partial view of gHMBCAD NMR spectrum of **Ru-4,7PEt** (400 MHz, CD$_3$CN, $J = 8$ Hz, 300K).

Table S8. Signal assignment in NMR spectra of **Ru-phen**.
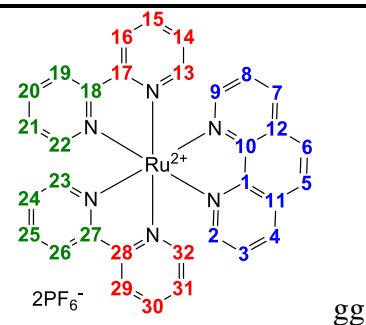
Assignment	Chemical shift (ppm)		J (Hz)		
	^{1}H	^{13}C	H–H		
1		148.4			
2	8.09	153.4	5.3 (3)	1.3 (4)	
3	7.74	132.0	8.3 (4)	5.3 (2)	
4	8.62	137.7	8.3 (3)	1.3 (2)	
5	8.24	128.9			
6	8.24	128.9			
7	8.62	137.7	8.3 (8)	1.3 (9)	
8	7.74	132.0	8.3 (7)	5.3 (9)	
9	8.09	153.4	5.3 (8)	1.3 (7)	
10		148.4			
11		131.1			
12		131.1			
13	7.54	152.7	5.6 (14)	1.5 (15)	0.8 (16)
14	7.22	128.2	7.7 (15)	5.6 (13)	1.3 (16)
15	7.99	138.5	8.2 (16)	7.7 (14)	1.5 (13)
16	8.49	125.0	8.2 (15)	1.3 (14)	0.8 (13)
17		157.9			
18		158.2			
19	8.53	125.1	8.3 (20)	1.3 (21)	0.8 (22)
20	8.10	138.7	8.3 (19)	7.7 (21)	1.5 (22)
21	7.45	128.4	7.7 (20)	5.6 (22)	1.3 (19)
22	7.85	152.9	5.6 (21)	1.5 (20)	0.8 (19)
23	7.85	152.9	5.6 (24)	1.5 (25)	0.8 (26)
24	7.45	128.4	7.7 (25)	5.6 (23)	1.3 (26)
25	8.10	138.7	8.3 (26)	7.7 (24)	1.5 (23)
26	8.53	125.1	8.3 (25)	1.3 (24)	0.8 (23)
27		158.2			
28		157.9			
29	8.49	125.0	8.2 (30)	1.3 (31)	0.8 (32)
30	7.99	138.5	8.2 (29)	7.7 (31)	1.5 (32)
31	7.22	128.2	7.7 (30)	5.6 (32)	1.3 (29)
32	7.54	152.7	5.6 (31)	1.5 (30)	0.8 (29)
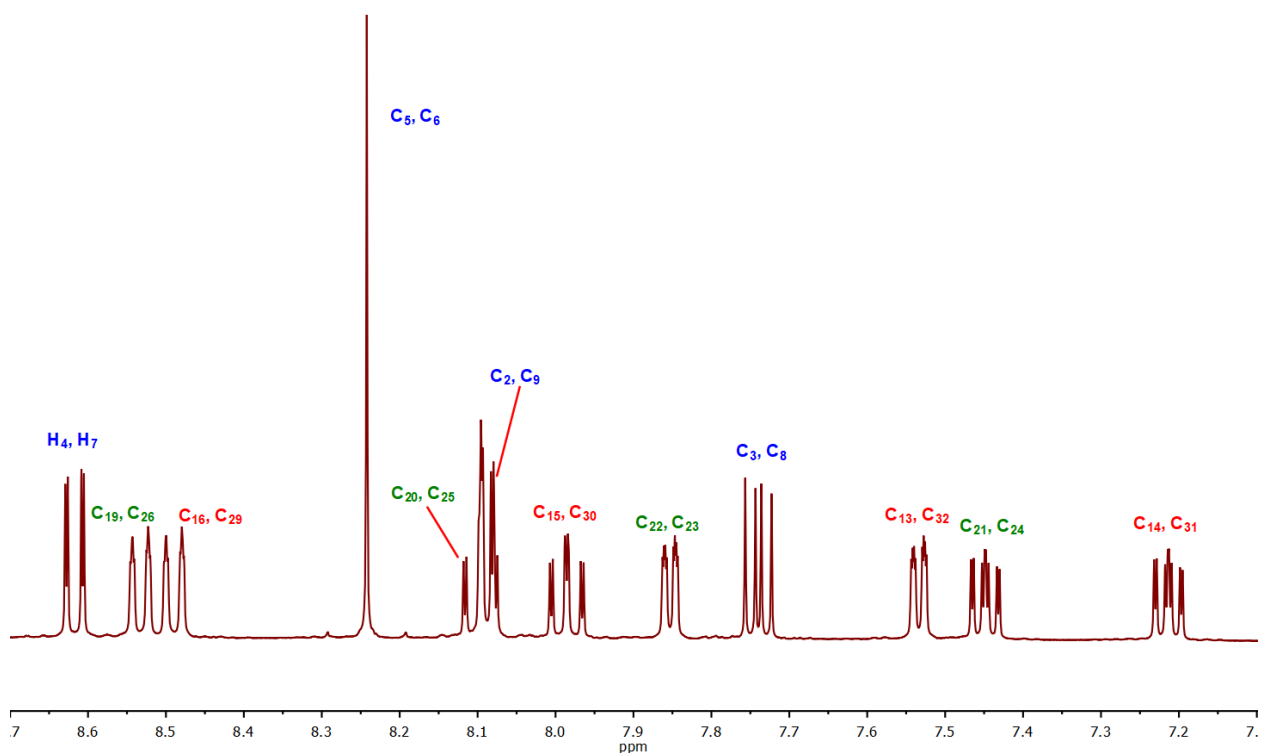
Figure S24. ^{1}H NMR spectrum of **Ru-phen** (400 MHz, CD$_3$CN, 300 K).
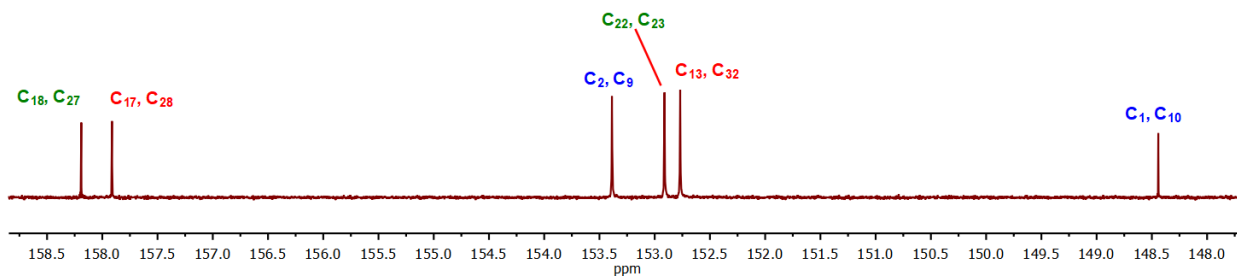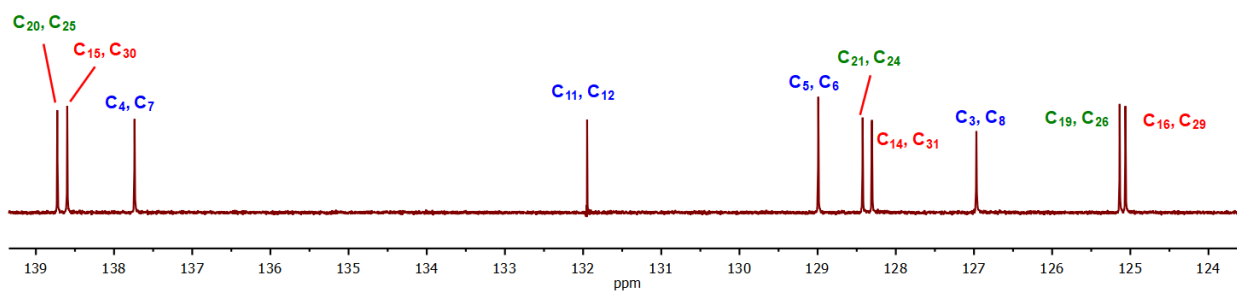
Figure S25. ^{13}C{^{1}H} NMR spectrum of **Ru-phen** (100 MHz, CD$_3$CN, 300 K).
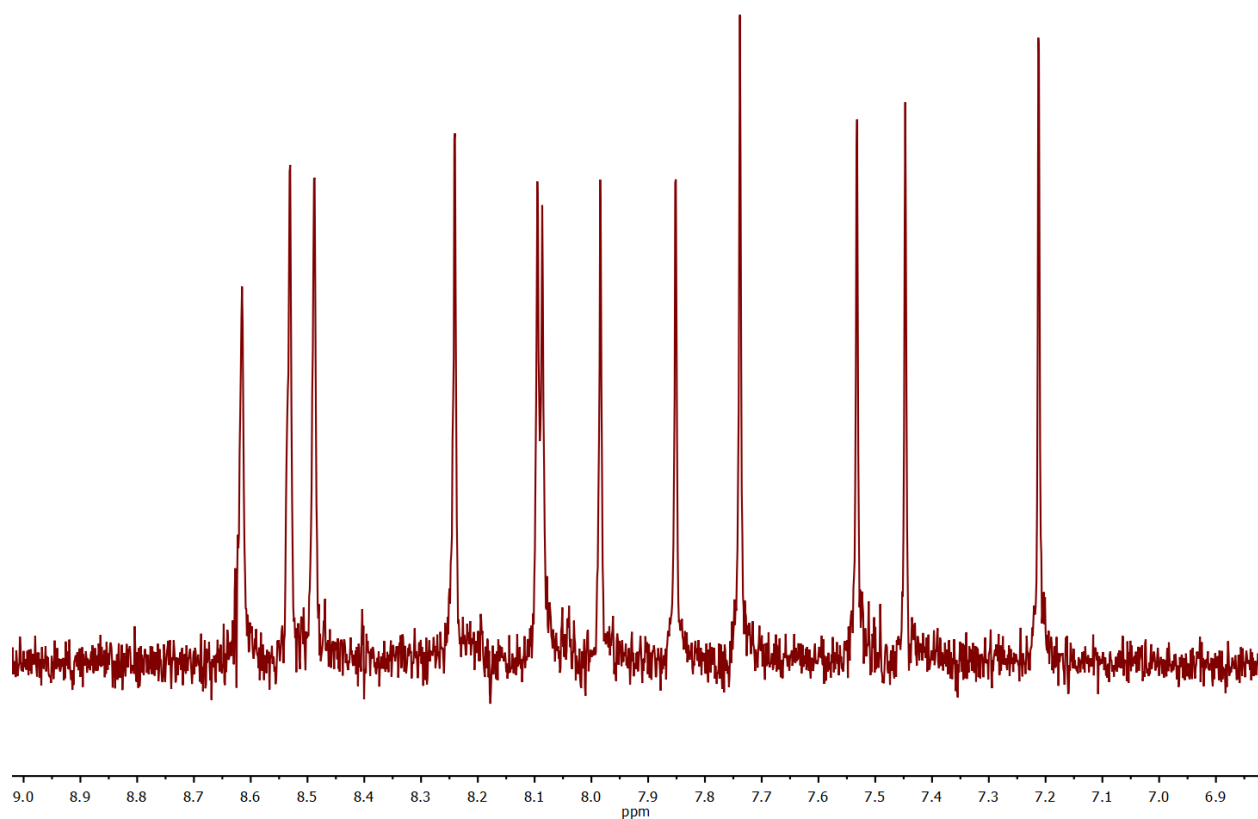
Figure S26. Aromatic region of PSYCHE ^{1}H NMR spectrum of **Ru-phen** (400 MHz, CD$_3$CN, 300 K).
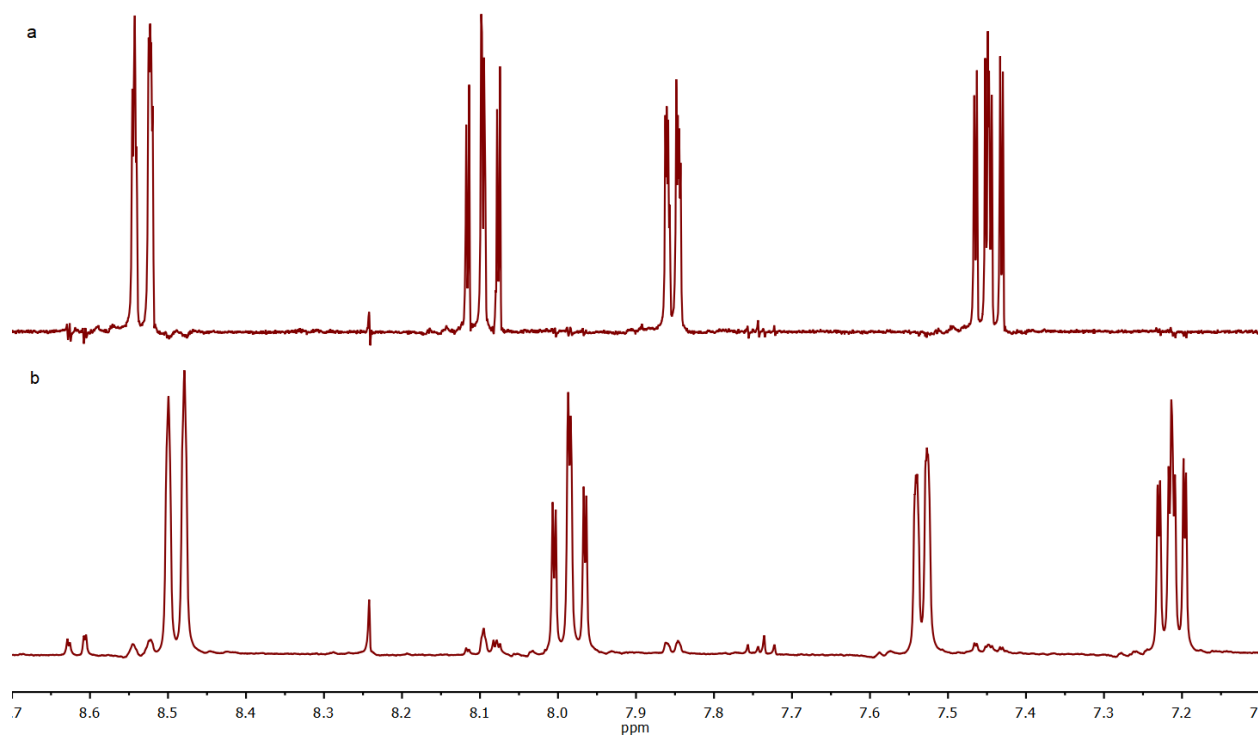
Figure S27. Selective ^{1}H TOCSY spectra of **Ru-phen** recorded with excitation at δ_H 7.21 ppm (a), and δ_H 7.44 ppm (b) (400 MHz, CD$_3$CN, 300 K).
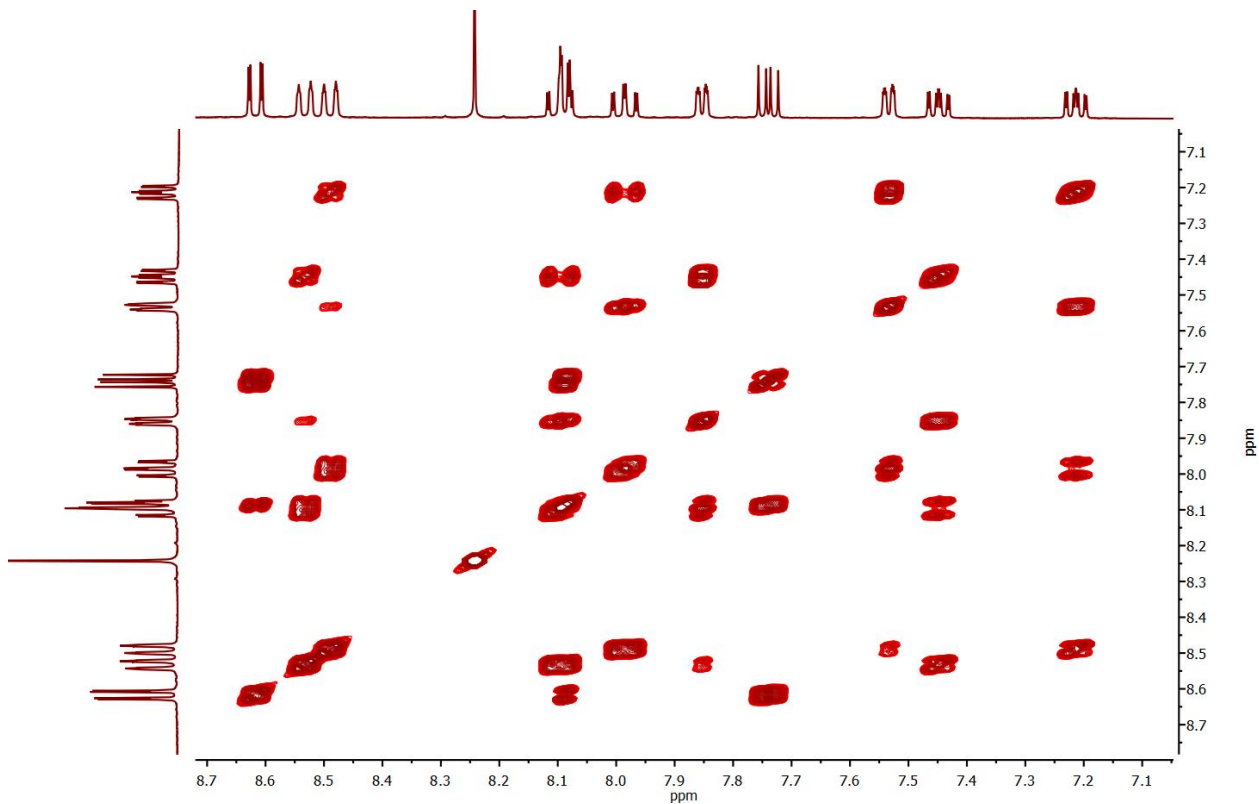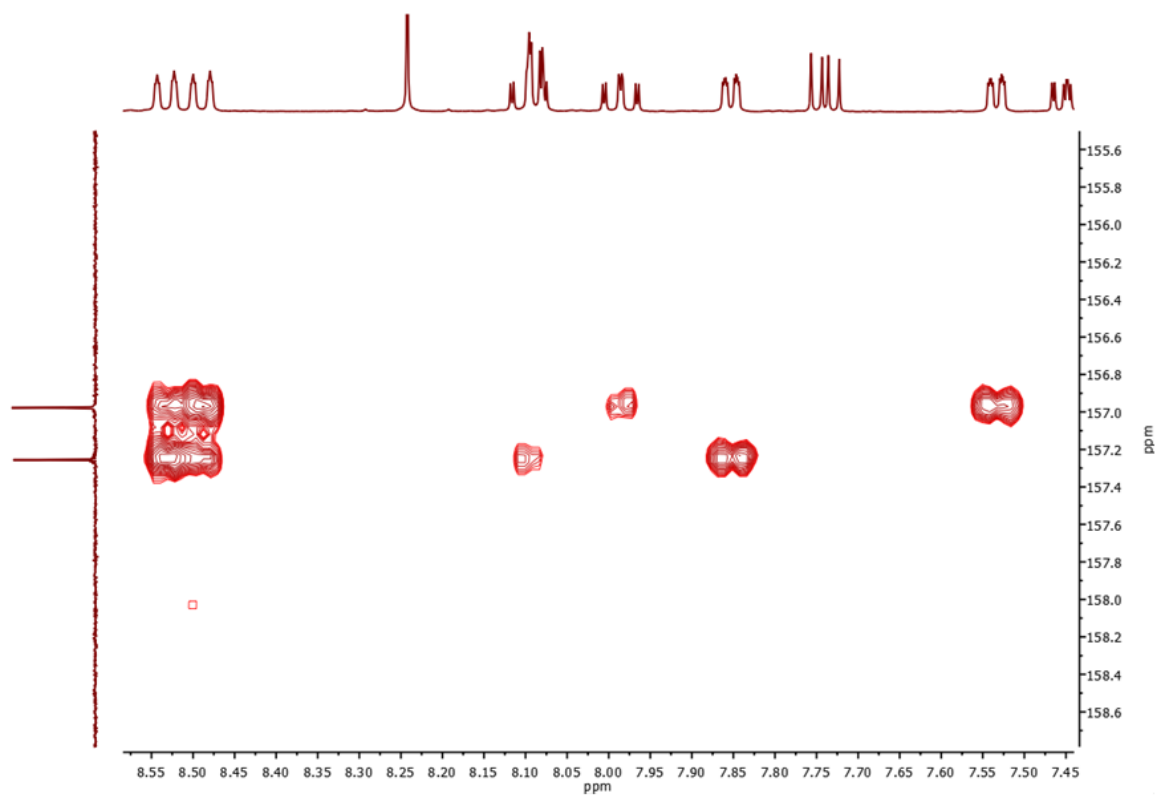
Figure S28. gCOSY ^{1}H NMR spectrum of **Ru-phen** (400 MHz, CD$_3$CN, 300K).
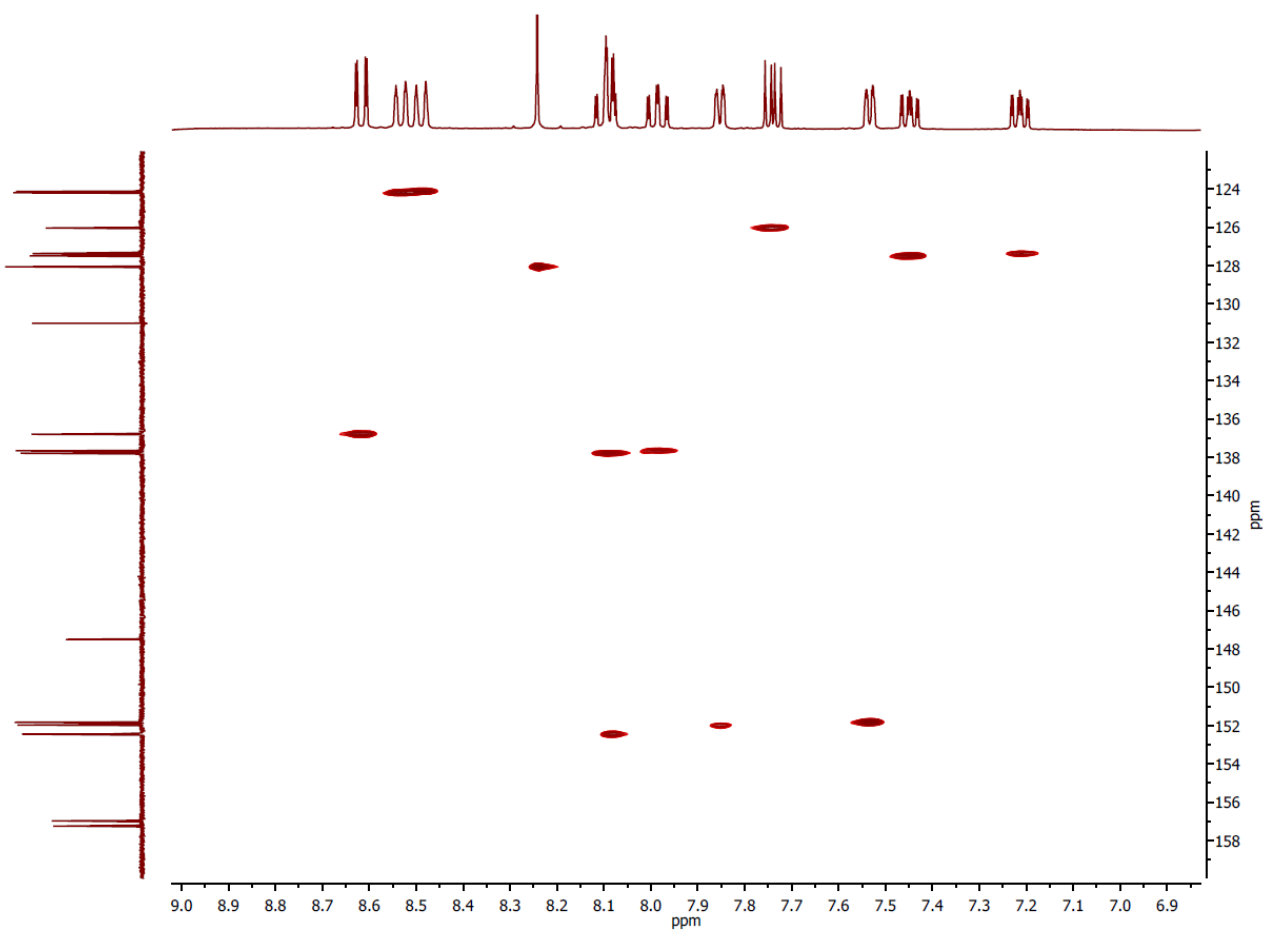
Figure S29. gHSQCAD NMR spectrum of **Ru-phen** (400 MHz, CD$_3$CN, 300K).
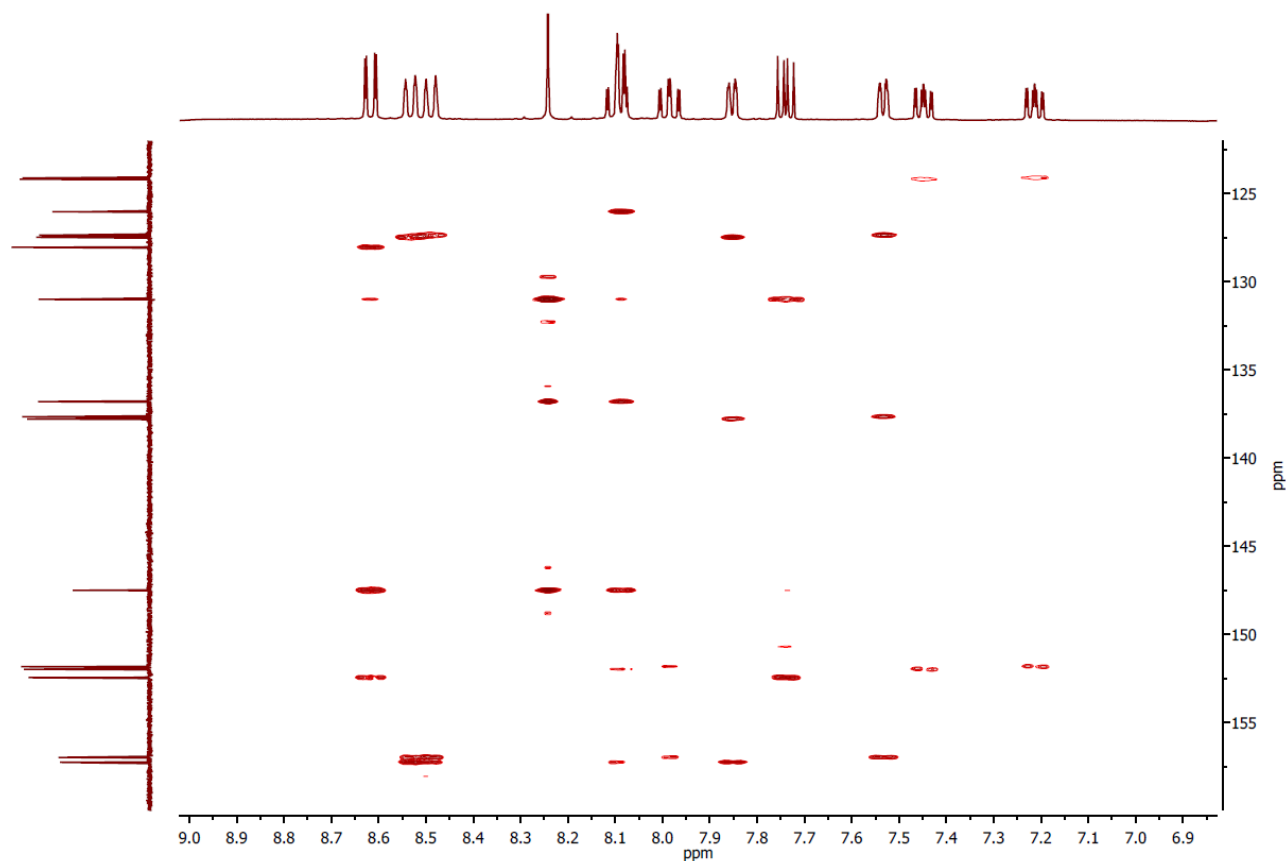
Figure S30. gHMBCAD NMR spectrum of **Ru-phen** (400 MHz, CD₃CN, 300K, J = 8 Hz).

Figure S31. Partial view of gHMBCAD NMR spectrum of **Ru-phen** (400 MHz, CD₃CN, 300K, J = 8 Hz).

7. Visible light photoredox-catalyzed functionalization of tertiary amines

Photoreactor setup
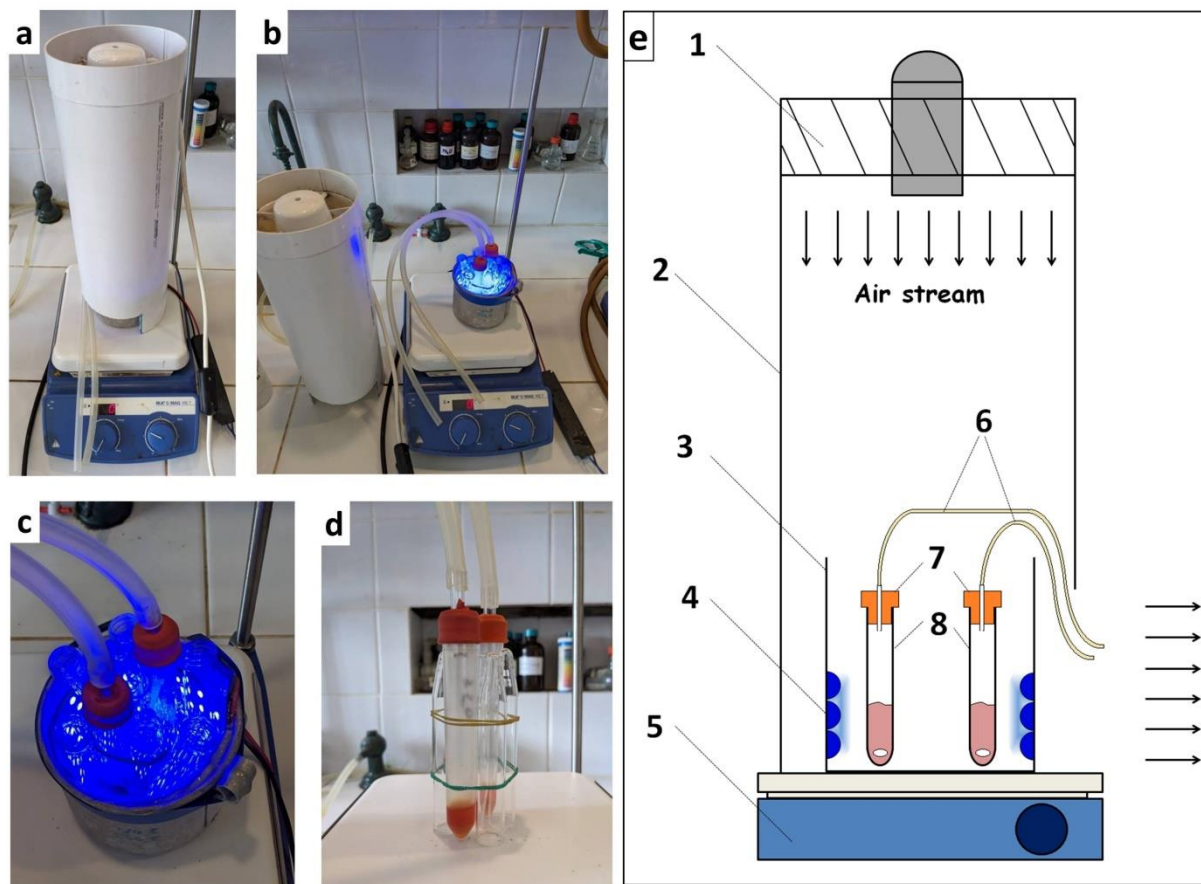
Figure S32. Homemade photoreactor setup: **a** – front view of the photoreactor; **b, c** – reaction tubes with glass inlets are fixed between LED; **d** – the reaction tubes; **e** –schematic representation of photoreactor setup; **1** – electric fan (16 W, 188 m^3/h); **2** – plastic protecting tube (d = 150 mm, h = 500 mm); **3** – aluminum cup (d = 110 mm); **4** – blue LED strip (LP SMD 5050, 300 Led, IP65, 12V, 12 W, 455 nm); **5** – magnetic stirrer (IKA® C-Mag HS 7); **6** – silicone hoses for a slow air access; **7** – rubber septums with glass outlets; **8** – fixed polypropylene centrifuge tubes (15 mL) equipped with magnetic stirring bars.

Table S9. Recycling of **Ru-4,7PHEt** in the nitromethylation of THIQ **1a**.
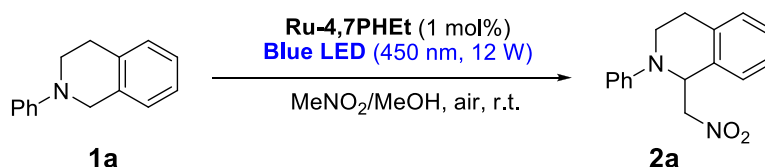
Cycle [1]	Time (h)	Conversion (%) [2]	Yield (%) [2]
1	10	93	83
2	10	85	70
3	10	97	84
4	10	94	79
5	10	77	67
6	10	80 [3]	-
	14	91	70
7	10	40 [3]	-
	19	81 [3]	-
	27	98	70

[1] Reaction conditions: **1a** (0.3 mmol), **Ru-4,7PHEt** (1 mol%), MeNO$_2$ (1.2 mL), MeOH (0.8 mL), air, blue LED (12 W), r.t.. [2] The yields and conversions were determined using NMR ^{1}H analysis of the reaction mixture. 1,3-Dimethoxybenzene was used as an internal standard. [3] Conversion was found using NMR ^{1}H analysis of the reaction mixture without an internal standard.

**Table S10.** Recycling of **Ru-bpy** in the nitromethylation of THIQ **1a**.
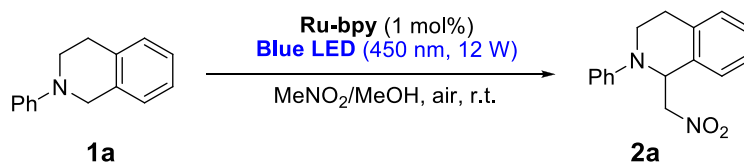
Cycle [1]	Time (h)	Conversion (%) [2]	Yield (%) [2]
1	10	91	73
2	10	30 [3]	-
	36	97	75

[1] Reaction conditions: **1a** (0.3 mmol), **Ru-bpy** (1 mol%), MeNO$_2$ (1.2 mL), MeOH (0.8 mL), air, blue LED (12 W), r.t.. [2] The yields and conversions were determined using NMR ^{1}H analysis of the reaction mixture. 1,3-Dimethoxybenzene was used as an internal standard. [3] Conversion was found using NMR ^{1}H analysis of the reaction mixture without an internal standard.

Representative examples of ^{1}H NMR analysis of the reaction mixtures in the aza-Henry reaction.
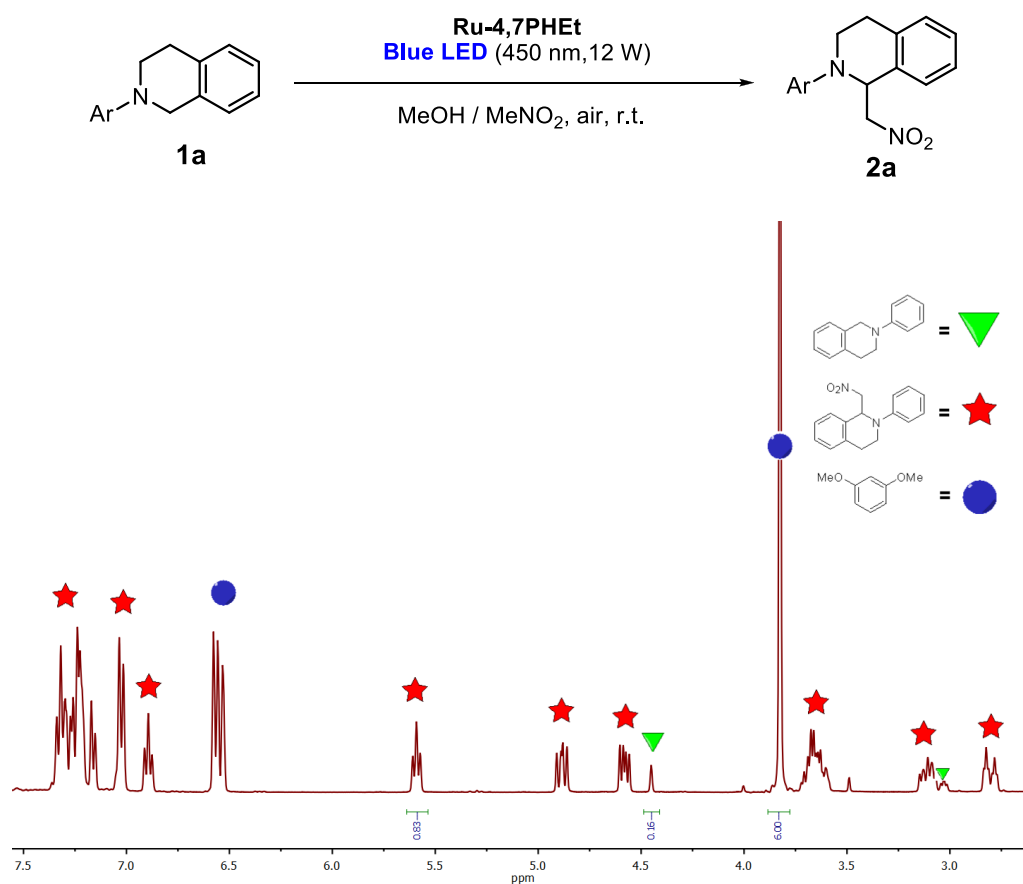
Figure S33. ^{1}H NMR spectrum of reaction mixture obtained in the 1st catalytic cycle of the nitromethylation of THIQ **1a** (400 MHz, CDCl$_3$, 298 K).
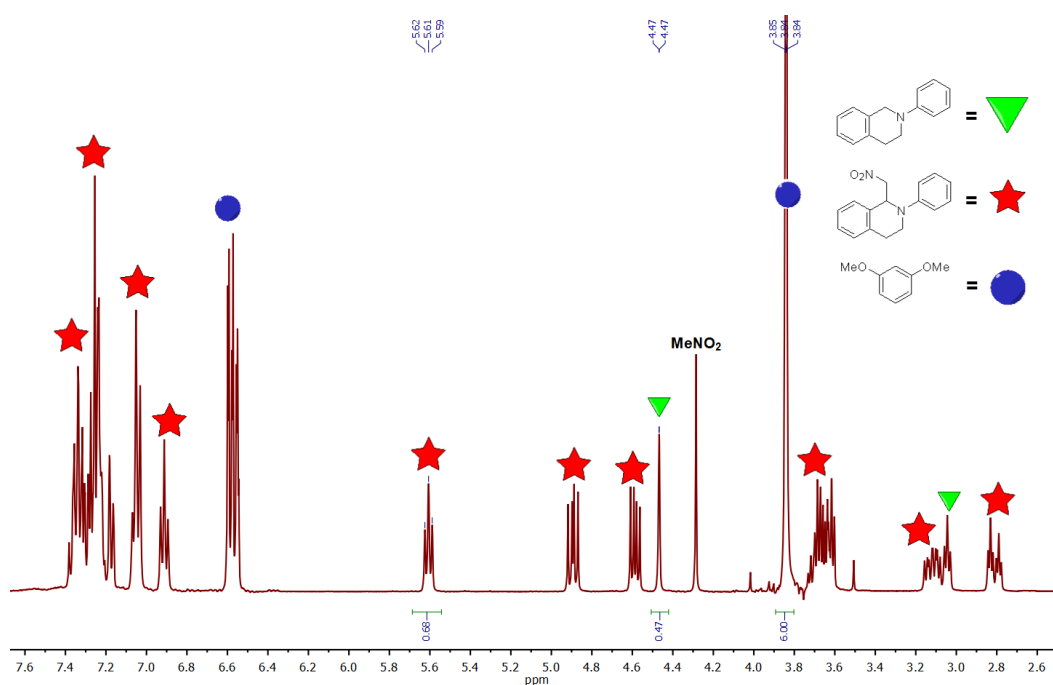

Figure S34. ^{1}H NMR spectrum of reaction mixture obtained in the 5th cycle of the nitromethylation of THIQ **1a** (400 MHz, CDCl$_3$, 298 K).

Table S11. Recycling of **Ru-4,7PHEt** in the phosphonylation of THIQ **1a**.
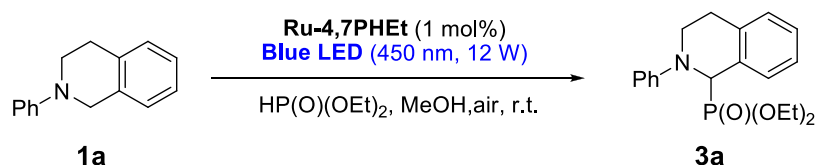
Cycle [1]	Time (h)	Conversion[2] (%)	Yield[2] (%)
1	4	98	86
2	4	93	70
3	4	83	64
4	4	77	64
5	4	78	63
6	4	69 [3]	-
	6	95	66
7	4	45 [3]	-
	8	67 [3]	-
	14	93	72

[1] Reaction conditions: **1a** (0.375 mmol), **Ru-4,7PHEt** (1 mol%), HP(O)(OEt)$_2$ (62 µL, 0.488 mmol, 1.3 equiv.), MeOH (1.5 mL), air, blue LED (12 W), r.t.. [2] The yields and conversions were determined using NMR ^{1}H analysis of the reaction mixture. 1,3-Dimethoxybenzene was used as an internal standard. [3] Conversion was found using NMR ^{1}H analysis of the reaction mixture without an internal standard.

Table S12. Recycling of **Ru-bpy** in the phosphonylation of THIQ **1a**.
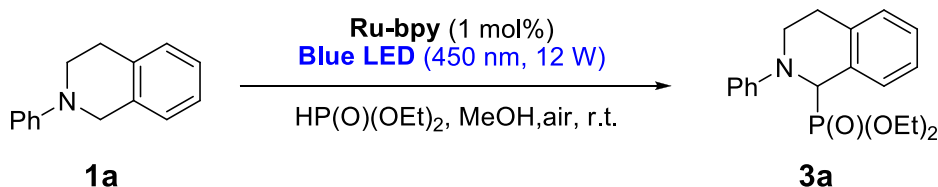
Cycle [1]	Time (h)	Conversion[2] (%)	Yield[2] (%)
1	4	70 [3]	-
	6	100	64
2	6	54 [3]	-
	16	93	68

[1] Reaction conditions: **1a** (0.375 mmol), **Ru-bpy** (1 mol%), HP(O)(OEt)$_2$ (62 µL, 0.488 mmol, 1.3 equiv.), MeOH (1.5 mL), air, blue LED (12 W), r.t.. [2] The yields and conversions were determined using NMR ^{1}H analysis of the reaction mixture. 1,3-Dimethoxybenzene was used as an internal standard). [3] Conversion was found using NMR ^{1}H analysis of the reaction mixture without an internal standard.

Representative examples of ^1H NMR analysis of the reaction mixtures in the phosphonylation reaction.
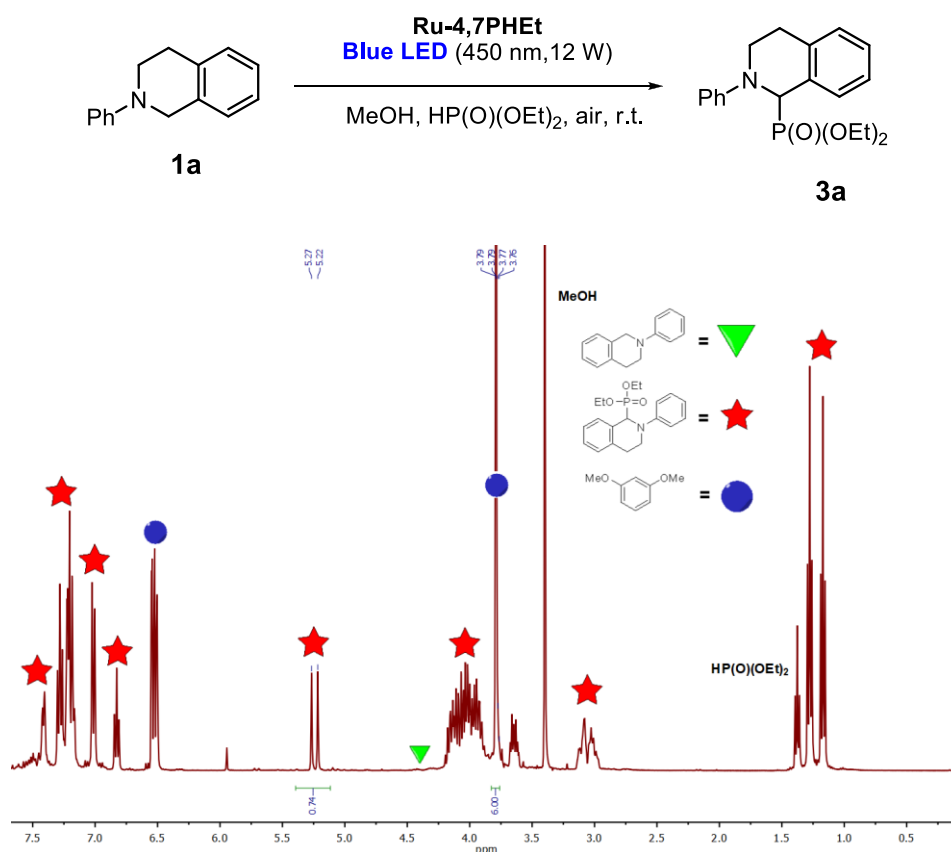
Figure S35. ^{1}H NMR spectrum of reaction mixture obtained in the 1st cycle of the phosphonylation of THIQ **1a** (400 MHz, CDCl$_3$, 298 K).
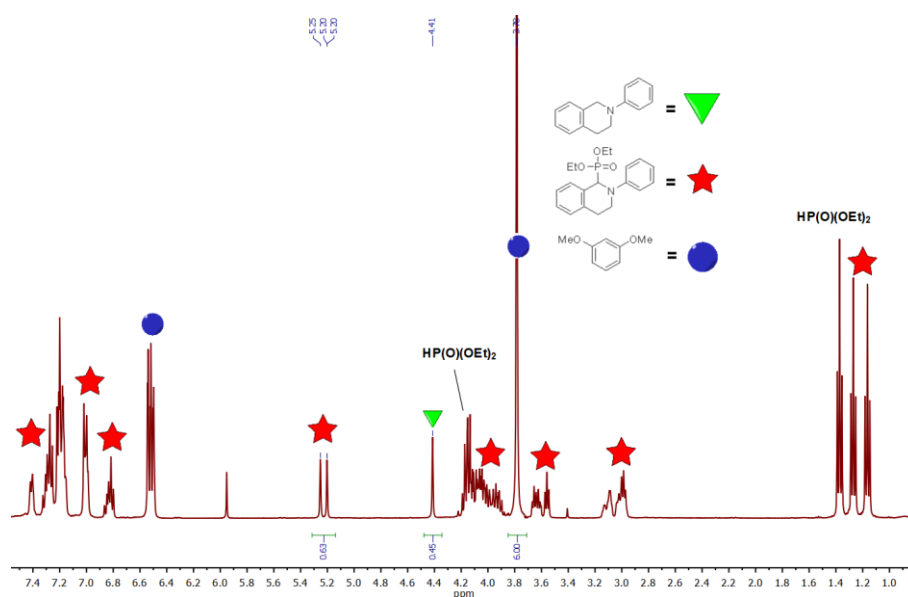
Figure S36. ^{1}H NMR spectrum of reaction mixture obtained in the 5th cycle of the phosphonylation of THIQ **1a** (400 MHz, CDCl$_3$, 298 K).

Table S13. Comparison of TON and TOF values for **Ru-4,7PHEt** and **Ru-bpy** catalysts.[1]

Reaction	Catalyst	TON (number of cycles)	TOF (1st cycle), h^{-1}	Average TOF, (number of cycles), h^{-1}
Nitromethylation	**Ru-4,7PHEt**	523 (7 cycles)	8.3	5.7 (7 cycles)
	Ru-bpy	148 (2 cycles)	7.3	3.2 (2 cycles)
Phosphonylation	**Ru-4,7PHEt**	485 (7 cycles)	21.4	12 (7 cycles)
	Ru-bpy	132 (2 cycles)	10.6	6 (2 cycles)

[1] The values were calculated from the data given in the tables S9–S12.
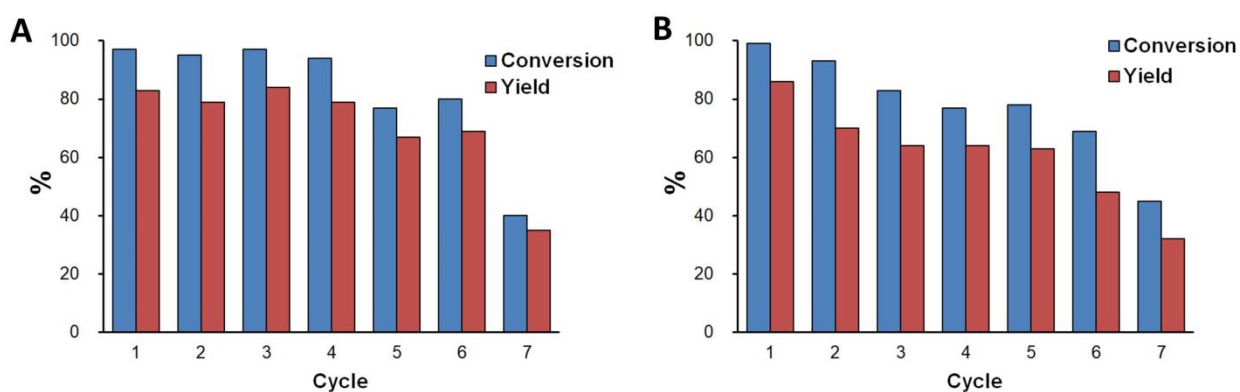
Figure S37. (A) Recycling **Ru-4,7PHEt** in the nitromethylation of THIQ **1a**. The irradiation time was 10 h. (B) Recycling **Ru-4,7PHEt** in the phosphonylation of THIQ **1a**. The irradiation time was 4 h.

8.   Spectral characterization of Ru(II) complexes

UV–vis spectra of Ru(II) complexes
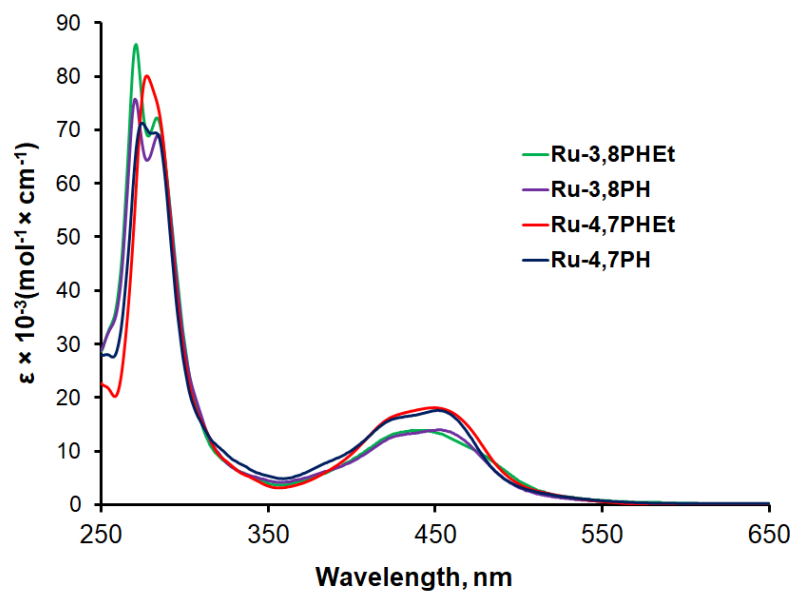
Figure S38. UV–vis spectra (ε as function of wavelength) of complexes **Ru-3,8PHEt**, **Ru-3,8PH**, **Ru-PHEt** and **Ru-4,7PH** in water.

NMR-spectra of Ru(II) complexes.
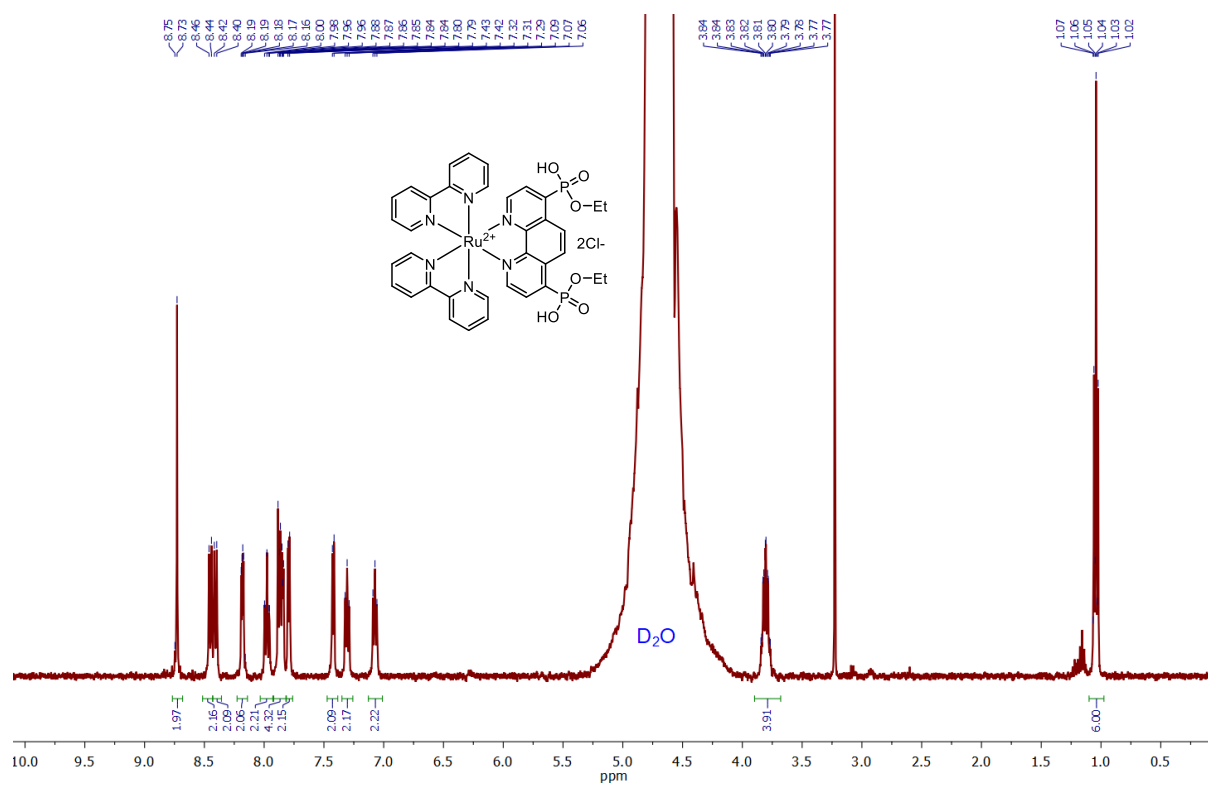
Figure S39. ^{1}H NMR spectrum of **Ru-4,7PHEt** (400 MHz, D$_2$O, 300 K).
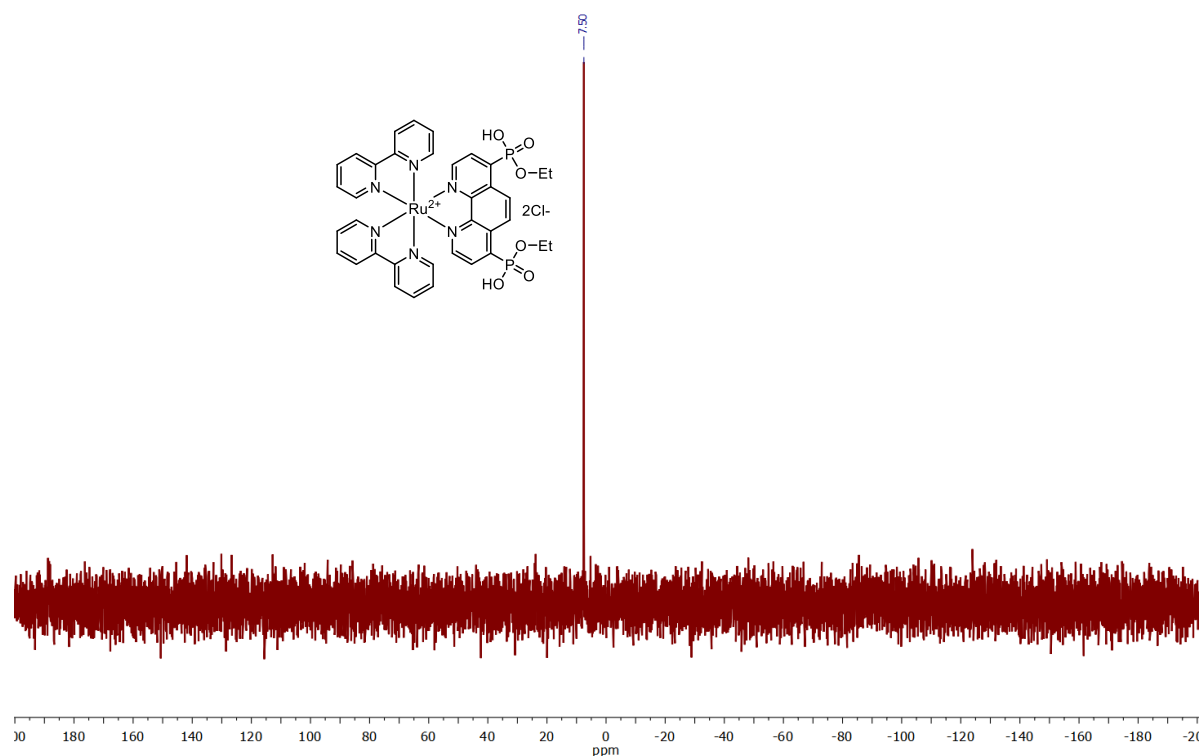
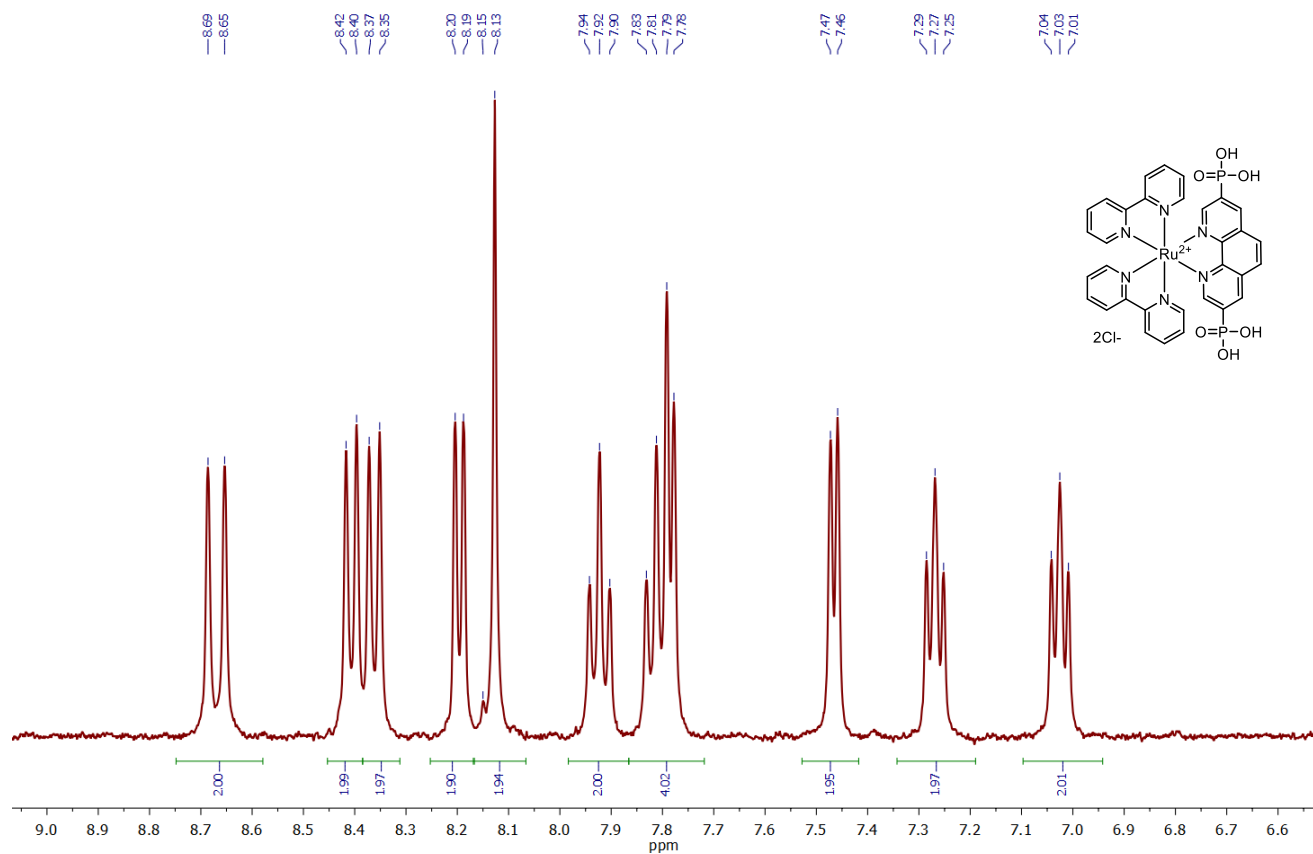**Figure S40.** ^{31}P NMR spectrum of **Ru-4,7PHEt** (161.9 MHz, D$_2$O, 300 K).
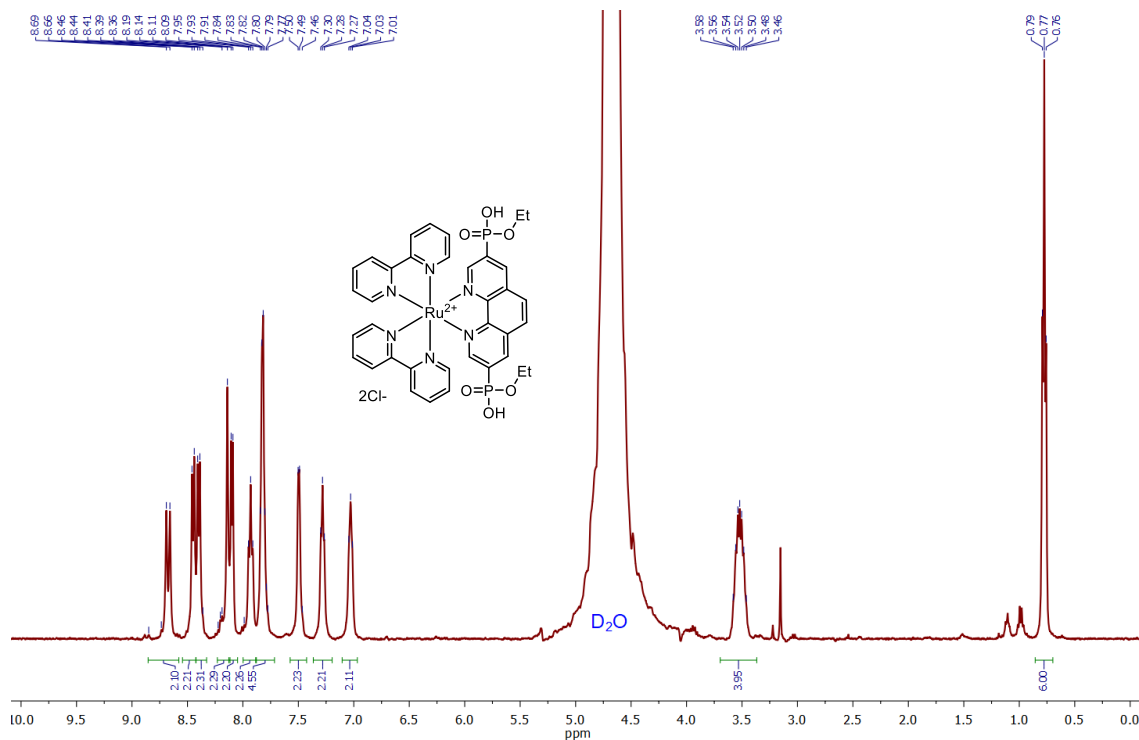
Figure S41. ^{1}H NMR spectrum of **Ru-3,8PHEt** (400 MHz, D$_2$O, 300 K).
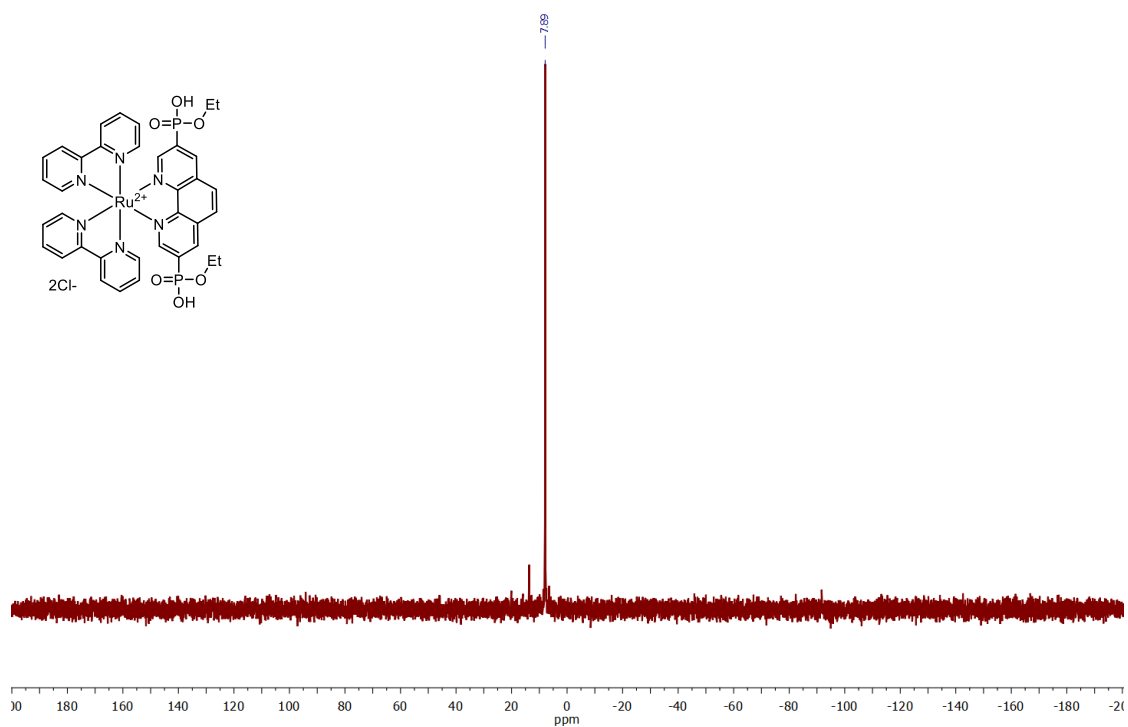
Figure S42. ^{31}P NMR spectrum of **Ru-3,8PHEt** (161.9 MHz, D$_2$O, 300 K).
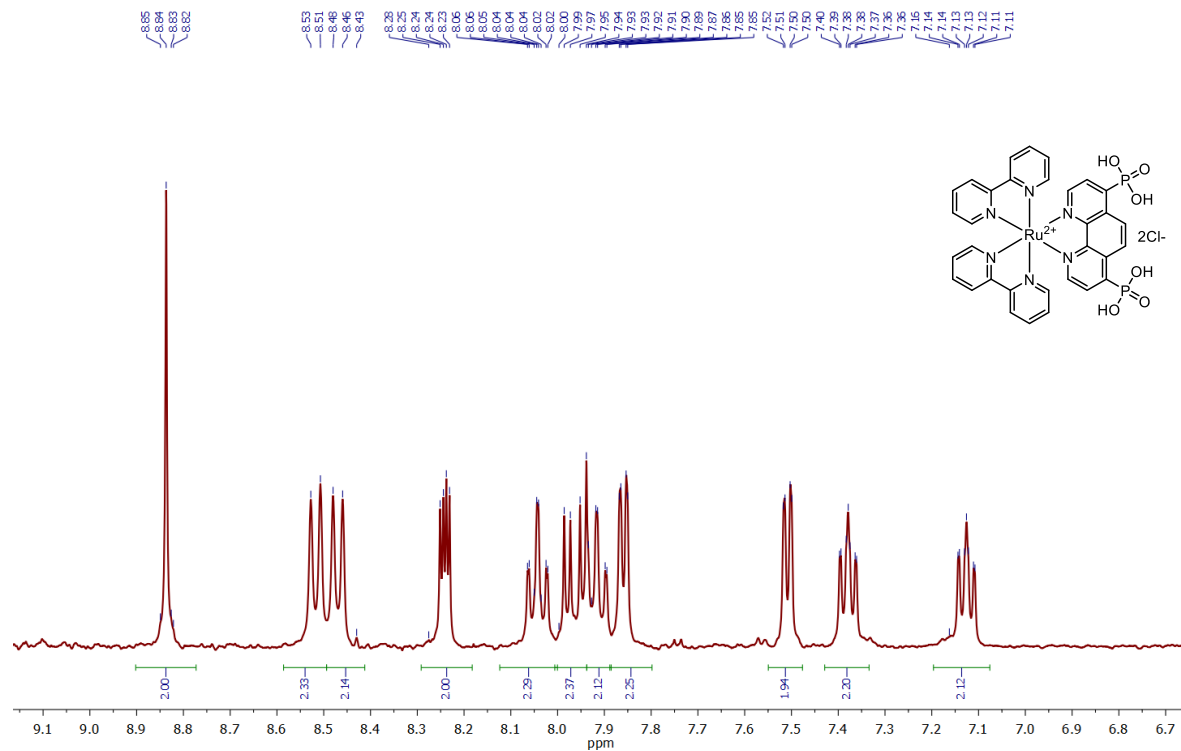
Figure S43. ^{1}H NMR spectrum of **Ru-4,7PH** (400 MHz, D$_2$O, 300 K).
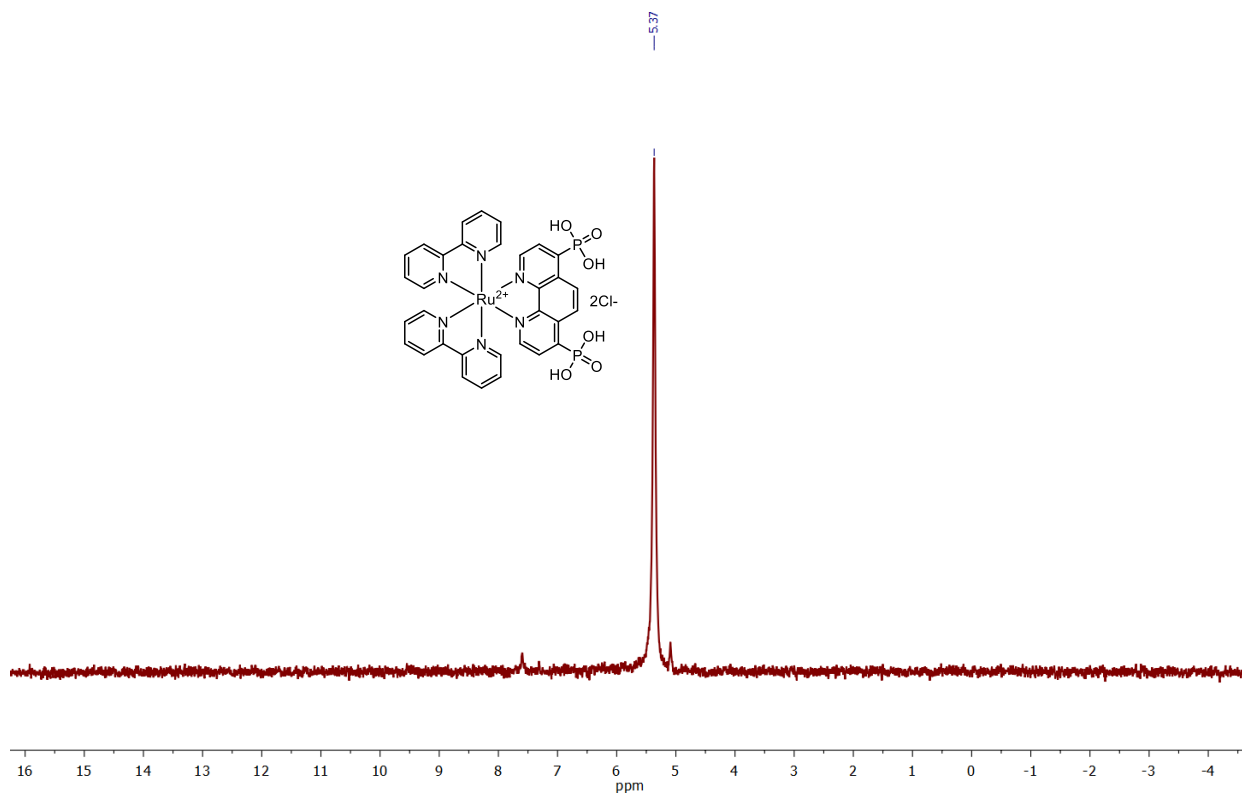
Figure S44. ^{31}P NMR spectrum of **Ru-4,7PH** (161.9 MHz, D$_2$O, 300 K).

Figure S45. ^{1}H NMR spectrum of **Ru-3,8PHEt** (400 MHz, D$_2$O, 300 K).
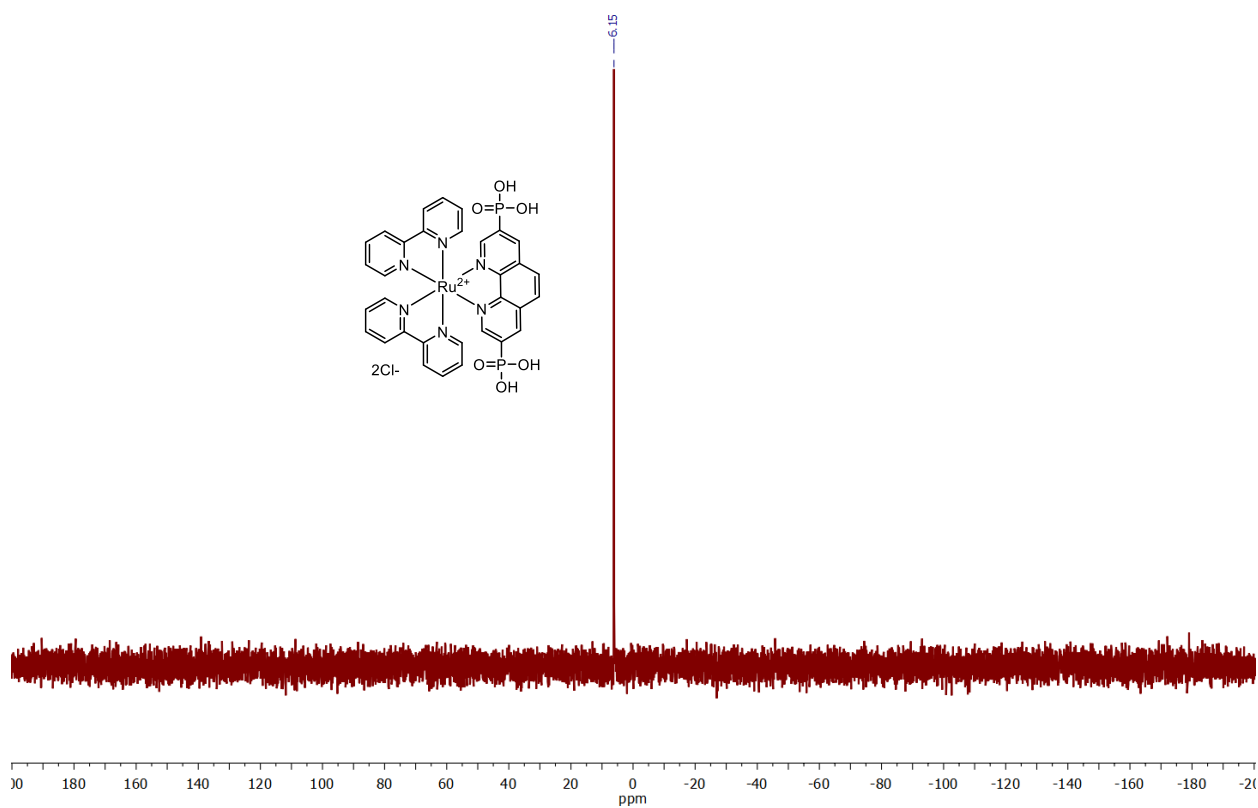
Figure S46. ^{31}P NMR spectrum of **Ru-3,8PHEt** (161.9 MHz, D$_2$O, 300 K).
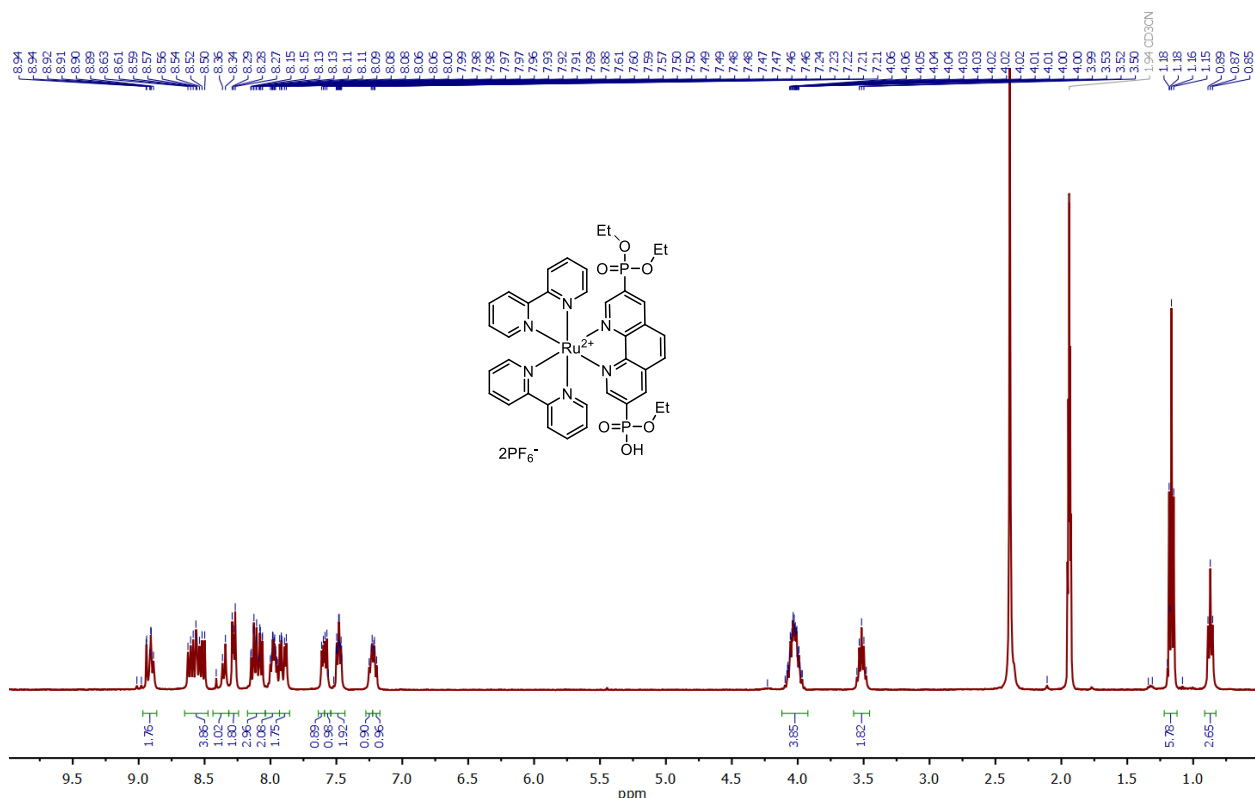
Figure S47. ^{1}H NMR spectrum of **Ru-3,8PH$_1$Et$_3$** (400 MHz, CD$_3$CN, 298 K).
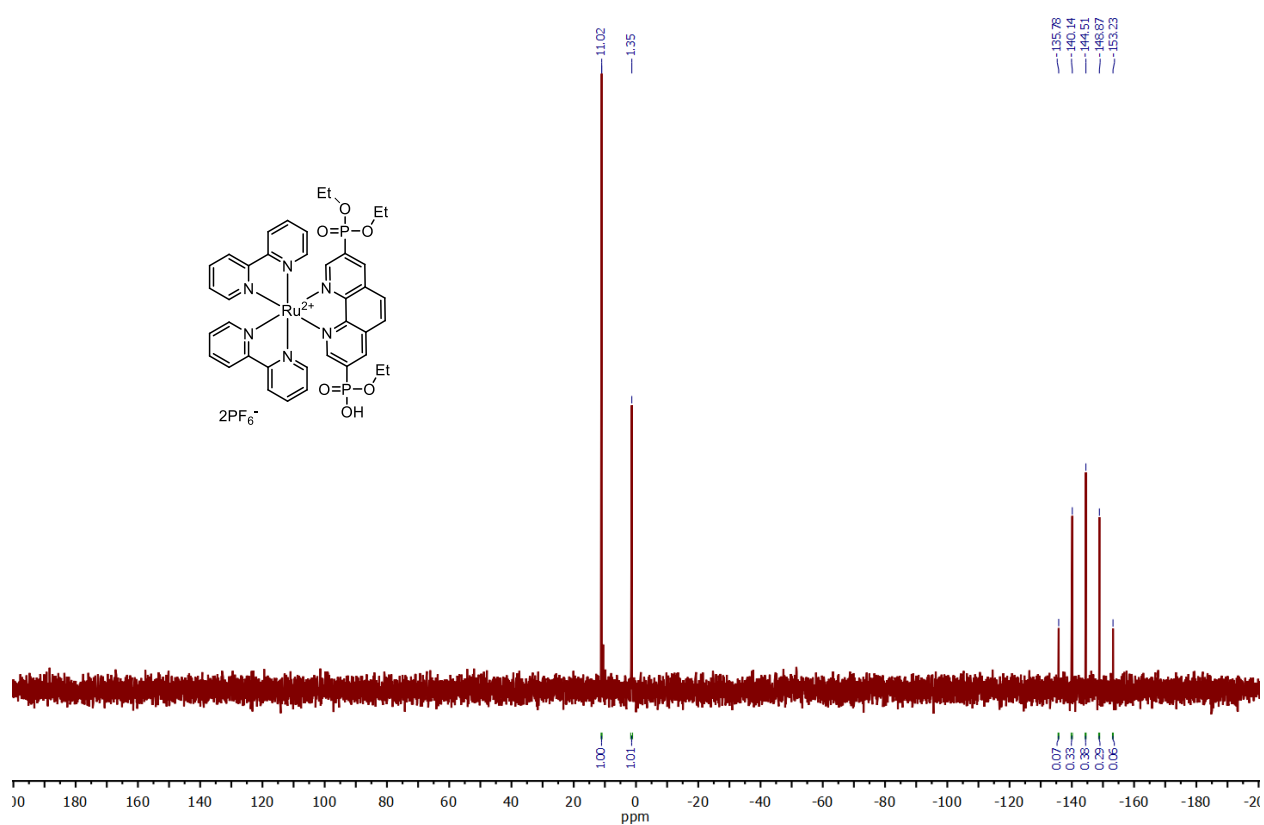
Figure S48. ^{31}P NMR spectrum of **Ru-3,8PH$_1$Et$_3$** (161.9 MHz, CD$_3$CN, 300 K).
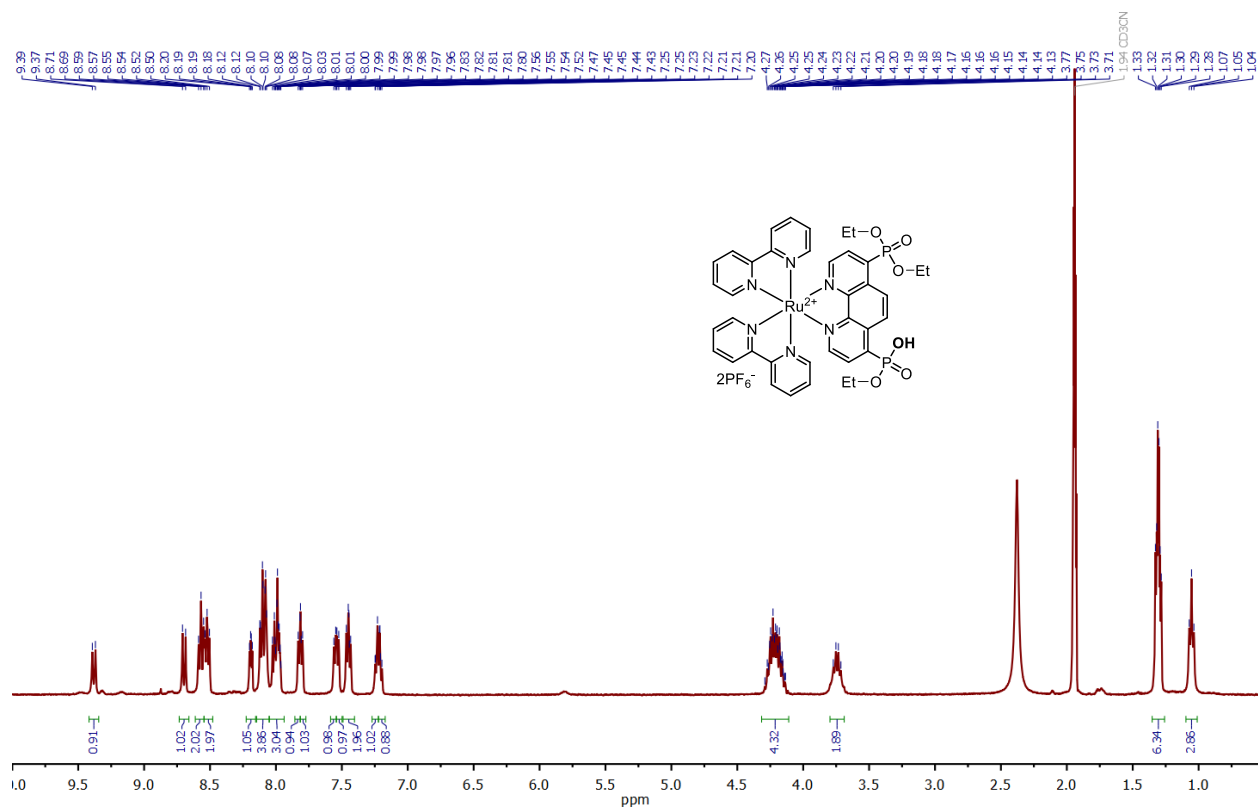
Figure S49. ^{1}H NMR spectrum of **Ru-4,7PH$_1$Et$_3$** (400 MHz, CD$_3$CN, 300 K).
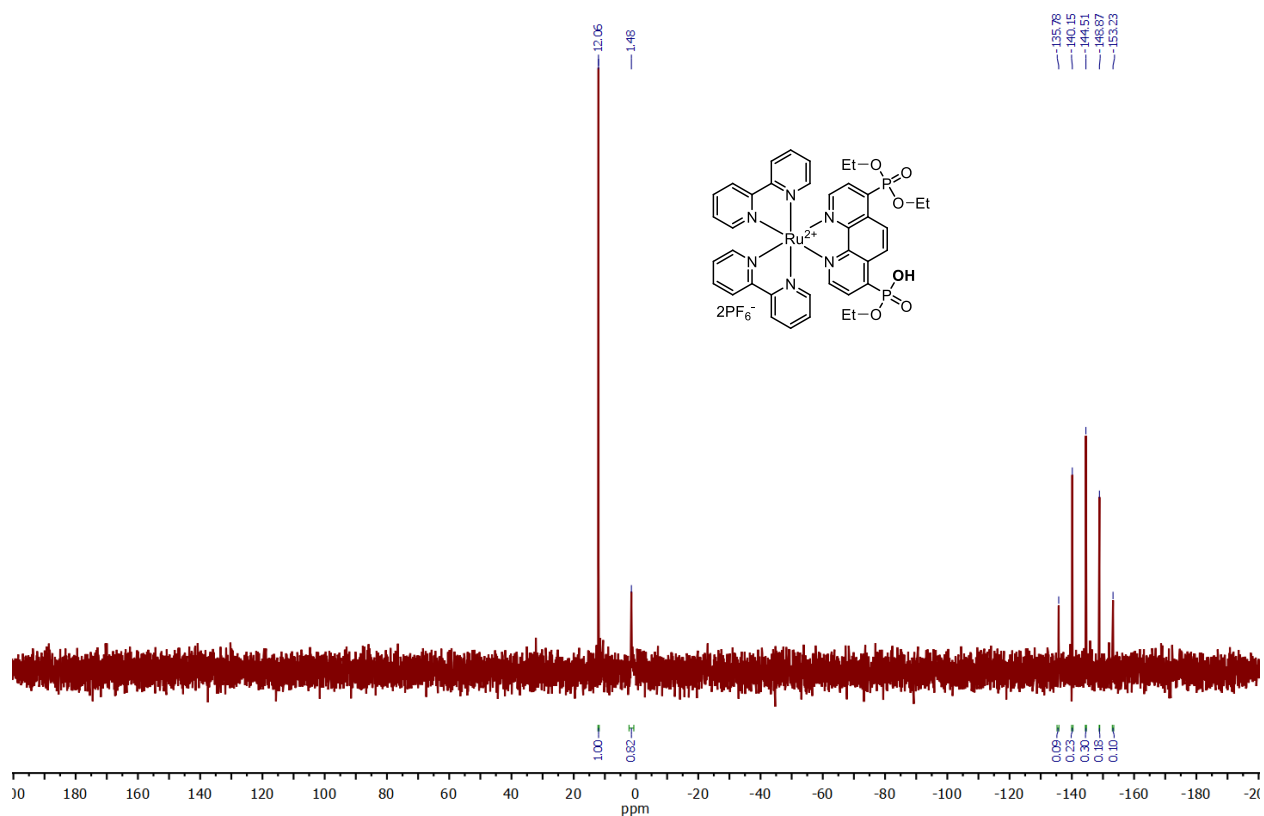
Figure S50. ^{31}P NMR spectrum of **Ru-4,7PH$_1$Et$_3$** (161.9 MHz, CD$_3$CN, 300 K).

*IR spectra of Ru(II) complexes **Ru-Pcat-A**.*
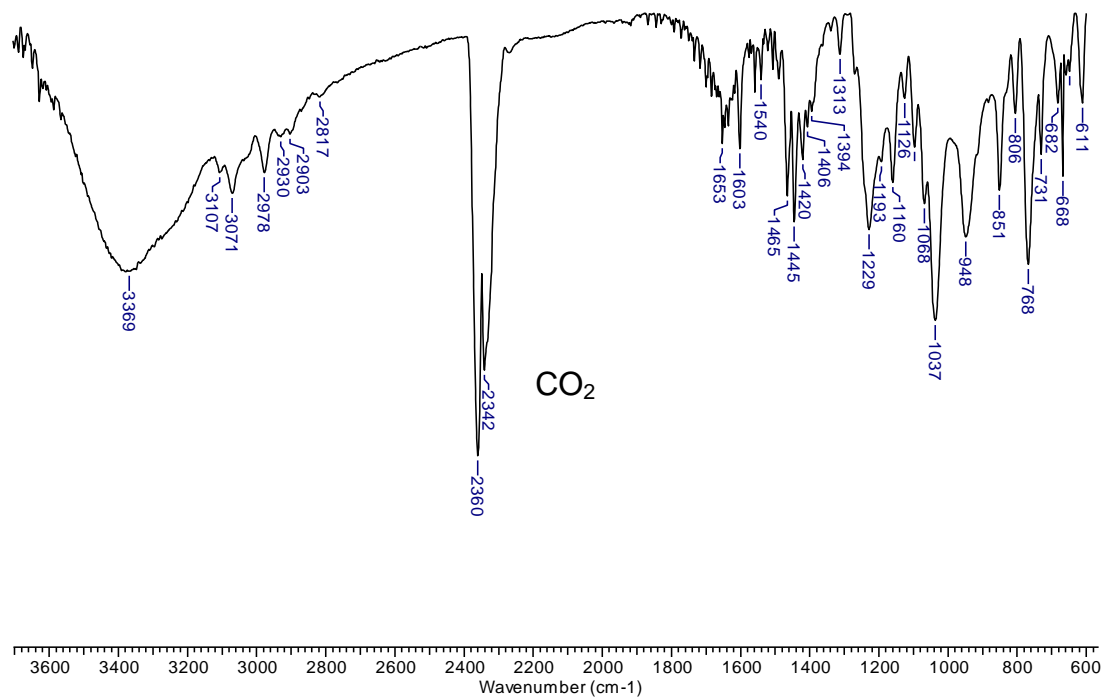
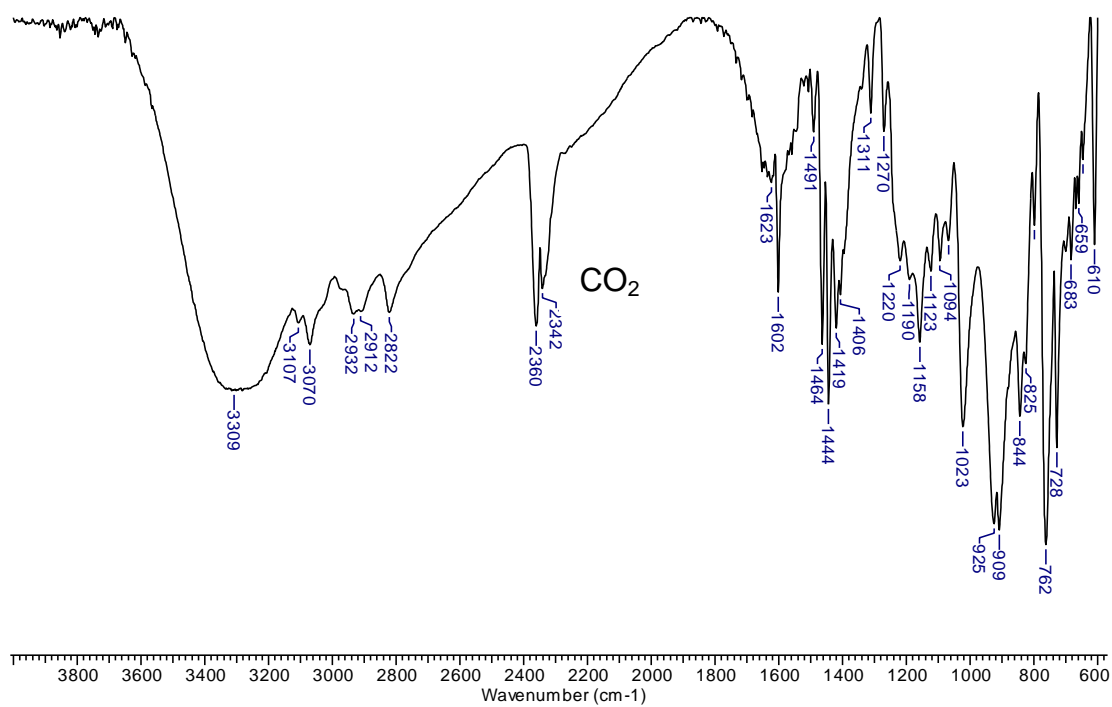**Figure S51**. IR spectrum of **Ru-4,7PHEt** (neat).
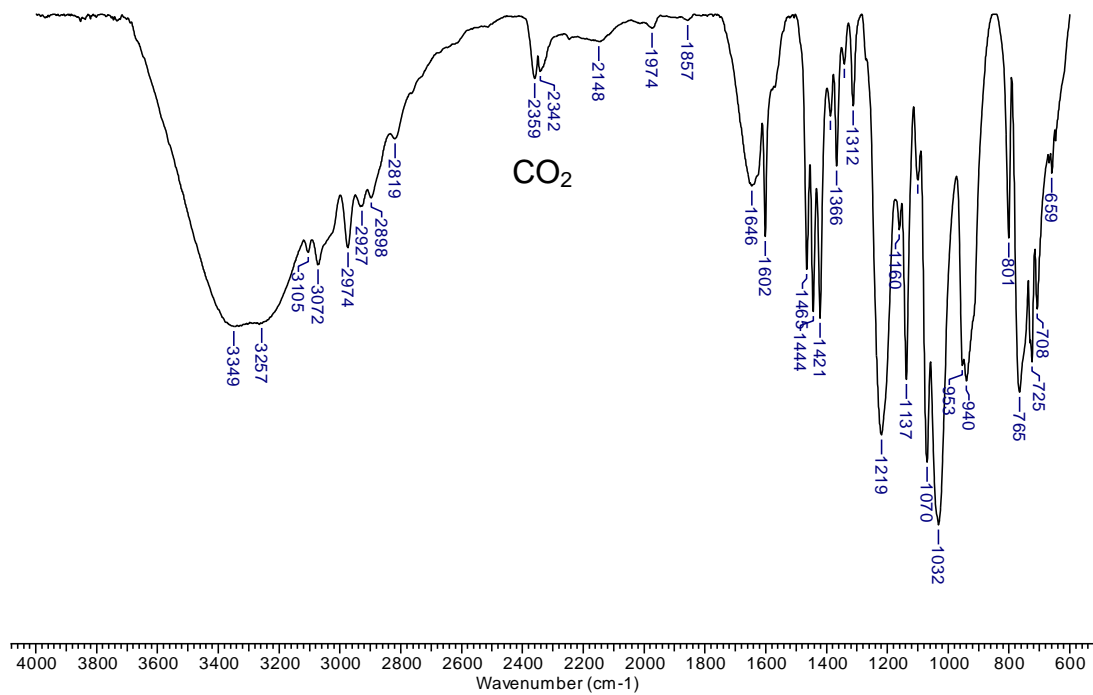

Figure S52. IR spectrum of **Ru-4,7PH** (neat).

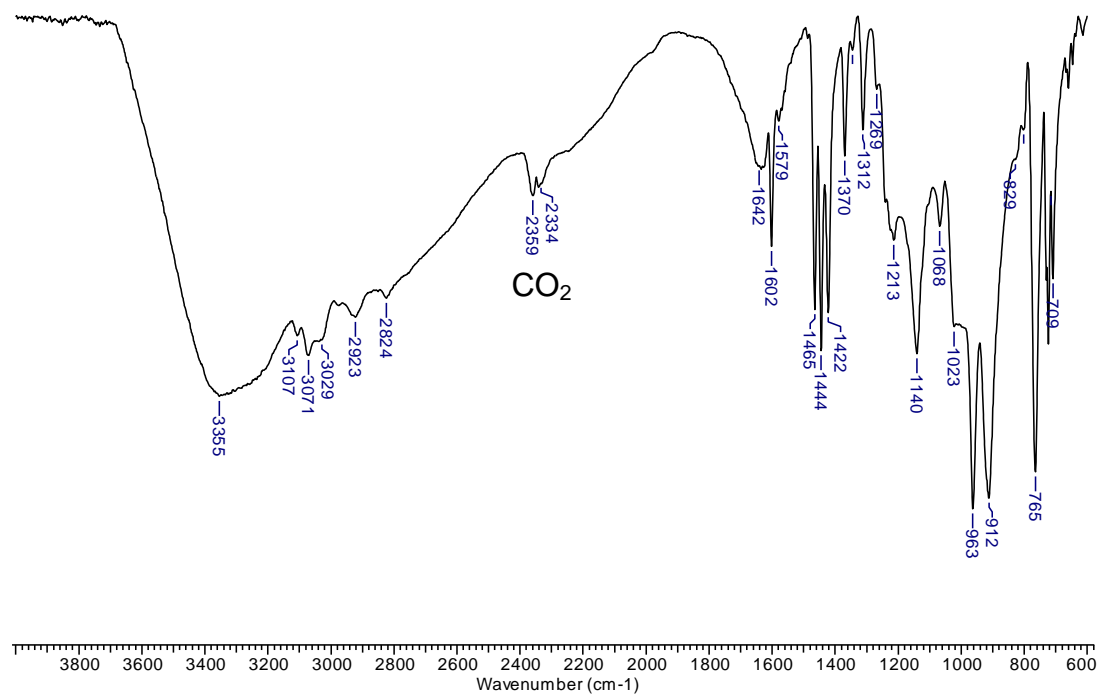**Figure S53**. IR spectrum of **Ru-3,8PHEt** (neat).

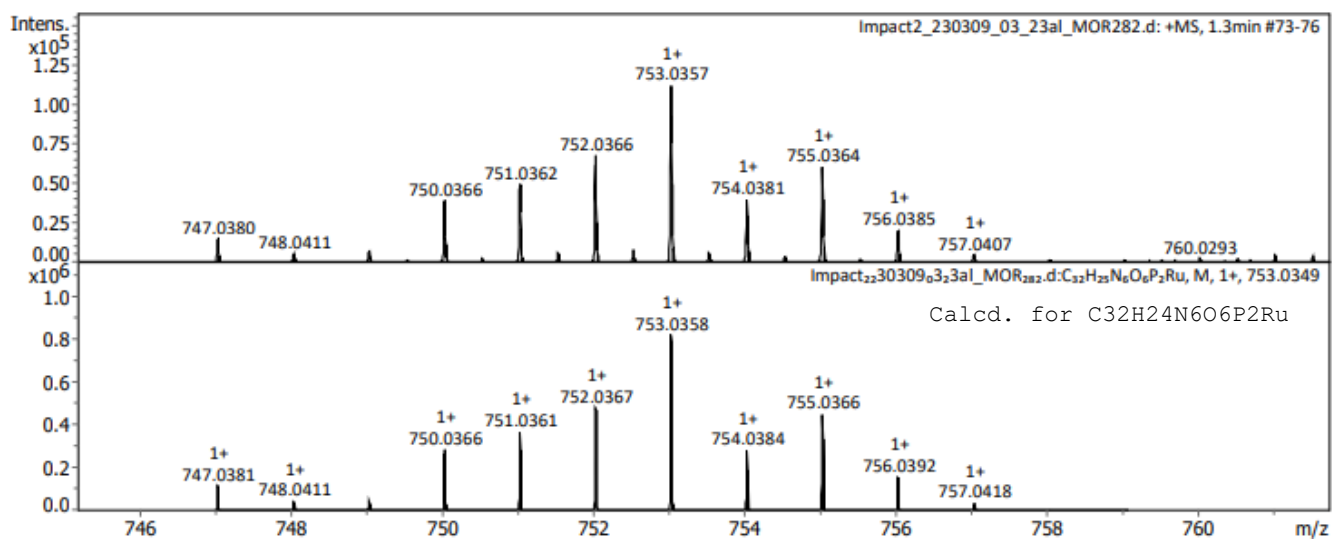**Figure S54**. IR spectrum of **Ru-3,8PH** (neat).

Mass-spectra of Ru(II) complexes.

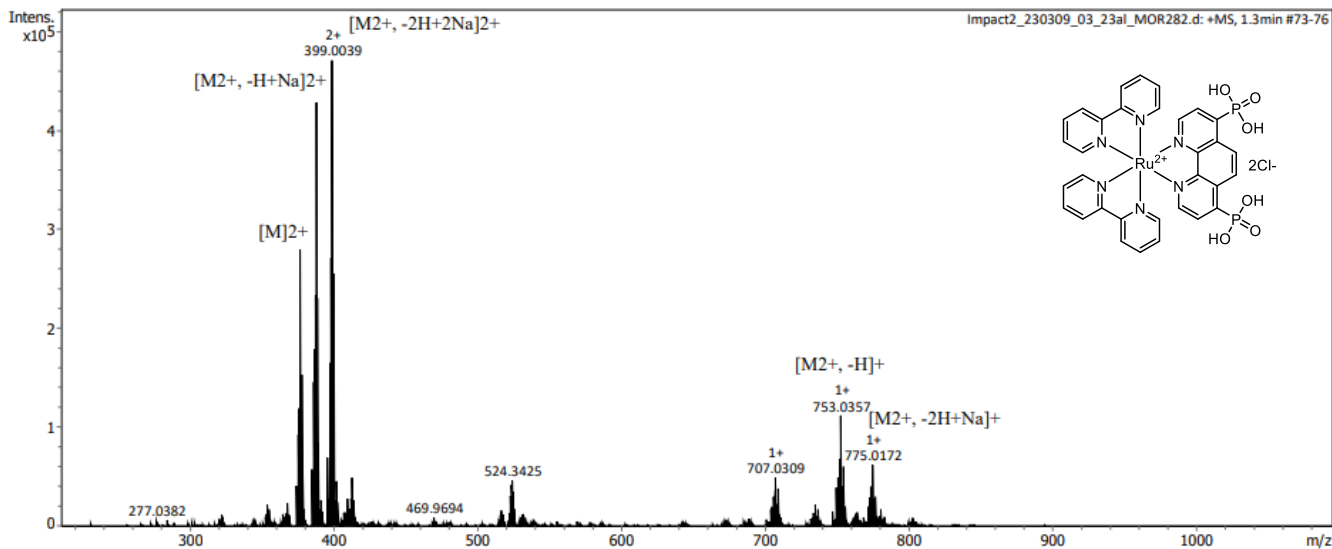**Figure S55.** HR-ESI mass spectrum of **Ru-4,7PHEt**.
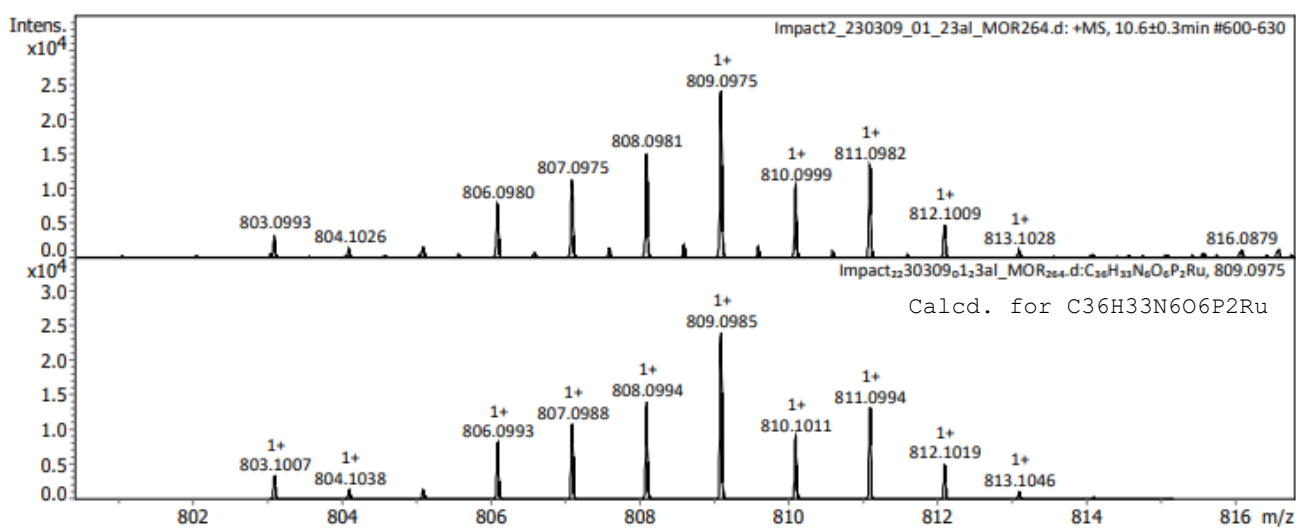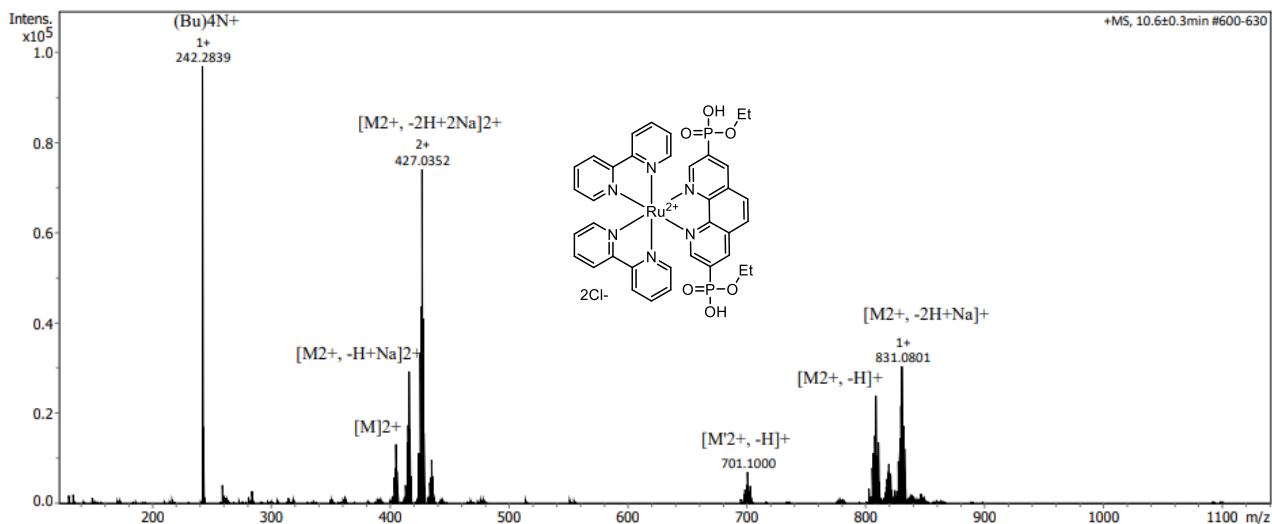
Figure S56. HR-ESI mass spectrum of **Ru-4,7PH**.

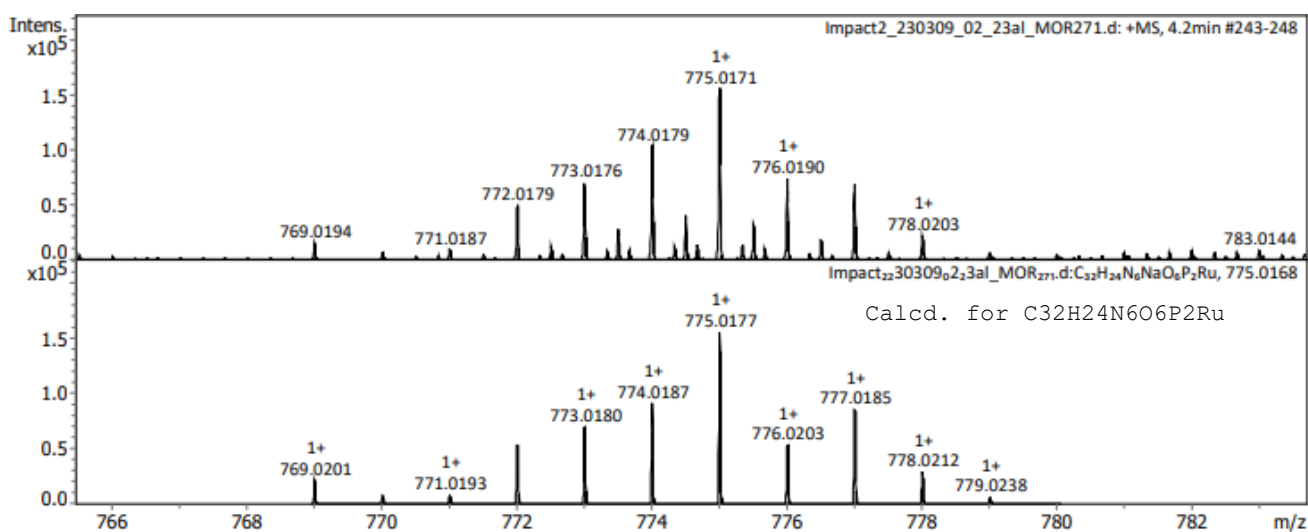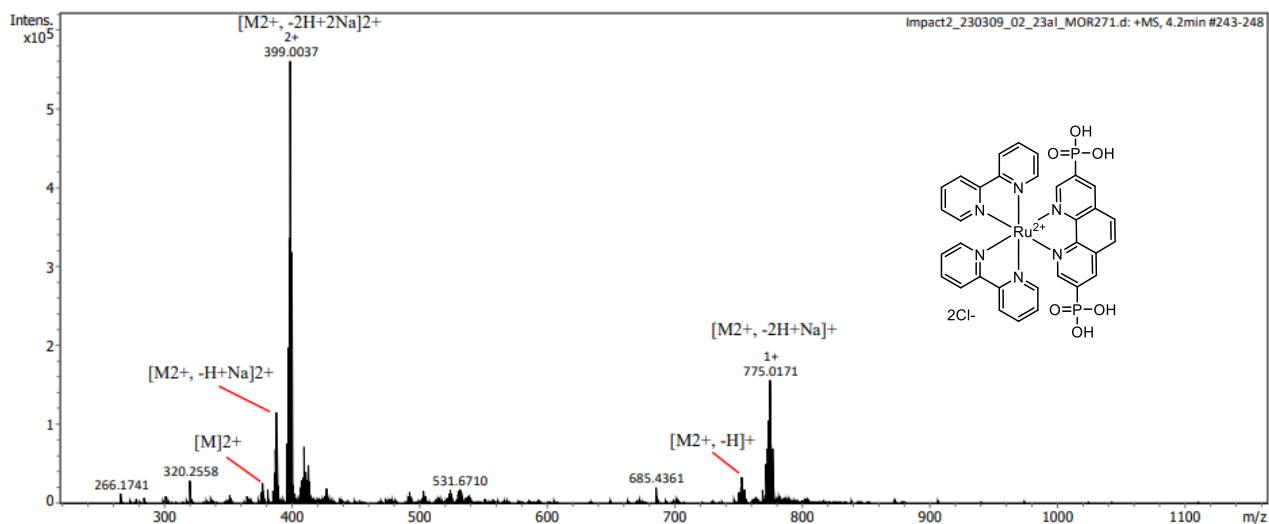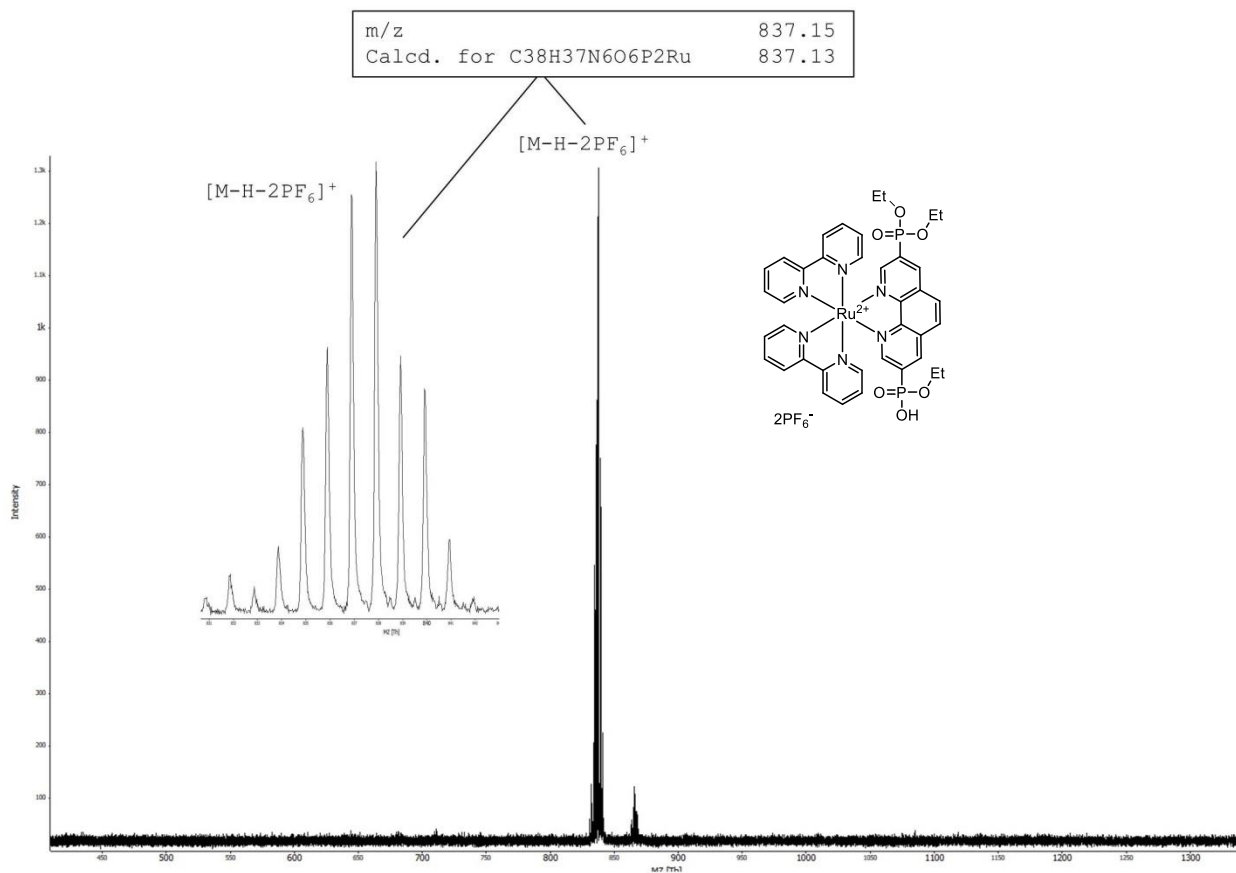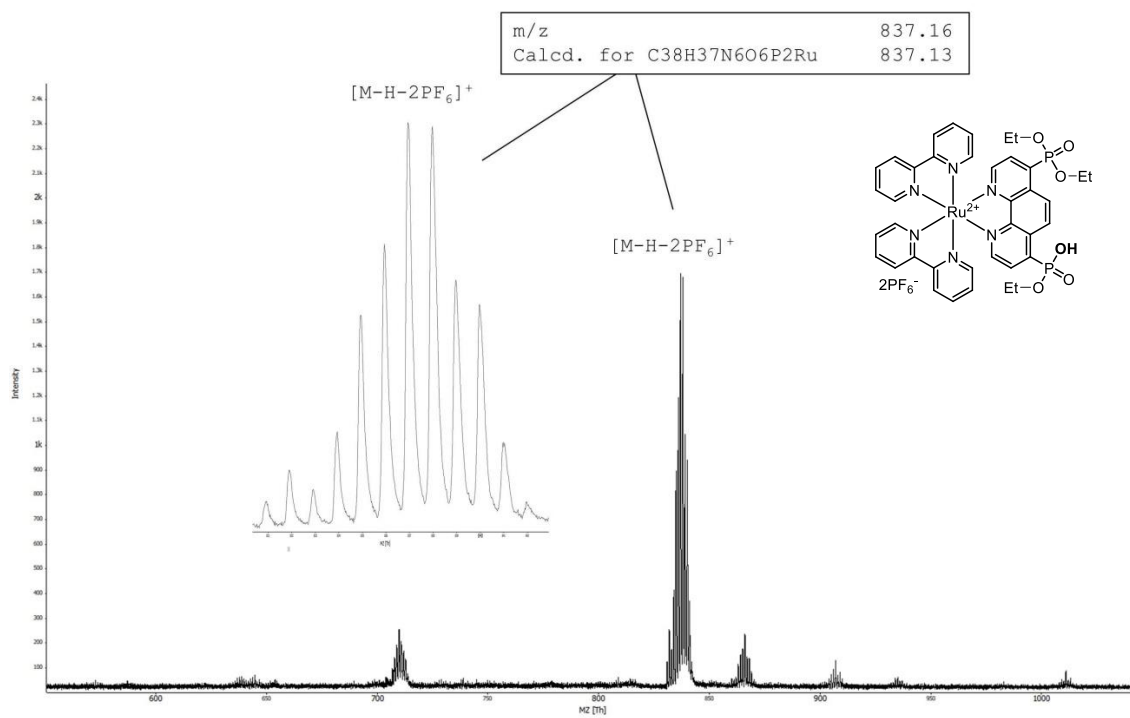**Figure S57.** HR-ESI mass spectrum of **Ru-3,8PHEt**.

.

Figure S58. HR-ESI mass spectrum of **Ru-3,8PH**.

Figure S59. MALDI-TOF spectrum of **Ru-3,8PH₁Et₃**.

Figure S60. MALDI-TOF spectrum of **Ru-4,7PH₁Et₃**.

9. References

(1) Jiang, J.-X.; Li, Y.; Wu, X.; Xiao, J.; Adams, D. J.; Cooper, A. I. Conjugated microporous polymers with rose bengal dye for highly efficient heterogeneous organo-photocatalysis. *Macromolecules* **2013,** *46,* 8779–8783.

(2) Martín-García, I.; Alonso, F. Synthesis of dihydroindoloisoquinolines through copper-catalyzed cross-dehydrogenative coupling of tetrahydroisoquinolines and nitroalkanes. *Chem. – Eur. J.* **2018,** *24,* 18857–18862.

(3) Nelyubina, Y. V.; Troyanov, S. I.; Antipin, M. Y.; Lyssenko, K. A., Why oxonium cation in the crystal phase is a bad acceptor of hydrogen bonds: a charge density analysis of potassium oxonium bis(hydrogensulfate). *J. Phys. Chem. A* **2009,** *113* (17), 5151–5156.

(4) Nelyubina, Y. V.; Barzilovich, P. Y.; Antipin, M. Y.; Aldoshin, S. M.; Lyssenko, K. A., Cation–π and lone Pair–π interactions combined in one: the first experimental evidence of $(H_3O\text{-}lp)^+\cdots\pi$-system binding in a crystal. *ChemPhysChem* **2011,** *12* (16), 2895–2898.

(5) Ananyev, I. V.; Barzilovich, P. Y.; Lyssenko, K. A., Evidence for the Zundel-like Character of Oxoethylidenediphosphonic Acid Hydrate. *Mendeleev Commun.* **2012,** *22* (5), 242-244.

(6) Morozkov, G. V.; Abel, A. S.; Filatov, M. A.; Nefedov, S. E.; Roznyatovsky, V. A.; Cheprakov, A. V.; Mitrofanov, A. Y.; Ziankou, I. S.; Averin, A. D.; Beletskaya, I. P.; Michalak, J.; Bucher, C.; Bonneviot, L.; Bessmertnykh-Lemeune, A. Ruthenium(II) complexes with phosphonate-substituted phenanthroline ligands: synthesis, characterization and use in organic photocatalysis. *Dalton Trans.* **2022,** *51,* 13612–13630.

(7) Zenkov, I. S.; Yakushev, A. A.; Abel, A. S.; Averin, A. D.; Bessmertnykh-Lemeune, A. G.; Beletskaya, I. P. Photocatalytic activity of ruthenium(II) complex with 1,10-phenanthroline-3,8-dicarboxylic acid in aerobic oxidation reactions. *Russ. J. Org. Chem.* **2021,** *57,* 1398–1404.

(8) Tzalis, D.; Tor, Y. Stereochemically-defined supramolecular architectures: diastereomerically-pure multi-Ru[II] complexes. *J. Am. Chem. Soc.* **1997,** *119,* 852–853.

(9) Abel, A. S.; Zenkov, I. S.; Averin, A. D.; Cheprakov, A. V.; Bessmertnykh-Lemeune, A. G.; Orlinson, B. S.; Beletskaya, I. P. Tuning the luminescent properties of ruthenium(II) amino-1,10-phenanthroline complexes by varying the position of the amino group on the heterocycle. *ChemPlusChem* **2019,** *84,* 498–503.

(10) Ye, B.-H.; Ji, L.-N.; Xue, F.; Mak, T. C. W. Synthesis, characterization and crystal structure of ruthenium(II) polypyridyl complexes. *Transition Met. Chem.* **1999,** *24,* 8–12.